

**The Cardioprotective Role of Renin-Angiotensin System  
Antagonists in the Prevention of  
Bevacizumab and Sunitinib Mediated Cardiotoxicity**

by

Viktoriya Mozolevska

A Thesis submitted to the Faculty of Graduate Studies of  
The University of Manitoba  
in partial fulfillment of the requirements of the degree of

MASTER OF SCIENCE

Department of Physiology and Pathophysiology  
Max Rady College of Medicine, Rady Faculty of Health Sciences  
University of Manitoba  
Winnipeg, Manitoba, Canada

Copyright © 2017 by Viktoriya Mozolevska

## **Abstract**

**Background:** Despite the beneficial effects of chemotherapy agents in improving overall survival of cancer patients, cardiovascular damage remains a serious complication of many anti-cancer therapies. Two types of targeted therapy currently in use for colorectal (CRC) and renal cell cancer (RCC) are the monoclonal antibody Bevacizumab (BVZ) and the tyrosine kinase inhibitor Sunitinib (SNT), respectively. An unexpected side effect of these two anti-cancer agents is an increased risk of cardiotoxicity. One of the key mechanisms involved in the development of BVZ or SNT mediated cardiac damage is activation of renin-angiotensin system (RAS). Although heart failure drugs including RAS antagonists are commonly used after cardiac dysfunction is detected in the CRC and RCC settings, their prophylactic role in the prevention of cardiotoxicity due to BVZ or SNT has yet to be elucidated.

**Objective:** To investigate whether prophylactic administration of RAS antagonists will attenuate the cardiotoxic side effects of BVZ or SNT in a chronic *in vivo* murine model.

**Methods:** A total of 194 C57Bl/6 male mice received: i) 0.9% saline; ii) BVZ; or iii) SNT for 4 weeks. Within each arm, mice were administered daily prophylactic treatment either with water, Hydralazine, Aliskiren, Perindopril, or Valsartan via oral gavage for the entire study period. Hydralazine served as a positive control due to its inability to antagonize the RAS pathway. Following serial echocardiographic and hemodynamic assessments for 4 weeks, the hearts were collected for histological and biochemical analyses.

**Results:** In our chronic model of BVZ or SNT induced cardiotoxicity, prophylactic addition of Hydralazine effectively attenuated hypertension due to BVZ or SNT but was

not overall cardioprotective. Similarly, RAS antagonists completely prevented the rise in MAP regardless of the targeted agent used. The echocardiographic findings revealed a significant decrease in LVEF from  $72\pm 3\%$  at baseline to  $41\pm 2\%$  at week 4 in BVZ treated mice. Prophylactic treatment with Aliskiren, Perindopril or Valsartan was partially cardioprotective with LVEF values of  $57\pm 2\%$ ,  $50\pm 2\%$ , and  $51\pm 3\%$  at the end of the study, respectively. Similarly, in mice treated with SNT alone, LVEF decreased from  $73\pm 4\%$  at baseline to  $34\pm 3\%$ . Addition of Aliskiren, Perindopril, or Valsartan significantly improved LVEF values to  $54\pm 2\%$ ,  $45\pm 2\%$ , and  $44\pm 3\%$  at week 4, respectively. Moreover, animals treated with BVZ or SNT demonstrated increased loss of cellular integrity and myofibril disarray, which were partially attenuated by RAS antagonists. According to our biochemical findings, there was a 2.1- or 2.3-fold induction in apoptotic marker cleaved PARP in BVZ or SNT treated mice at week 4, respectively, which was partially attenuated by the prophylactic administration of Aliskiren, Perindopril, or Valsartan. Finally, a 7.7-fold increase in phosphorylation of p38 was observed in mice treated with SNT at the end of the study. RAS antagonists completely normalized the expression of this apoptosis inducing marker.

**Conclusion:** The prophylactic administration of RAS antagonists partially attenuated the cardiotoxic side effects of BVZ or SNT in a chronic *in vivo* murine model.

## **Acknowledgments**

First and foremost I would like to thank my supervisor Dr. Davinder Jassal for everything you have taught me during the course of my graduate program. Thank you from the bottom of my heart for your support, patience, understanding, mentorship, expertise, guidance, and all the precious advice you have given me. Thank you for challenging me and making me a better person and scientist! Words cannot describe how thankful I am for all the opportunities you provided me with! I am very thankful to my co-supervisor Dr. Pawan Singal for your continuous support, encouragement, and thoughtfulness. I would like to express my sincere gratitude to my committee members, including Dr. Jeffrey Wigle, Dr. Ian Dixon, and Dr. Amir Ravandi for their support, knowledge and belief in me. I would like to thank Dr. James Thliveris for his help and guidance with electron microscopy.

I would like to sincerely thank David Cheung – I would not have been able to finish this program without your tremendous help. Thank you to all the past and present members of the Cardiovascular Imaging laboratory, especially Vineet, Anna, Antonia, Ishika, Chantal, Kimberly, Bella, Bilal, Ryan, and Hilary – it has been a joy knowing and working with all of you! I would like to thank all the members of Muscle Cell Biochemistry laboratory for their support and specifically Navid Koleini. I truly appreciate all your support and words of encouragement. Thank you kindly to all the members of Molecular Pathophysiology laboratory, especially Raghu and Nina for their kindness and all the help. Dr. Andrea Edel, thank you for everything, your friendship and the time you took to help me prepare for my 3MT speech. I would like to acknowledge all the members of animal holding who helped me with this project and specifically Dana

– it has been so much fun working with you! Thank you to all the members of Institute of Cardiovascular Sciences who helped and supported me, including Gauri, Prathap, Elena, Stephanie, Aleksandra, Mihir, Zahra, Kairee, Natalie, Krista, Joseph and Rob. I owe deep gratitude to my previous mentors – Dr. Rushita Bagchi, Dr. Michael Czubryt, and Dr. Nasrin Mesaeli. Thank you for your mentorship and introducing me into the world of research!

I am extremely grateful to the following funding agencies, including the Mark and Patricia Smerchanski Studentship and Research Manitoba Studentship. Your financial support has allowed me to explore the project that can benefit heart health of cancer patients in the future.

Finally, I would like to sincerely thank my mom Irina, dad Igor, sister Svetlana, grandmother Svetlana, aunt Irina, uncle Dr. Alex Omelchenko, aunt Luda and my dear friend Samira! Thank you for always being there for me, for encouraging and supporting me in every way. You are my everything, and I love you very much! Thank you God for putting me through this journey for a reason!

I dedicate this thesis to  
my grandfathers and aunt who battled with cancer

# Table of Contents

<b>Abstract</b> .....	i
<b>Acknowledgements</b> .....	iii
<b>Table of Contents</b> .....	vi
<b>Table Synopsis</b> .....	ix
<b>Figure Synopsis</b> .....	x
<b>List of Equations</b> .....	xii
<b>List of Abbreviations</b> .....	xiii
<b>Chapter 1: Literature Review</b> .....	1
Cancer in Canada: Introduction .....	1
Cardio-Oncology.....	1
Colorectal Cancer: Prevalence, Risk Factors, Diagnosis, and Treatment.....	4
Monoclonal Antibody: Bevacizumab .....	6
Bevacizumab: Anti-cancer Mechanism .....	8
Bevacizumab: Cardiovascular Toxicity.....	10
i) <i>Murine Model</i> .....	14
ii) <i>Clinical Setting</i> .....	16
Renal Cell Carcinoma: Prevalence, Risk Factors, Diagnosis, and Treatment .....	18
Tyrosine Kinase Inhibitor: Sunitinib .....	22
Sunitinib: Anti-cancer Mechanism .....	23
Sunitinib: Cardiovascular Toxicity .....	26
i) <i>Murine Model</i> .....	27
ii) <i>Clinical Setting</i> .....	29

Prevention of Cardiotoxicity.....	31
i) <i>Statins</i> .....	32
ii) <i>Antioxidants</i> .....	33
iii) <i><math>\beta</math>-blockers</i> .....	34
iv) <i>RAS Antagonists</i> .....	35
<b>Chapter 2: Hypothesis, Objectives, and Study Rationale .....</b>	<b>38</b>
<b>Chapter 3: Materials and Methods .....</b>	<b>40</b>
Animal Model .....	40
Hemodynamics .....	43
Murine Echocardiography .....	43
Histological Analysis .....	44
Oxolipidomic Analysis .....	45
Western Blotting .....	46
Statistical Analysis.....	47
<b>Chapter 4: Results.....</b>	<b>49</b>
Hemodynamics: BVZ Treatment.....	49
Hemodynamics: SNT Treatment .....	51
Murine Echocardiography: BVZ Treatment.....	53
Murine Echocardiography: SNT Treatment .....	58
Histological Analysis: BVZ and SNT Treatment .....	63
Oxolipidomic Analysis .....	67
Western Blotting: BVZ Treatment.....	68
Western Blotting: SNT Treatment.....	70



<b>Chapter 5: Discussion</b> .....	73
BVZ and SNT Mediated Hypertension.....	74
BVZ and SNT Mediated Cardiotoxicity: Echocardiography.....	78
BVZ and SNT Mediated Cardiotoxicity: Histology .....	81
Mechanisms of BVZ and SNT Mediated Cardiotoxicity .....	84
Limitations .....	89
Future Directions .....	90
Clinical Implications .....	91
<b>Chapter 6: Conclusion</b> .....	92
<b>Chapter 7: References</b> .....	93

## Table Synopsis

Table 1: Echocardiographic data from C57Bl/6 mice treated with 0.9% Saline or BVZ  
with or without prophylactic anti-hypertensive medications from baseline to week 4.  
..... 54

Table 2: Echocardiographic data from C57Bl/6 mice treated with 0.9% Saline or SNT  
with or without prophylactic anti-hypertensive medications from baseline to week 4.  
..... 59

## Figure Synopsis

Figure 1: Angiogenesis and BVZ anti-cancer mechanism. ....	9
Figure 2: Bevacizumab and Sunitinib mediated cardiotoxicity .....	13
Figure 3: Chemical structure of Sunitinib.....	23
Figure 4: Mechanism of action of SNT .....	25
Figure 5: Experimental Methodology.....	42
Figure 6: Mean arterial pressure changes in BVZ treated mice prophylactically receiving anti-hypertensive medications .....	50
Figure 7: Mean arterial pressure changes in SNT treated mice prophylactically receiving anti-hypertensive medications .....	52
Figure 8: Changes in LVEDD in BVZ treated mice prophylactically receiving anti-hypertensive medications.....	56
Figure 9: Changes in LVEF in BVZ treated mice prophylactically receiving anti-hypertensive medications.....	57
Figure 10: Changes in LVEDD in SNT treated mice prophylactically receiving anti-hypertensive medications.....	61
Figure 11: Changes in LVEF in SNT treated mice prophylactically receiving anti-hypertensive medications.....	62
Figure 12: Structural alterations of mitochondria in all BVZ and SNT treatment arms...	64
Figure 13: Cellular alterations in BVZ treated mice prophylactically receiving anti-hypertensive medications.....	65
Figure 14: Cellular alterations in SNT treated mice prophylactically receiving anti-hypertensive medications.....	66

Figure 15: Changes in cleaved PARP expression in BVZ treated mice prophylactically receiving anti-hypertensive medications .....	69
Figure 16: Changes in cleaved PARP expression in SNT treated mice prophylactically receiving anti-hypertensive medications .....	71
Figure 17: Changes in phosphorylated p38 expression in SNT treated mice prophylactically receiving anti-hypertensive medications .....	72

## List of Equations

Equation 1: Left Ventricular Ejection Fraction .....	44
Equation 2: Fractional Shortening .....	44

## List of abbreviations

A	Aliskiren
ACE	Angiotensin converting enzyme
AMPK	5' adenosine monophosphate-activated kinase
Ang-II	Angiotensin II
ANOVA	One-way analysis of variance
APC	Adenomatous polyposis coli
ARBs	Angiotensin receptor blockers
ASICS	Avastin and Sutent induced cardiotoxicity study
ASK1	Apoptosis signal-regulating kinase
AT <sub>1</sub>	Type I angiotensin receptors
ATE	Arterial thromboembolic events
Bcl-xL	B-cell lymphoma-extra large
BEV-CAPIRI	Bevacizumab, capecitabine and irinotecan
bFGF	Basic fibroblast growth factor
BHT	Butylated hydroxytoluene
BMI	Body mass index
BSA	Bovine serum albumin
BVZ	Bevacizumab
CHF	Congestive heart failure
CM	Chloroform:methanol
CM-PBS	Chloroform:methanol – phosphate buffered saline
CRC	Colorectal cancer
CSF-1R	Colony stimulating factor-1 receptor
CT	Computed tomography
CTRCD	Cancer therapeutics related cardiac dysfunction
CV	Cardiovascular
DOX	Doxorubicin (Adriamycin)
EDTA	Ethylenediaminetetraacetic acid
FAP	Familial adenomatous polyposis
FASN	Fatty acid synthase
FDA	Food and Drug Administration
FLT3	FMS-like tyrosine kinase-3
FOBT	Fecal occult blood test
FOLFIRI	Infusional 5-FU/leucovorin and irinotecan
FOLFOX	Infusional 5-FU/leucovorin and oxaliplatin
FS	Fractional shortening
5-FU	5-fluorouracil
G6-31	Phage-derived anti-murine VEGF-A monoclonal antibody
GLS	Global longitudinal strain
GSSG	Glutathione disulfide
H	Hydralazine
HER2/ErbB2	Human epidermal growth factor receptor 2
HIF- $\alpha$	Hypoxia-inducible factor $\alpha$
HLRCC	Hereditary leiomyomatosis and renal cell carcinoma

HF	Heart failure
HMG-CoA	3-hydroxy-3-methylglutaryl-coenzyme A
HNPCC	Hereditary nonpolyposis colorectal cancer
HPLC	High performance liquid chromatography
HR	Heart rate
IFL	Irinotecan, bolus fluorouracil, and leucovorin
IFN- $\alpha$	Interferon- $\alpha$
IL-2	Interleukin-2
i.p.	Intraperitoneally
i.v.	Intravenous
IVS	Interventricular septum
JNK	c-Jun N-terminal kinase
KIT	Stem-cell factor receptor
LDL	Low-density lipoprotein
LV	Left ventricular
LVEDD	Left ventricular end-diastolic diameter
LVEF	Left ventricular ejection fraction
LVESD	Left ventricular end-systolic diameter
MAP	Mean arterial pressure
MAPK	Mitogen-activated protein kinase
MF	Milk-derived fat
MRI	Magnetic resonance imaging
NACA	N-acetyl cysteine amide
NAD <sup>+</sup>	Nicotinamide adenine dinucleotide
NO	Nitric oxide
NRVMs	Neonatal rat ventricular myocytes
OS	Oxidative stress
OxPC	Oxidized phosphatidylcholine
P	Perindopril
PAR	Poly(ADP-ribose)
PARP	Poly (ADP-ribose) polymerase
PAZ	Pazopanib
PBS	Phosphate buffered saline
PDGF	Platelet-derived growth factor
PDGFR	Platelet-derived growth factor receptor
PLAX	Parasternal long axis
PLAS	Parasternal short axis
PVDF	Polyvinylidene fluoride
PWT	Posterior wall thickness
RAS	Renin-angiotensin system
RCC	Renal cell carcinoma
RIPA	Radioimmunoprecipitation
ROS	Reactive oxygen species
SD	Standard deviation
SDS	Sodium dodecyl sulfate
SDS-PAGE	Sodium dodecyl sulfate polyacrylamide gel electrophoresis

SEM	Standard error mean
SNT	Sunitinib
SR	Strain rate
TAC	Transverse aortic constriction
TBARS	Thiobarbituric acid reactive substance
TBST	Tris Buffered Saline with 0.1% Tween 20
TKR	Tyrosine kinase receptor
TRZ	Trastuzumab
TTE	Transthoracic echocardiography
TVI	Tissue velocity imaging
V	Valsartan
VEGF-A	Vascular endothelial growth factor A
VEGFR-2	Vascular endothelial growth factor receptor 2
V <sub>endo</sub>	Endocardial systolic velocity
VHL	von Hippel-Lindau



## **Chapter 1: Literature Review**

### **Cancer in Canada: Introduction**

Cancer is a major public health concern and the leading cause of death in Canada.<sup>1</sup> It accounts for 30.2% of all deaths in this population and surpasses the mortality due to cardiovascular disorders.<sup>1</sup> Approximately 1 in 2 Canadians will be affected by cancer in their lifetime, and 1 in 4 individuals will die of this disease.<sup>1</sup> Males are more likely to be afflicted with cancer than females,<sup>1</sup> and the majority of the individuals diagnosed with cancer are over the age of 50.<sup>1</sup> Approximately 24 Canadians received a cancer diagnosis each hour, contributing to 206,200 new cases reported in 2017.<sup>1</sup> Moreover, 9 individuals died from cancer each hour, accounting for 80,800 Canadians that year.<sup>1</sup> Although lung, breast, colorectal, and prostate are the most prevalent cancer types diagnosed,<sup>1</sup> bladder, melanoma, and kidney cancers are also common in this population.<sup>1</sup>

### **Cardio-Oncology**

Cardio-oncology is an evolving discipline that aims to sustain the cardiovascular health of patients receiving cancer therapy.<sup>2</sup> The need for this field emerged due to the increasing survivorship of cancer patients<sup>3-5</sup> and recognition that traditional and novel anti-cancer agents can adversely affect cardiac function.<sup>6-10</sup> The focus of cardio-oncology includes:<sup>11</sup> a) identification of cancer patients at the highest risk of cardiotoxicity;<sup>11</sup> b) detection and prevention of cardiovascular injury; c) cardiotoxicity treatment;<sup>11</sup> and d) development of a multidisciplinary approach in the management of cancer patients with cardiotoxicity.<sup>11</sup>

The meaning of cardiotoxicity differs among various professional societies.<sup>12</sup> It is defined by the National Cancer Institute as “toxicity that affects the heart”.<sup>12, 13</sup> The Cardiac Review and Evaluation Committee proposed drug-induced cardiotoxicity due to

anti-cancer drugs as follows:<sup>14, 15</sup> i) cardiomyopathy with evident reduction in left ventricular ejection fraction (LVEF); ii) symptoms associated with congestive heart failure (CHF); iii) signs of CHF such as tachycardia; and iv) decrease in LVEF from baseline with values  $\geq 5\%$  to  $< 55\%$  with accompanying signs or symptoms of heart failure (HF), or asymptomatic decrease in LVEF ranging from  $\geq 10\%$  to  $< 55\%$ , without accompanying signs or symptoms of HF.<sup>14, 15</sup> However, the American Society of Echocardiography and European Association of Cardiovascular Imaging recently identified cancer therapeutics related cardiac dysfunction (CTRCD) as a reduction in LVEF of  $> 10\%$  to a value  $< 53\%$  that requires a subsequent confirmation by imaging within 2 to 3 weeks.<sup>12, 16</sup>

Two types of CTRCD have been reported in the literature.<sup>7, 12, 16, 17</sup> Type I CTRCD is considered to be irreversible and is associated with the use of anthracycline antibiotics, particularly doxorubicin (DOX).<sup>12, 16, 17</sup> This chemotherapeutic agent, which treats breast cancer, lymphoma, and leukemia, causes permanent damage to cardiomyocytes.<sup>7, 16, 17</sup> The mechanism of DOX associated cardiac toxicity involves inhibition of type II topoisomerase leading to mitochondrial dysfunction, increase in oxidative stress, myofibril disarray, and cellular death.<sup>7, 12, 18-20</sup> The most common cardiovascular side effects observed with anthracyclines include dilated cardiomyopathy, arrhythmia, acute myocarditis and/or pericarditis.<sup>20</sup> Type I CTRCD is also found to be dose dependent.<sup>7, 16</sup> Patients who receive the cumulative DOX dose of  $400 \text{ mg/m}^2$  have up to 5% risk of developing HF, whereas exposure to  $700 \text{ mg/m}^2$  elevates this risk to an approximate 48%.<sup>9, 21-23</sup>

Type II CTRCD is reversible and is not dependent on the administered chemotherapeutic dose.<sup>7, 12, 17</sup> There are no structural abnormalities observed in the

myocardium with this form of CTRCD.<sup>12, 7, 24, 25, 26</sup> Type II dysfunction is commonly associated with the use of a humanized monoclonal antibody trastuzumab (TRZ),<sup>12,7,27</sup> an agent that targets breast and gastric cancer cells overexpressing the human epidermal growth factor receptor 2 (HER2/ErbB2).<sup>7,27,28</sup> Common cardiovascular toxicities of TRZ include supraventricular tachycardia, cardiomyopathy, decrease in LVEF, and/or CHF.<sup>20, 29</sup> Other novel targeted agents that can lead to type II CTRCD include lapatinib, imatinib, sorafenib, pertuzumab, bortezomib, bevacizumab, and sunitinib.<sup>7,25, 29</sup>

During the initial visit at a cardio-oncology clinic, assessing patients at high risk for cardiotoxicity is based on the following factors:<sup>2,12,7,25, 30</sup> a) patient's characteristics – age, established cardiovascular (CV) disease, existing CV risk factors, metabolic malfunctions, hypersensitivity to the drugs, prior chemotherapy, and radiation exposures;<sup>2,11,12,7, 31</sup> b) cancer-related factors include anatomic location, type, and stage of cancer;<sup>12</sup> and c) cancer therapy factors including specific drug(s) used, the dosage, frequency and route of administration as well as sequence and timing between the drugs.<sup>2, 7, 12, 25, 30, 31</sup> Cardio-oncology team members including cardiologists, medical oncologists, nurse practitioners, nurses, dietitians, pharmacists, and social workers, meet with cancer patients to evaluate their global health needs.<sup>2, 32</sup> A collaborative approach among team members is used to create the most effective treatment strategy for patients at high risk of cardiotoxicity.<sup>2,32</sup> In this cancer population, the goal of cardio-oncology interventions is to optimize cardiac health of patients enabling them to complete the proposed cancer treatment.<sup>2,11,32</sup>

## **Colorectal Cancer: Prevalence, Risk Factors, Diagnosis, and Treatment**

Colorectal cancer (CRC) is the third most common cancer type and the fourth leading cause of death from cancer in the world.<sup>33-35</sup> Nearly 1.2 million people are affected by this cancer every year, and 608,000 individuals die from it.<sup>33-35</sup> The majority of CRC cases occur in the developed countries,<sup>34-36</sup> where the incidence of colon cancer is 2 times higher than that of rectal cancer.<sup>37</sup> In Canada, CRC is the second most commonly diagnosed cancer, and it is more prevalent in men than women.<sup>1</sup> The lifetime probabilities of developing CRC in men and women are 7.4% and 6.4%, respectively.<sup>1</sup> In 2017, approximately 26,800 Canadians were diagnosed with CRC, and 9,400 died from the disease.<sup>1</sup> An estimated 870 new cases of CRC cancer were reported in Manitoba, with a 5-year age-standardized net survival of 60%.<sup>1</sup>

CRC is classified by origin into two forms.<sup>34</sup> Up to 94% of the diagnosed individuals have sporadic CRC.<sup>34,38-40</sup> Risk factors for developing CRC include increasing age, male sex, and previous history of CRC or polyps.<sup>33, 34, 39</sup> Environmental factors including sedentary lifestyle, obesity, diabetes mellitus, smoking, high alcohol consumption, and diet high in red meat increase the risk for CRC.<sup>33, 37,34, 39</sup> Moreover, duration of inflammatory bowel disease and resulting degree of colorectal inflammation elevate the risk for CRC.<sup>34,39</sup> The hereditary form accounts for 5-10% of CRC cases.<sup>34</sup> It is represented mainly by two syndromes, familial adenomatous polyposis (FAP) and hereditary nonpolyposis colorectal cancer (HNPCC).<sup>34,39,40</sup> FAP is a rare autosomal dominant disorder caused by the germline mutation in the adenomatous polyposis coli (*APC*) gene.<sup>34, 41</sup> This condition is characterized by the presence of hundreds to thousands of polyps that develop in childhood or adolescence.<sup>34, 41, 42</sup> HNPCC, also known as Lynch

syndrome, is an autosomal dominant condition with germline mutations in one of the mismatch repair genes (*MSH2*, *MLH1*, *MSH6*, *PMS2*).<sup>34, 39, 41</sup> The main feature of almost all colorectal tumours in patients with this syndrome is microsatellite instability.<sup>34,39,42</sup> Notably, other molecular mechanisms involved in the development of CRC are chromosome instability and aberrant DNA methylation.<sup>40, 43, 44</sup>

In the early stages of the disease, patients with CRC may not experience any symptoms.<sup>37</sup> The diagnosis is made when patients have persistent symptoms or as the result of CRC screening.<sup>37</sup> Signs and symptoms associated with this CRC include:<sup>37, 45</sup> a) abdominal pain; b) change in bowel habits ; c) rectal bleeding or blood in stool; d) nausea or vomiting; and/or e) presence of anemia.<sup>37, 45</sup> Surveillance for CRC is important in order to effectively diagnose and prevent this disease as well as to reduce mortality in this population.<sup>34,39,46</sup> The current screening modalities include the fecal occult blood test (FOBT), the Cologuard stool test, colonoscopy, flexible sigmoidoscopy, computed tomography (CT) colonography, and double-contrast barium enema.<sup>47-50</sup> In Canadians over 50 years of age with no family history of CRC, the national screening guidelines recommend FOBT to be performed every 2 years, followed by either flexible sigmoidoscopy or colonoscopy every 5 or 10 years, respectively.<sup>51</sup> Each of the screening procedures has different risks and benefits.<sup>34, 39, 48, 49</sup> By assessing the entire colon, polyps are removed,<sup>34, 49</sup> and tissue biopsy can be taken during colonoscopy.<sup>34</sup> Bleeding and bowel perforation are possible side effects.<sup>48, 49</sup> Moreover, this procedure is less effective in finding the ascending colon cancer.<sup>48</sup> On the other hand, FOBT and flexible sigmoidoscopy are less invasive and safe but might not be as efficacious as colonoscopy with regards to prevention of cancer.<sup>34,39,49</sup>

Treatment of CRC is multifactorial, including the combination of surgery, radiation, 5-fluorouracil (5-FU) based chemotherapy, and novel targeted agents.<sup>33, 34, 37, 39</sup> As the primary treatment strategy, the current surgical approach for patients includes either open or laparoscopic resection of CRC.<sup>33, 39</sup> Laparoscopic colectomy is the common procedure for colon cancer removal,<sup>34, 39</sup> whereas total mesorectal excision is performed in patients with rectal cancer.<sup>33, 34, 39</sup> In up to 30% of CRC patients, who have the metastatic (stage IV) form of the disease at diagnosis, surgical removal of hepatic, pulmonary or peritoneal metastasis is also necessary in order to both extend survival and improve quality of life.<sup>37, 52, 53</sup> Radiotherapy diminishes the risk of recurrence in patients with stage II and III CRC.<sup>34, 37</sup> However, no standardized guidelines exist for stage IV CRC, and radiation is used as the palliative approach to alleviate symptoms or delay tumour growth.<sup>34, 37</sup> A total of ten separate drugs have been currently approved for the treatment of metastatic CRC, and their use is determined on the patient's characteristics and tumour features.<sup>54</sup> FOLFOX (infusional 5-FU/leucovorin and oxaliplatin) and FOLFIRI (infusional 5-FU/leucovorin and irinotecan) are considered the standard first-line chemotherapy regimens for stage IV cancer.<sup>37, 55, 55, 54</sup> The addition of molecular targeted agent, including Bevacizumab, further improves response rates and prolongs overall survival of patients with metastatic CRC.<sup>34, 37, 56</sup>

### **Monoclonal Antibody: Bevacizumab**

An increased understanding of the molecular mechanisms of CRC has led to the development of the monoclonal antibody Bevacizumab (Avastin).<sup>57-61</sup> In 2004, the United States Food and Drug Administration (FDA) approved its use as the first-line treatment of metastatic CRC in combination with fluoropyrimidine based chemotherapeutic agents.<sup>39, 62, 63</sup> The clinical study by Hurwitz *et al.*<sup>56</sup> was the first to demonstrate that untreated

metastatic CRC patients who received irinotecan, bolus fluorouracil, and leucovorin (IFL) with bevacizumab (BVZ), had a median duration of overall survival of 20.3 months, as compared to 15.6 months in patients administered IFL with placebo ( $p < 0.001$ ).<sup>56</sup> These results demonstrated a 34% reduction in the risk of death in the BVZ treated group.<sup>56</sup> Moreover, the group receiving IFL with BVZ had an increased duration of progression free survival (10.6 months vs. 6.2 months;  $p < 0.001$ ).<sup>56</sup> The overall response rate was significantly higher in the group treated with IFL and BVZ as compared to the group administered IFL and placebo (44.8% vs. 34.8%;  $p = 0.004$ ).<sup>56</sup> The study by Degirmenci *et al.*<sup>64</sup> reported that the patients who received BVZ with capecitabine and irinotecan (BEV-CAPIRI) had mean progression free survival of 16.2 months and overall survival of 25.3 months, as compared to 10.2 months and 15.2 months, respectively, in patients given chemotherapy alone.<sup>64</sup>

The recommended dose of BVZ for the treatment of metastatic CRC is 5 mg/kg or 10 mg/kg once every 2 weeks when used together with 5-FU based chemotherapy.<sup>37, 58</sup> This antibody is administered as an intravenous infusion over 90 minutes during the initial visit.<sup>58, 63</sup> If this infusion is well tolerated, and no immune reaction occurs, the second infusion is administered over 60 minutes, and all subsequent infusions are administered over the period of 30 minutes.<sup>58, 63</sup> The elimination half-life of this targeted agent is relatively long, ranging from 12 to 22 days.<sup>58, 59, 63, 65</sup> BVZ related side effects include headache, fever, cardiovascular events, rash, proteinuria, diarrhea, and/or gastrointestinal perforation.<sup>58</sup> This monoclonal antibody is also used for the treatment of non-squamous non-small cell lung cancer, glioblastoma, metastatic renal cell carcinoma, cervical cancer as well as epithelial ovarian, fallopian tube, or primary peritoneal cancer.<sup>59, 65, 66</sup>

## **Bevacizumab: Anti-cancer Mechanism**

Angiogenesis is the process of forming new blood vessels.<sup>57, 67</sup> It is important in embryonic development, reproduction, and wound healing and is controlled by various pro- and anti-angiogenic factors.<sup>63, 67, 68</sup> Angiogenesis plays an essential role in growth, progression, and metastasis of tumour cells.<sup>59</sup> In order for the tumour to grow beyond 1-2 mm in size and obtain sufficient nutrients and oxygen, overexpression and secretion of pro-angiogenic factors are favoured.<sup>63, 67, 68</sup> Vascular endothelial growth factor (VEGF)-A is the key pro-angiogenic factor in tumour angiogenesis and is upregulated in a variety of cancer types, including CRC.<sup>57, 68-70</sup> High circulating levels of VEGF in CRC patients correlated with elevated risk of metastasis and poor prognosis.<sup>63, 68, 71</sup> Tumour cells increase levels of VEGF-A in response to hypoxia, hypoglycemia, oncogenes, and/or by inactivation of tumour suppressor genes.<sup>63, 67, 68, 72</sup>

VEGF-A is responsible for regulating vascular proliferation and permeability.<sup>67</sup> This factor has an anti-apoptotic function for endothelial cells in newly formed blood vessels.<sup>67, 73</sup> VEGF-A is a homodimeric glycoprotein that belongs to the family of growth factors that include VEGF-B, VEGF-C, VEGF-D, VEGF-E, and placental growth factor.<sup>67,68, 74</sup> VEGF-A is the most abundant form and has at least 7 different isoforms that range in molecular weight from 34 to 42 kDa.<sup>55,75</sup> VEGF-A signals mainly via VEGF receptor 2 (VEGFR-2),<sup>75</sup> which is highly expressed by endothelial cells involved in angiogenesis and by circulating bone-marrow derived endothelial progenitor cells.<sup>57, 72</sup> The binding of VEGF-A to VEGFR-2 results in proliferation of endothelial cells, vascular permeability, tumour growth, and protection against apoptosis (Figure 1).<sup>68,72</sup>



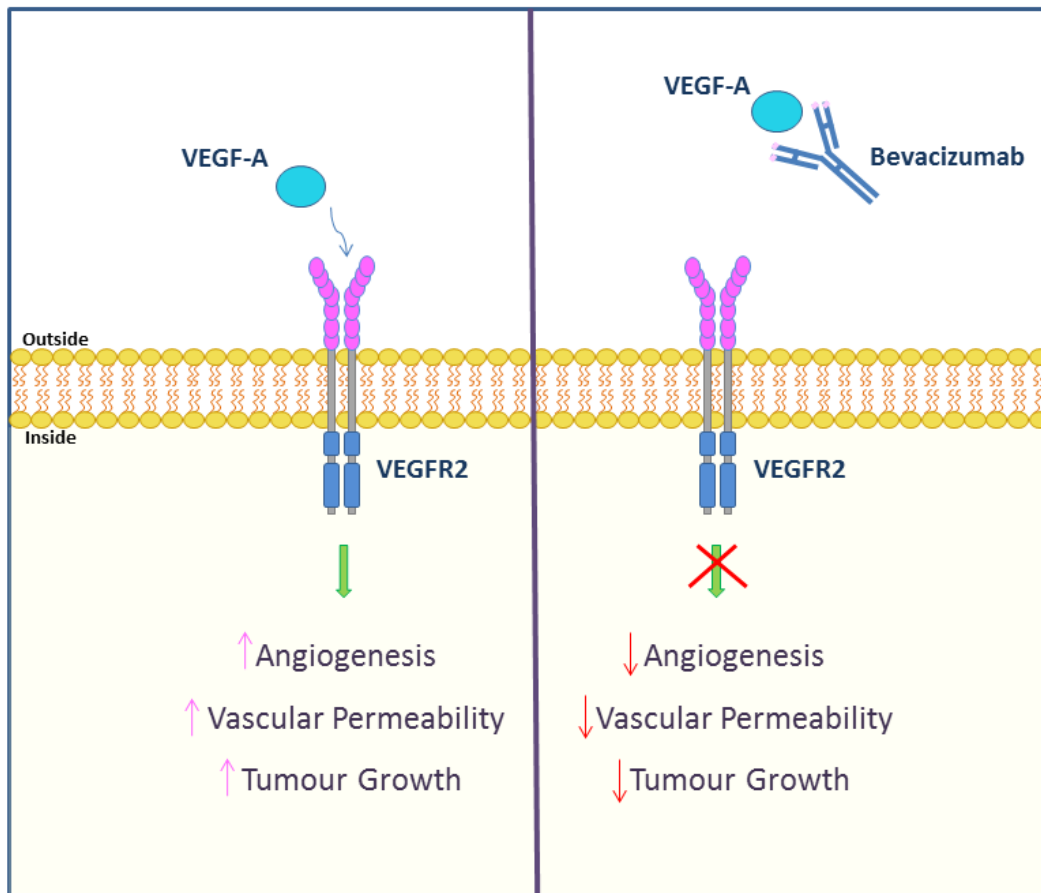


**Figure 1: Angiogenesis and BVZ anti-cancer mechanism.**

Tumour angiogenesis is a complex process involving the interaction between VEGF-A and VEGFR-2. The monoclonal antibody BVZ inhibits VEGF-A extracellularly, thereby decreasing vascular proliferation and tumour growth.<sup>59, 68, 71, 72, 76-78</sup>

VEGF receptor signaling stimulates the RAS pathway, thereby activating the RAF-MEK-ERK and the PI3K-Akt cascades.<sup>72, 74, 75, 79-82</sup> The latter leads to phosphorylation of endothelial nitric oxide synthase and subsequent nitric oxide (NO) formation.<sup>75, 83</sup>

The agent BVZ is a humanized recombinant monoclonal antibody that targets all isoforms of VEGF-A.<sup>59, 60</sup> The antibody's structure is 93% human, and the murine portion of 7% comprises complementarity-determining regions that bind this growth factor.<sup>59, 63</sup>

BVZ neutralizes soluble VEGF-A and, by steric hindrance, does not allow further receptor binding.<sup>58</sup> This inhibition reduces tumour proliferation and blood vessels development (Figure 1).<sup>59,84</sup>

Tumour angiogenesis is characterized by formation of vessels with structural and functional abnormalities, including irregular vascular network and hyperpermeability.<sup>59,63,68,85,86</sup> These blood vessels generally have increased diameter, length, density, and interstitial fluid pressure, altering the delivery of nutrients and therapeutic agents.<sup>63</sup> Inhibition of VEGF-A leads to more normalized tumour vasculature, decreased interstitial pressure, and restoration of normal blood supply.<sup>59, 87</sup> Normalization of vessels, hence, enhances the effectiveness of concomitantly administered chemotherapeutic drugs and increases vulnerability to radiation.<sup>68, 69, 84, 86</sup> A study by Willett *et al.*<sup>87</sup> demonstrated that a single intravenous infusion of BVZ at a dose of 5 mg/kg in patients with non-metastatic rectal cancer produced direct and rapid anti-vascular effects in tumours.<sup>87</sup> In particular, BVZ diminished tumour blood perfusion and volume, microvascular density, interstitial fluid pressure, and the amount of circulating endothelial and progenitor cells.<sup>68, 87</sup> This antibody also improved the fraction of vessels with pericyte coverage.<sup>87</sup>

### **Bevacizumab: Cardiovascular Toxicity**

Although BVZ decreases tumour growth, improves progression-free and overall survival, and increases response rates in patients with metastatic CRC,<sup>56,64,88,89, 90</sup> this anti-cancer therapy is associated with an increased risk of cardiovascular disease.<sup>63, 91-93</sup> The common cardiotoxic side effects observed include new or worsening hypertension, myocardial infarction, and/or thromboembolic events.<sup>62,63,68</sup> Moreover, BVZ may cause left ventricular (LV) systolic dysfunction and heart failure.<sup>29,91,94</sup> This drug mediated

cardiotoxicity is thought to occur via the following mechanisms:<sup>95-103</sup> i) decrease in NO production leading to vasoconstriction, increased peripheral vascular resistance, sodium retention, and, consequently, elevation in blood pressure; ii) microvascular rarefaction – decrease in the density of arterioles and capillaries; iii) elevated levels of pro-hypertensive factors, such as endothelin-1; and/or iv) activation of the renin-angiotensin system (RAS).<sup>95-103</sup>

A myriad of literature demonstrates that the RAS pathway is one of the critical regulators in the pathophysiology of BVZ mediated cardiac dysfunction.<sup>97,101, 104, 105</sup> The RAS involves the secretion of renin from the juxtaglomerular cells in the kidney. This protease enzyme cleaves angiotensinogen into angiotensin I, which is then converted to angiotensin II (Ang-II) by angiotensin converting enzyme (ACE) inhibitor.<sup>97, 106-108</sup> Ang-II subsequently activates type I angiotensin (AT<sub>1</sub>) receptors leading to vasoconstriction as well as increased sodium and water reabsorption, thereby elevating blood pressure.<sup>101,106-108</sup> Interestingly, mice possess two types of AT<sub>1</sub> receptors, including AT<sub>1a</sub> and AT<sub>1b</sub>.<sup>109</sup> Being the closest homologue to the human AT<sub>1</sub> receptor, the murine AT<sub>1a</sub> isoform is predominantly expressed in the key organ systems, including kidney, heart, and vasculature, and is responsible for blood pressure regulation and vasoconstriction.<sup>108-110</sup> Persistent activation of the RAS pathway, however, results in cardiac hypertrophy and heart failure.<sup>94,111</sup>

The potential mechanism for BVZ induced cardiotoxicity includes increased expression of Ang-II, leading to an increase in oxidative stress (OS) by enhancing reactive oxygen species (ROS) production and diminishing antioxidant reserve (Figure 2).<sup>112-119</sup> Ang-II induced OS leads to activation of members of the mitogen-activated protein kinase

(MAPK) family, including apoptosis signal-regulating kinase (ASK1), c-Jun N-terminal kinase (JNK) and p38.<sup>120-124</sup> Activated JNK and p38, which correlate with cardiomyocyte apoptosis and cardiac pathologies, increase expression of pro-apoptotic genes [Bax, Caspase-3, and poly (ADP-ribose) polymerase (PARP)] and decrease expression of anti-apoptotic genes [B-cell lymphoma-extra large (Bcl-xL)].<sup>121-123, 125-127</sup> This overall cascade leads to the induction of apoptosis and ultimately heart failure as shown in Figure 2.<sup>106, 116,</sup>

118-120, 127, 128,114,118

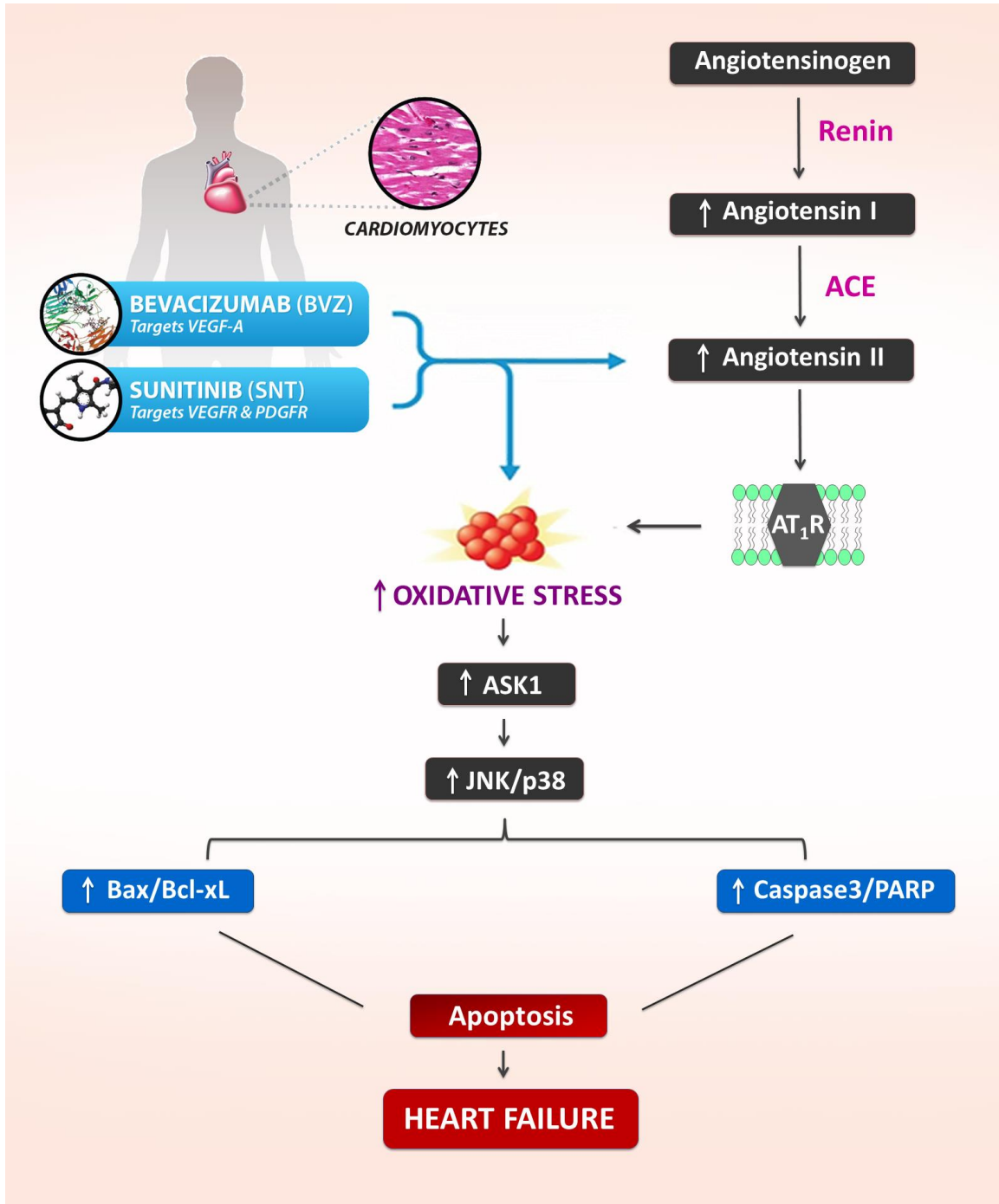


**Figure 2: Bevacizumab and Sunitinib mediated cardiotoxicity.**

In experimental models of cardiac injury due to BVZ or SNT, up-regulation of RAS results in an increase in oxidative stress, leading to downstream activation of the ASK1/MAPK pathway, and finally increased cardiac apoptosis and heart failure.<sup>116, 117, 120-122, 127</sup>

### **i) Murine Model**

Various animal studies have reported the damaging cardiovascular side effects associated with the administration of BVZ.<sup>105, 113, 129</sup> A study by Belchik *et al.* evaluated wild-type C57Bl/6 mice that were treated with a phage-derived anti-murine VEGF-A monoclonal antibody (G6-31) once every 2 weeks (10 mg/kg intraperitoneally (i.p.)).<sup>105</sup> After 5 weeks of follow-up, mice treated with the antibody had increased plasma angiotensin II concentrations as compared to sham control mice.<sup>105</sup> Antibody treated animals developed systemic hypertension leading to concentric LV remodeling and diminished stroke volume.<sup>105</sup> Of note, contractile function of the left ventricle was not impaired in these mice.<sup>105</sup> Giordano *et al.* reported that VEGF-A plays an important role in the heart.<sup>130</sup> By selectively deleting this gene from cardiomyocytes, mice had thin-walled, dilated, and hypovascular hearts with evidence of contractile dysfunction.<sup>130</sup>

Chen *et al.* studied the orthotopic mouse tumour models of human colorectal and breast cancers.<sup>129</sup> Once these tumors were established in mice, they were treated with BVZ at 10 mg/kg biweekly through tail vein injection. Moreover, BVZ treated mice were administered 15 mg/kg of 5-FU once per week (i.p.).<sup>129</sup> The results of this study showed that treatment with BVZ and 5-FU resulted in severe left ventricular systolic dysfunction, elevated troponin I serum levels, and increased cardiac fibrosis.<sup>129</sup>

Serial assessment of LVEF using echocardiography is an important diagnostic tool to monitor cardiac function during anti-cancer drug administration.<sup>131-133</sup> A reduction in LVEF signifies that irreversible cardiac injury may have already occurred.<sup>113, 132, 134</sup> In fact, this method is unable to detect early changes in LV systolic function and is highly dependent on the underlying hemodynamic state.<sup>131, 135</sup> Novel echocardiographic indices, including tissue velocity and strain imaging, are more sensitive in predicting early LV

function.<sup>131, 134-137</sup> By evaluating one point in the myocardium relative to the transducer, tissue velocity imaging measures endocardial systolic velocity ( $V_{\text{endo}}$ ).<sup>133</sup> In a murine model,  $V_{\text{endo}}$  is measured in cm/s, and value below 2 cm/s suggests the presence of early subtle myocardial dysfunction.<sup>134,131</sup> Strain imaging assesses two points in the myocardium relative to each other and calculates strain rate (SR), which is the rate of tissue deformation.<sup>133, 138</sup> SR is reported as seconds<sup>-1</sup>, and its decline below 20 s<sup>-1</sup> attribute to the abnormalities in cardiac function in an animal model.<sup>132-134, 138</sup> Various basic science and clinical studies have established the role of tissue velocity and strain imaging in the early detection of cardiac dysfunction due to DOX and TRZ in the breast cancer setting.<sup>131, 132, 134,135,138</sup>

Recently, our group evaluated whether these novel echocardiographic parameters can detect early evidence of BVZ mediated cardiotoxicity in an acute murine model.<sup>113</sup> Mice treated with BVZ (10 mg/kg) developed systemic hypertension as early as day 7, which continued to increase by day 14 of the study.<sup>113</sup> Although conventional LVEF values decreased at day 13 in mice administered BVZ,  $V_{\text{endo}}$  and SR started to significantly decline at day 8, confirming early evidence of subclinical LV systolic dysfunction.<sup>113</sup> Histological analysis demonstrated an increased loss of cell integrity and dilatation of smooth endoplasmic reticulum in BVZ treated animals.<sup>113</sup> Moreover, these animals had increased levels of oxidized phosphatidylcholine (OxPC), a marker of OS, and an elevated expression of Caspase-3 at day 14.<sup>113</sup> Therefore, early evidence of BVZ mediated cardiac damage was confirmed in this acute animal model.<sup>113</sup>

## ii) Clinical Setting

Treatment with BVZ has been associated with the development of various cardiovascular complications.<sup>63, 91, 93, 94</sup> Hypertension is the most common adverse event seen in BVZ treated patients with an overall incidence rate of up to 35%.<sup>29,94,93</sup> Approximately 9-15% of patients developed severe hypertension (grade 3 and 4) in phase 2 trials.<sup>94</sup> The grading system of the Common Terminology Criteria for Adverse Events defines grade 3 hypertension as the state that requires more than one drug or more intensive therapy management than used previously.<sup>139</sup> Grade 4 hypertension is described when a patient develops a hypertensive crisis.<sup>139</sup> In the recently described phase 3 trial by Hurwitz *et al.*, the prevalence of grade 3 hypertension was 11%.<sup>56</sup> Hypertension due to BVZ administration can develop at any time during treatment and may be dose related.<sup>63,94</sup> In particular, low doses (5 mg/kg every 2 weeks) of this targeted agent increases the risk of developing hypertension by 3 times, whereas high doses (10 mg/kg every 2 weeks) increase this risk by 7.5 times.<sup>94,90</sup> The presence of hypertension is an indication that the monoclonal antibody against VEGF-A is effective in treating metastatic CRC.<sup>95, 98, 112</sup> Antihypertensive medications should be initiated in this situation, and blood pressure should be monitored weekly for the duration of the first cycle of cancer treatment and then every 2 – 3 weeks during the cancer therapy.<sup>11</sup> If patients do not develop hypertension, the treatment strategy for cancer should be altered.<sup>91,98,95</sup>

The risk of stroke, myocardial infarction, coronary artery disease, and death due to cardiac causes is twice as high in patients who are treated with BVZ.<sup>140</sup> A systematic review reported the incidence of developing high-grade CHF of 0.9% in BVZ treated patients.<sup>141</sup> Administration of higher doses (5.0 mg/kg per week) of this monoclonal antibody was associated with a greater risk of severe CHF as compared to lower doses (2.5



mg/kg per week).<sup>141</sup> The incidence of developing LV systolic dysfunction and heart failure ranges from 1.7% to 3%.<sup>93,142</sup> A retrospective study by our group assessed the prevalence of BVZ induced cardiac dysfunction in patients with CRC at CancerCare Manitoba from 2010 to 2011.<sup>143</sup> We identified that 25% of this patient population (19/76) developed LV systolic dysfunction as measured by a LVEF value of less than 40%.<sup>143</sup>

Arterial thromboembolic events (ATEs), including arterial thrombosis, angina, myocardial or cerebral ischemia/infarct, are also prevalent among patients taking BVZ.<sup>94</sup> The overall incidence of high-grade myocardial ischemia was 1.5% in 2,322 patients treated with BVZ.<sup>144</sup> Scappaticci *et al.* performed a pooled analysis of 5 randomized controlled studies and evaluated 1,745 BVZ treated patients with metastatic colorectal, breast, or non-small cell lung cancer.<sup>145</sup> They reported an overall incidence of ATEs of about 4%, whereas the incidence of angina/MI was found to be 1.5%.<sup>145</sup> Patients treated with this monoclonal antibody can develop ATEs at any time during the therapy; however, the median time to the first event is approximately 3 months.<sup>145</sup> Moreover, researchers have identified that the risk factors for ATEs include previous history of these events and individuals with age of 65 years or more.<sup>145</sup> Importantly, as the use of the novel targeted agent BVZ poses adverse effects on the cardiovascular system, the current care should focus on prevention of this drug mediated dysfunction in patients with CRC.

## **Renal Cell Carcinoma: Prevalence, Risk Factors, Diagnosis, and Treatment**

Renal cell carcinoma (RCC) is a major health concern as it is the 14<sup>th</sup> most common cancer type in the world.<sup>146, 147,148</sup> Nearly 295,000 people are affected by this cancer every year, and 134,000 individuals die from it.<sup>149</sup> Individuals who reside in developed countries are more than 4 times as likely to acquire RCC than those living in developing countries.<sup>110</sup> In Canada, RCC is the tenth most commonly diagnosed cancer and is more prevalent in men than women.<sup>1</sup> The lifetime probabilities of developing RCC are 1.8% in men and 1.1% in women.<sup>1</sup> In 2017, approximately 6,600 Canadians were diagnosed with RCC and 1,900 died from the disease.<sup>1</sup> Moreover, the 5-year age-standardized net survival constitutes 67% for both sexes in the country.<sup>1</sup> In Manitoba, RCC is the sixth and the ninth most detected cancer in males and females, respectively, representing a total of 235 estimated new cases.<sup>1</sup>

RCC originates in the convoluted tubule within the kidney<sup>147</sup> and is classified into 3 histologic types.<sup>146, 149-151</sup> The first type is clear cell carcinoma in up to 80% of all diagnosed RCC affecting the proximal convoluted tubule.<sup>147,152</sup> Under histologic examination, cells have clear cytoplasm due to buildup of cholesterol esters, glycogen, and phospholipids.<sup>111</sup> The development of clear cell carcinoma is primarily caused by sporadic loss, mutation or methylation of tumor suppressor gene named von Hippel-Lindau (*VHL*).<sup>147, 152, 153</sup> In addition, mutations in chromatin remodeling genes (*PBRM1*, *SETD2*, *BAP1*) and in mTOR pathway genes (*PIK3CA*, *PTEN*, and *MTOR*) have been identified with this cancer type.<sup>150, 152, 153</sup>

Papillary RCC is the second histologic type of RCC and is noted in up to 15% of RCC.<sup>150, 151</sup> It also affects proximal convoluted tubule<sup>152</sup> and is commonly observed in patients with kidney transplant.<sup>147</sup> Papillary RCC is further subdivided into 2 types.<sup>150</sup>

Type I tumours have a single or double layer of small cuboidal cells with scanty basophilic cytoplasm.<sup>154,155,156</sup> Type II papillary tumour cells are larger with eosinophilic cytoplasm and are arranged in an irregular manner.<sup>154,155</sup> Increased expression of VEGFR2 was identified in the epithelium of this tumour type.<sup>157</sup> Patients with type II papillary cancer had higher incidence of nodal and distant metastasis, necrosis, and poor outcome as compared to patients with type 1 tumour.<sup>157</sup>

The third type, chromophobe RCC, is found in approximately 5% of all RCC cases.<sup>147,150</sup> As this tumour does not typically metastasize, patients with this type of kidney cancer have the best prognosis.<sup>147</sup> As the majority of RCC have sporadic origin, hereditary form accounts for up to 8% of the diagnosed cases.<sup>151</sup> The most common hereditary syndromes include:<sup>150-152</sup> i) VHL syndrome: This autosomal dominant disease involves combinations of hemangioblastomas of central nervous system or retina, pheochromocytomas, RCC, endolymphatic sac tumour, papillary cystadenoma of the epididymis, neuroendocrine pancreatic tumours;<sup>151</sup> ii) Hereditary papillary RCC is an autosomal dominant condition characterized by mutations in the proto-oncogene *MET* and less aggressive type I papillary cancer;<sup>152,150,151</sup> iii) Hereditary leiomyomatosis and RCC (HLRCC) is an autosomal dominant disease that is associated with mutations in the Krebs' cycle gene *FH*.<sup>151</sup> This condition represents a more aggressive type II papillary cancer that metastasizes early in the disease onset.<sup>152,150,151</sup>

Risk factors associated with the development of RCC include hypertension, acquired cystic kidney disease, chronic kidney disease, dialysis, family history of kidney cancer, increasing age and cigarette smoking.<sup>146, 149, 158,159</sup> Although obesity places patients at a higher risk for developing RCC,<sup>160</sup> Albiges *et al.* discovered that patients with

metastatic RCC treated with targeted therapy had a greater median overall survival if they had higher body mass index (BMI) than patients with low BMI (25.6 vs. 17.1 months).<sup>160,161</sup> Expression of the fatty acid synthase (*FASN*) gene may be implicated with patient's survival.<sup>160, 161</sup> They demonstrated that *FASN* expression was downregulated in patients with a high BMI than in patients with normal BMI, and median overall survival was longer in patients with low *FASN* expression (36.8 vs. 15.0 months; p=0.002).<sup>161</sup>

In the early stages of the disease, patients with RCC do not demonstrate any symptoms or signs.<sup>162</sup> RCC is typically discovered in its advanced stage during diagnostic imaging for different medical conditions, and approximately 20% of patients present with metastatic RCC at the time of diagnosis.<sup>149, 163,162,164</sup> Imaging techniques, including chest x-ray, abdominal CT, and magnetic resonance imaging (MRI) are the complementary modalities used for the detection of RCC.<sup>149,165</sup> Staging of RCC includes tumour size, lymph node involvement, characterization of the contralateral kidney, and abdominal metastases.<sup>165</sup> Abdominal MRI may be used in the following situations:<sup>165</sup> a) if the patient has allergy to contrast; b) to evaluate renal mass during pregnancy; c) in the case of diminished kidney function; and d) in order to assess tumour involvement in the inferior vena cava.<sup>165</sup> Chest x-ray is usually performed to evaluate and confirm the presence of metastasis.<sup>165</sup> Symptoms that may be indicative of advanced disease include weight loss, coughing, bone pain, a lump in the abdomen, edema of lower extremities, and abnormal liver function.<sup>163, 165</sup> The most common laboratory parameters evaluated include complete blood count, creatinine, glomerular filtration rate, alanine transaminase, aspartate aminotransferase, alkaline phosphatase, corrected calcium levels.<sup>165</sup> Biopsy is a useful diagnostic tool for determining the histologic characterization of tumour.<sup>165</sup> As no national

screening guidelines exist for this patient population in Canada,<sup>166</sup> individuals at the high risk of developing RCC are encouraged to maintain healthy weight and blood pressure, reduce smoking, and perform regular physical examination by their physicians.<sup>149, 159</sup>

Treatment strategies for patients with RCC include surgical resection, radiotherapy, and systemic therapy.<sup>147</sup> Partial or radical nephrectomy is performed depending on the tumour location and its stage.<sup>149, 153, 167</sup> Other approaches that can be used to remove renal tumours less than 3 cm in diameter include radiofrequency ablation and cryotherapy.<sup>165,168</sup> These techniques are suitable for patients with high surgical risks and offer fewer complications; however, the recurrence rate of tumour cells may be higher compared to partial nephrectomy.<sup>149,153,165</sup> For patients with metastatic RCC, cytoreductive nephrectomy is recommended prior to initiation of systemic therapy.<sup>153,165</sup> This surgery involves the removal of primary gross tumour, thereby reducing the burden of tumour size and significantly improving overall survival and disease-free state.<sup>169, 170</sup> Radiation therapy may also be beneficial for patients with metastatic RCC, as it controls bleeding, reduces pain from the tumour, alleviates symptoms originating from metastases, and stabilizes brain metastases.<sup>171</sup> Non-targeted immunotherapies including interleukin-2 (IL-2) and interferon- $\alpha$  (IFN- $\alpha$ ) were the first systemic drugs approved for the management of metastatic RCC.<sup>147, 150,166</sup> However, due to many toxic side effects and low median overall survival of nearly 12 months, the use of these drugs is now limited.<sup>150, 166, 171</sup> With an increased understanding of pathophysiologic mechanisms of RCC development, the systemic therapy encompasses various targeted agents including pazopanib, sorafenib, axitinib, temsirolimus, everolimus, and sunitinib.<sup>147, 153,171,166</sup>

### **Tyrosine Kinase Inhibitor: Sunitinib**

Sunitinib (Sutent; SNT), an oral small molecule tyrosine kinase inhibitor and a structural analogue of indolin-2-one, was approved for the treatment of advanced RCC in 2006 (Figure 3).<sup>172, 173</sup> The clinical study by Motzer *et al.* was the first to demonstrate the superiority of SNT over IFN- $\alpha$  in patients with untreated metastatic RCC.<sup>164, 174</sup> In this trial, an improved response rate (47% vs. 12%;  $p < 0.001$ ) and progression-free survival (11 vs. 5 months;  $p < 0.001$ ) were reported in the SNT group than in the IFN- $\alpha$  group.<sup>174</sup> Moreover, patients treated with SNT had median overall survival of 26.4 months as compared to 21.8 months in patients receiving IFN- $\alpha$  ( $p = 0.051$ ).<sup>174</sup>

SNT is distributed as the malate salt or sunitinib malate.<sup>175, 176</sup> The recommended dosage for metastatic RCC patients is 50 mg/day for the duration of 4 weeks followed by a 2 week period without this medication.<sup>173, 177</sup> The dosage and schedule of SNT can be optimized according to patient's health condition in order to obtain the most benefit from the treatment.<sup>164, 171, 174, 177, 178</sup> SNT is metabolized into its active N-desethyl metabolite SU12662 primarily by the cytochrome P450 enzyme in the liver.<sup>177, 179, 180</sup> The half-lives of SNT and SU12662 are 40-60 hours and 80-110 hours, respectively.<sup>175, 180</sup> The total oral clearance of SNT is 34-62 liters/hour. The primary route of elimination of this targeted drug is via feces.<sup>177, 180</sup> Patient's age, sex, body weight, and the type of tumour do not affect the pharmacokinetic profile of SNT.<sup>177</sup>

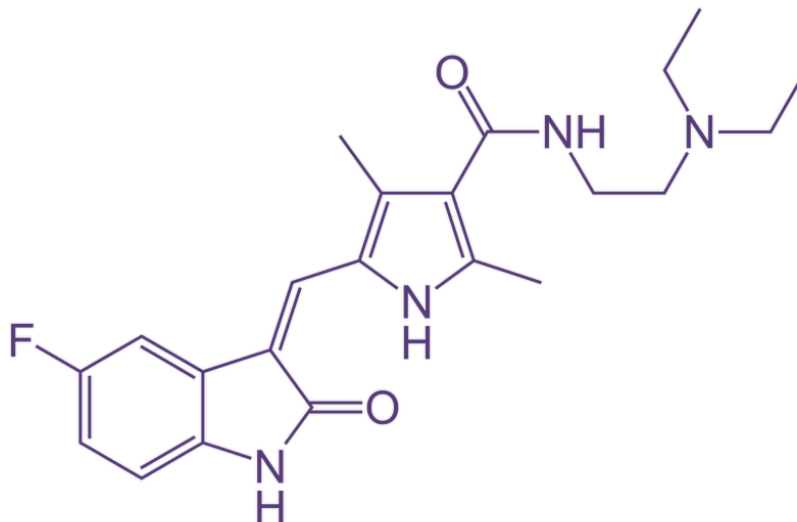


**Figure 3: Chemical structure of Sunitinib.**

Sunitinib is a butanedioic acid, hydroxyl-, (2S)-, compound with N-[2-(diethylamino)ethyl]-5-[(Z)-(5-fluoro-2-oxo-1H-indol-3-ylidene)methyl]-2,4-dimethyl-1H-pyrrole-3-carboxamide.<sup>175</sup>

SNT related side effects include fatigue, hypothyroidism, nausea, diarrhea, skin discoloration, and cardiovascular events.<sup>172</sup> This novel targeted agent has also been approved for the treatment of gastrointestinal stromal and metastatic pancreatic neuroendocrine tumours.<sup>175</sup>

### **Sunitinib: Anti-cancer Mechanism**

The development of RCC in the majority of patients occurs sporadically, mainly due to inactivation of the *VHL* tumor suppressor gene.<sup>180, 181</sup> VHL regulates the response of tissues to a low oxygen environment.<sup>181</sup> This protein adds ubiquitin to hypoxia-inducible factor  $\alpha$  (HIF- $\alpha$ ), thereby targeting it for proteasome degradation and halting the downstream signaling.<sup>182,166,181</sup> A mutation in VHL causes aberrant accumulation of HIF-

$\alpha$ , leading to overexpression of VEGF, platelet-derived growth factors (PDGF), and transforming growth factor (TGF) alpha and beta.<sup>150, 166, 182-184</sup> Overexpression of tyrosine kinase and serine/threonine receptors may promote tumour angiogenesis, proliferation, and metastasis.<sup>164, 177</sup>

Tyrosine kinase receptors (TKR) are transmembrane proteins that are located at the cell surface and transduce extracellular signals to the cell.<sup>172, 180</sup> The receptor monomer is composed of an extracellular ligand-binding domain, a transmembrane domain, as well as intracellular domain which possesses tyrosine kinase activity.<sup>172, 180</sup> The kinase domain contains ATP-binding cleft that has adenine, sugar, and phosphate-binding sites.<sup>180</sup> Ligand binding promotes receptor dimerization and autophosphorylation of specific tyrosine residues of the intracellular domains.<sup>172</sup> Tyrosine kinase activation induces various signaling pathways that are important in cell proliferation, differentiation, migration, survival, and angiogenesis (RAF-MEK-ERK, PI3K-Akt-mTOR, Src).<sup>180, 185, 172, 186</sup> VEGFR signaling plays an important role in angiogenesis and vascular permeability, as do PDGF-A, PDGF-B, PDGF-C, and PDGF-D that bind to PDGF receptors (PDGFR- $\alpha$  and PDGFR- $\beta$ ).<sup>172</sup> PDGFR signaling is essential in pericyte recruitment, vascular maturation, and stability.<sup>180</sup> Approximately 30% of TKR including stem-cell factor receptor (KIT) and FMS-like tyrosine kinase-3 (FLT3) are found mutated or overexpressed in different cancer types.<sup>185,187</sup> Moreover, PDGRF, basic fibroblast growth factor (bFGF) and its receptor are also expressed in a variety of tumours.<sup>172</sup>

SNT is a tyrosine kinase inhibitor that targets various TKR including: i) VEGFR 1-3; ii) PDGFR- $\alpha$  and PDGFR- $\beta$ ; iii) FLT3; iv) KIT; v) colony stimulating factor-1 receptor (CSF-1R), vi) RET, and vii) bFGF (Figure 4).<sup>172, 180, 188, 187</sup> This novel inhibitor possesses



hydrophobic properties and competes with ATP by presenting up to three hydrogen bonds to the ATP-binding site of intracellular domain.<sup>180</sup> The ability of SNT to inhibit various tyrosine kinases downregulates tumour angiogenesis and vasculature and leads to an improved anti-tumour response.<sup>189</sup>

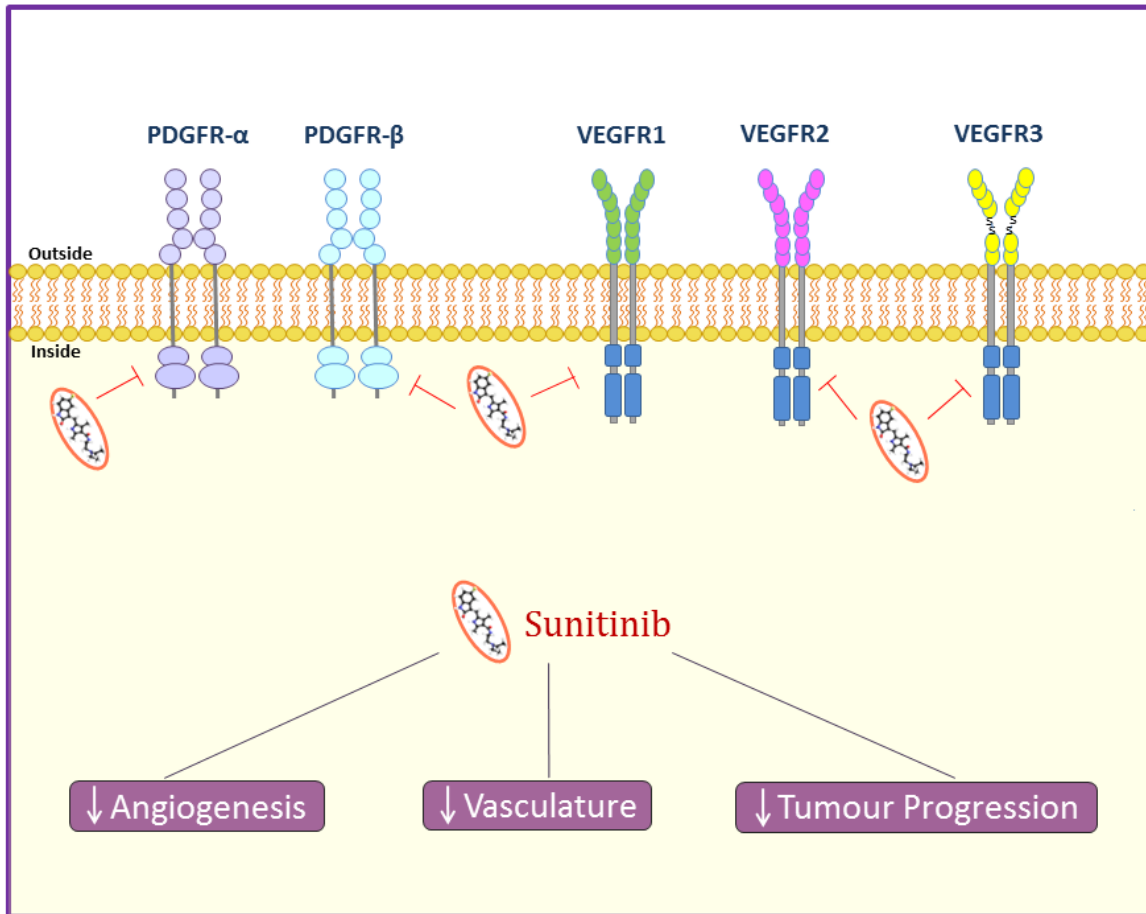


**Figure 4: Mechanism of action of SNT.**

The novel targeted agent Sunitinib exerts its action by inhibiting various tyrosine kinase receptors, thereby decreasing tumour proliferation, vascular permeability, and angiogenesis.<sup>76-78, 190, 191</sup>

## **Sunitinib: Cardiovascular Toxicity**

Although SNT diminishes tumour growth, improves progression-free and overall survival, and enhances response rates in metastatic RCC, this novel agent is associated with a number of cardiovascular side effects.<sup>91, 93, 139, 192</sup> The most common cardiotoxic side effects of SNT include hypertension, LV dysfunction, and/or heart failure.<sup>91, 176, 193, 194</sup> Bradycardia and QT prolongation are also rarely observed in SNT treated patients.<sup>91, 195, 196</sup> LV apical ballooning (Takotsubo) syndrome and reversible acute cardiomyopathy have also been noted in patients with RCC treated with SNT.<sup>197, 198</sup>

As the sites for ATP binding are highly conserved,<sup>180</sup> non-selective inhibitor SNT targets more than 50 kinases, thereby causing cardiac toxicity.<sup>188, 199, 200</sup> Moreover, this drug related cardiac damage is thought to occur via the following possible mechanisms: 1) decreased nitric oxide signaling; 2) increased endothelin-1 production; 3) capillary rarefaction; 4) inhibition of AMP-activated kinase; 5) mitochondrial damage; and/or 6) activation of RAS pathway.<sup>100, 139, 201-205</sup> However, a myriad of literature suggests that the RAS pathway is the main regulator of SNT mediated cardiotoxicity.<sup>97, 101, 104, 201</sup> The potential mechanism for the development of this cardiac damage involves upregulation of Ang-II, resulting in an increase in OS and subsequent activation the MAPK family of proteins, including ASK1, JNK and p38.<sup>112, 113, 115-124</sup> Activation of JNK and p38 enhances expression of pro-apoptotic proteins (Bax, Caspase-3, and PARP) and diminishes the expression of anti-apoptotic proteins (Bcl-xL).<sup>121, 125, 126, 204, 205</sup> This overall cascade leads to cardiomyocyte apoptosis and ultimately heart failure as denoted in Figure 2.<sup>106, 114, 116, 118-120, 127, 128</sup>

### **i) Murine Model**

Various animal studies have investigated the adverse cardiovascular side effects associated with the administration of SNT.<sup>113, 187</sup> Recently, our group evaluated whether novel echocardiographic parameters, including  $V_{\text{endo}}$  and SR, can detect early evidence of SNT mediated cardiotoxicity in a murine model.<sup>113</sup> Mice treated with SNT (40 mg/kg/day) developed systemic hypertension as early as day 7 which continued to increase throughout the duration of the study.<sup>113</sup> Although conventional LVEF values decreased at day 13 in mice administered SNT,  $V_{\text{endo}}$  and SR started to significantly decline at day 8, confirming early subclinical LV systolic dysfunction.<sup>113</sup> Electron microscopy demonstrated an increased loss and disruption of myofibrils in the animals treated with SNT. These mice had a significant increase in OxPC and elevated expression of Caspase-3 protein.<sup>113</sup>

In order to confirm that the RAS pathway and Ang-II induced OS play a primary role in the development of this cardiac dysfunction, we performed a pilot study using a transgenic mouse model homozygous for the disrupted angiotensin type 1 receptor gene (AT1<sub>a</sub>R-KO).<sup>206</sup> AT1<sub>a</sub>R-KO mice were administered either 0.9% saline or SNT (40 mg/kg/day) via oral gavage for a total of 14 days.<sup>113</sup> Our results demonstrated that in mice treated with SNT, LVEF did not change significantly from baseline to the study end-point (74±2% vs. 71±2%; p<0.05). There was no evidence of LV systolic dysfunction in these mice.

Chu *et al.* evaluated the effect of SNT in the *in vitro* setting.<sup>187</sup> Treatment of neonatal rat ventricular myocytes (NRVMs) with 1µM SNT resulted in increased release of cytochrome C from mitochondria after 30 and 48 hours.<sup>187</sup> These cardiomyocytes underwent apoptosis as evidenced by elevated caspase-9 activity and the number of

apoptotic cells.<sup>187</sup> In an *in vivo* animal model of wild-type Swiss-Webster mice, cardiomyocyte abnormalities, including swelling of mitochondria and disrupted cristae, were observed after 12 days of administration of SNT (40 mg/kg/day).<sup>187</sup> No significant changes in blood pressure were noted in these mice.<sup>187</sup> To investigate the effect of SNT and high blood pressure on heart function, mice were given regular chow or chow mixed with SNT (10 mg/kg/day) for 2 weeks.<sup>187</sup> For the duration of the second week, 0.9% saline or the  $\alpha$ -adrenergic drug phenylephrine (30 mg/kg/d) was co-administered.<sup>187</sup> The rise in systolic blood pressure was seen in mice receiving phenylephrine alone and SNT with phenylephrine.<sup>187</sup> However, treatment with SNT resulted in a 7-fold increase in apoptosis of cardiomyocytes.<sup>187</sup>

Inhibition of PDGF signalling may be another possible explanation for the cardiac damage noted in the animals treated with SNT.<sup>188, 207</sup> Transverse aortic constriction (TAC) in mice with cardiac-specific PDGFR- $\beta$  deletion resulted in dilated left ventricles, pulmonary edema, hypertrophy, secondary fibrosis, and clinical evidence of heart failure.<sup>207</sup> Expression of phosphorylated p38, ERK1/2, JNK, and AKT proteins were downregulated in these animals.<sup>207</sup> Interestingly, the number of apoptotic cardiomyocytes was significantly elevated compared to control animals, suggesting that PDGFR- $\beta$  signaling may be involved in activation of proteins that protect the heart in the setting of pressure overload.<sup>207</sup> The same research group has also evaluated the effect of TAC in mice treated with SNT (40 mg/kg/d) for 14 days.<sup>208</sup> Although mice did not develop pulmonary edema or cardiac hypertrophy in this pressure overload model, they had impaired cardiac function and increased fibrosis. The levels of PDGFR- $\beta$  protein were diminished in TAC mice receiving SNT.<sup>208</sup>

## ii) Clinical Setting

Treatment with SNT has been linked with the onset of a number of cardiovascular complications.<sup>93, 98, 139, 192</sup> Hypertension is the most frequent cardiac adverse event noted in SNT treated patients.<sup>139, 195, 209, 210</sup> Up to 53% of patients developed new or worsening hypertension in a variety of clinical studies.<sup>164, 187, 210, 211</sup> A retrospective trial evaluated patients with imatinib-resistant gastrointestinal stromal tumours receiving up to 4 cycles of SNT.<sup>187</sup> The development of hypertension (>150/100 mmHg) was noted in 47% of study participants.<sup>187, 193</sup> The incidence of grade 3 hypertension was observed by the third cycle of SNT treatment in 17% of patients.<sup>187</sup>

Azizi and colleagues reported on metastatic RCC patients who had unilateral nephrectomy, received 2 cycles of SNT, and monitored their home blood pressure.<sup>212</sup> By week 4, all normotensive patients were diagnosed with hypertension. In all hypertensive patients, blood pressure increased by the end of the first week of SNT treatment.<sup>212</sup> However, subsequent blood pressure values were similar to baseline, most likely due to the fact that hypertension was controlled with appropriate medications.<sup>212</sup> Development of new or worsening hypertension in metastatic RCC patients is associated with an improved response to SNT treatment, longer time to disease progression, and better overall survival.<sup>211</sup> The presence of hypertension may be a surrogate marker that the tyrosine kinase inhibitor SNT is effective in treating metastatic RCC.<sup>195, 211</sup>

LV systolic dysfunction and heart failure are common side effects due to SNT and have relatively high incidence among RCC patients.<sup>91, 213, 214</sup> Telli and colleagues discovered that 15% of patients treated with SNT developed symptomatic left ventricular dysfunction within 22 to 435 days of therapy.<sup>214</sup> These study participants presented with heart failure signs with LVEF values of less than 40%.<sup>214</sup> A review performed by Hall *et*

*al.* analysed 101 metastatic RCC patients treated with SNT and reported the incidence of heart failure and reduced LVEF to be 32% and 15%, respectively.<sup>210</sup> An international expanded-access trial, which evaluated 4543 metastatic RCC patients receiving SNT, stated that cardiac failure was present in 17 participants, including 3 who died from this therapy related side effect.<sup>215</sup> Less than 1% of patients treated with this targeted agent had congestive cardiac failure.<sup>215</sup> Chu and colleagues evaluated a cohort of patients with gastrointestinal tumours and found that 1% of patients receiving SNT had myocardial infarction and 8% developed CHF.<sup>187,193</sup> Approximately 19% of SNT treated participants had a decrease in LVEF values of more than 15%.<sup>187, 193</sup> Histological evaluation of biopsy tissues revealed the presence of cardiac hypertrophy and abnormal mitochondria in patients who developed SNT induced LV dysfunction and CHF.<sup>187,193</sup>

Our ongoing ‘Avastin and Sutent induced cardiotoxicity study’ (ASICS) is investigating whether novel echocardiographic parameters can detect the early evidence of CTRCD in CRC and RCC patients receiving BVZ, SNT, or pazopanib (PAZ).<sup>216</sup> PAZ is a tyrosine kinase inhibitor also used in the treatment of metastatic RCC.<sup>166, 171</sup> Cardiac dysfunction related to cancer drug administration was observed in 8% of the study population. These patients experienced a significant decrease in LVEF from 63% to 51% at 3 months of follow-up. Significant changes in systolic global longitudinal strain (GLS) were detected as early as 1 month after targeted therapy initiation. In this study, GLS decreased by 13% in one month and by 24% by the third month of treatment, thereby confirming early evidence of CTRCD.<sup>138, 217, 218</sup> Overall, in a population of CRC and RCC patients, GLS was able to detect early evidence of cardiotoxicity as compared to traditional LVEF values.<sup>219</sup>

## Prevention of Cardiotoxicity

Although novel echocardiographic techniques may allow for the early detection of LV systolic dysfunction in CRC and RCC patients,<sup>131, 133-135, 137</sup> the more important question is whether this cardiac injury can be prevented at the onset.<sup>220</sup> Protecting cardiovascular health during cancer therapy may be an effective approach to improve patients' quality of life and overall survival.<sup>104,30</sup> A key strategy for primary prevention may be to focus on treating patients who have the highest risk for developing LV dysfunction due to cancer therapy administration.<sup>17, 220, 221</sup> Individuals at increased risk are those with diabetes, CV disorder (hypertension, coronary artery disease), CV risk factors (smoking, obesity, alcohol use, sedentary lifestyle, diet), advanced age, exposures to radiation and cardiotoxins.<sup>11, 17, 221, 222</sup> Potential treatment interventions may involve adjustment of chemotherapy dosages, prescription of less cardiotoxic agents, and use of cardioprotective drugs.<sup>221,17</sup>

No established or consensus guidelines currently exist on the use of prophylactic therapies as primary prevention of chemotherapy mediated cardiotoxicity.<sup>3, 221,11,220</sup> In 2016, the Canadian Cardiovascular Society<sup>11</sup> suggested the following medications for patients at the high risk for cardiac complications due to anti-cancer therapy: i) ACE inhibitor; ii) angiotensin receptor blocker; iii)  $\beta$ -blocker; and/or iv) statin.<sup>11</sup> A number of clinical trials have focused their attention on prevention of cardiac damage in breast cancer, sarcoma, lymphoma, and leukemia patients treated with anthracyclines.<sup>11, 220</sup> Due to the small study size and variable results, limited evidence is currently available on the prophylactic use of various cardiac medications.<sup>220</sup> Hence, more studies are warranted to

explore the role of cardioprotective agents against chemotherapy related cardiotoxicity in a variety of cancer settings.<sup>11,220</sup>

Selection of particular prophylactic agent is determined by the underlying mechanisms of chemotherapy induced cardiac damage.<sup>5,223</sup> Some cardioprotective drugs may diminish oxidative stress, mitochondrial damage and/or apoptosis of cardiomyocytes, while others may decrease the workload on the heart.<sup>5,223</sup> In the setting of chemotherapy mediated cardiotoxicity, the cardioprotective role of statins, antioxidants,  $\beta$ -blockers and RAS antagonists have been investigated in a number of basic science and clinical studies.<sup>5, 21, 220, 224-229</sup>

### **i) Statins**

Statins are 3-hydroxy-3-methylglutaryl-coenzyme A (HMG-CoA) reductase inhibitors that decrease low-density lipoprotein (LDL) cholesterol by elevating LDL receptor synthesis.<sup>230, 231</sup> These drugs are used in the treatment of hyperlipidemia and for the primary and secondary prevention of myocardial infarction and stroke.<sup>232</sup> Statins possess antioxidative, anti-inflammatory, and immunomodulatory properties.<sup>21, 228, 233,234</sup> They have also had cardioprotective effects in the cancer setting.<sup>5, 224, 229, 235, 21</sup> In an *in vivo* model of DOX mediated cardiac dysfunction, 4 days of pre-treatment with fluvastatin resulted in improved systolic function.<sup>21, 228</sup> Moreover, an increased expression of the anti-oxidant superoxide dismutase 2 and attenuation in cardiac nitrotyrosine, apoptotic and inflammatory mediators were found in mice receiving fluvastatin.<sup>21, 228</sup> In another model, mice prophylactically treated with atorvastatin 1 hour before DOX administration demonstrated a decrease in oxidative stress and cellular damage within the myocardium.<sup>231</sup>



In the clinical setting, Chotenimitkhun *et al.*<sup>235</sup> demonstrated that treatment with statins prevented a decline in LVEF in patients receiving anthracycline-based chemotherapy.<sup>235</sup> Similarly, Acar and colleagues evaluated the cardioprotective role of atorvastatin in anthracycline mediated cardiomyopathy.<sup>236, 237</sup> In their study, one group of patients took daily prophylactic atorvastatin (40mg) prior to chemotherapy administration (1 per month), and another group received chemotherapy alone.<sup>236, 237</sup> In the statin treated group, LVEF values remained unchanged after 6 months while a significant decrease in LVEF was observed in the control group.<sup>236, 237</sup> Corroborating the echocardiographic findings, C-reactive protein levels were low in the statin treated group as compared to controls.<sup>236, 237</sup> In a separate observational study, Seicean *et al.*<sup>224</sup> followed patients for a mean duration of 2.4 years and found a lower incidence of heart failure and cardiac-related mortality in women with breast cancer who received statins during anthracycline based chemotherapy.<sup>224</sup>

## **ii) Antioxidants**

Anti-oxidants, including probucol and N-acetyl cysteine amide (NACA), have cardioprotective properties in preventing cardiac dysfunction due to chemotherapy.<sup>238, 239</sup> Probucol is a lipid-lowering agent known to decrease serum low- and high-density lipoprotein cholesterol,<sup>240,241</sup> and it has been used for the prevention and treatment of atherosclerotic CV disorders.<sup>241</sup> This drug also possesses potent anti-oxidative and anti-inflammatory properties.<sup>241, 242</sup> Probucol protected against doxorubicin (DOX) mediated cardiomyopathy and heart failure in rats by maintaining anti-oxidant reserve, decreasing cardiomyocyte apoptosis and preventing detrimental hemodynamic changes.<sup>243-245</sup> In a murine model of DOX and TRZ induced cardiac dysfunction, prophylactic treatment with Probucol lessened degeneration of myofibrils and decreased cardiac apoptosis.<sup>239</sup>

Although Probucol may be an effective prophylactic agent in *in vivo* settings of chemotherapy mediated cardiotoxicity,<sup>239</sup> its safety is yet to be investigated in clinical trials.

NACA is a novel thiol form of N-acetylcysteine that is able to pass through the cellular membrane.<sup>246,238</sup> This drug was found to have anti-oxidant and free radical scavenging properties, thus having the potential to treat diseases related to oxidative stress.<sup>246, 247,248</sup> The cardioprotective role of NACA has been investigated in embryonic rat cardiomyocytes treated with DOX.<sup>249</sup> In the *in vitro* setting, NACA attenuated oxidative stress by increasing activities of anti-oxidant enzymes and decreasing reactive oxygen species and lipid peroxidation.<sup>249</sup> However, NACA treatment did not prevent DOX mediated cell death.<sup>249</sup> This anti-oxidant drug was also shown to be partially cardioprotective in an acute model of DOX and TRZ induced cardiotoxicity.<sup>238</sup> In this study, mice received prophylactic administration of NACA with DOX and/or TRZ for 10 days.<sup>238</sup> In mice receiving both anti-cancer agents, NACA partially prevented adverse cardiovascular remodeling, cardiomyocyte damage, oxidative stress, and apoptosis.<sup>238</sup>

### **iii) $\beta$ -blockers**

$\beta$ -blockers inhibit  $\beta$ -adrenoreceptors and have mainly been used for the treatment of CV diseases including hypertension, LV systolic dysfunction, valvular heart disease, and arrhythmias.<sup>223, 232,250</sup> These drugs have potential anti-cancer, anti-oxidant, and anti-apoptotic properties.<sup>5,223,232,251,252</sup> A number of clinical trials have investigated whether these inhibitors can exert cardioprotective effects against chemotherapy induced cardiac dysfunction.<sup>252, 253</sup> In a small randomized, placebo-controlled study, anthracycline treated patients received prophylactic treatment with the  $\beta$ -blocker carvedilol (12.5 mg/day).<sup>252</sup>

After 6 months, carvedilol protected overall LV function and prevented anthracycline mediated cardiomyopathy.<sup>252</sup> In the OVERCOME trial, prophylactic treatment with both carvedilol and the ACE inhibitor enalapril prevented the development of LV systolic dysfunction in patients with hematological malignancies receiving chemotherapy.<sup>254</sup> The recent MANTICORE study investigated whether the  $\beta$ -blocker bisoprolol or ACE inhibitor perindopril would exert cardioprotective effects in breast cancer patients treated with TRZ.<sup>255</sup> After a mean follow-up of 350 days, bisoprolol attenuated the decrease in LVEF as compared to perindopril and placebo groups.<sup>255</sup> However, adverse LV remodeling associated with TRZ treatment was not prevented by either prophylactic agents.<sup>255</sup>

#### **iv) RAS Antagonists**

RAS antagonists comprise a group of blood pressure lowering medications that include direct renin inhibitor (Aliskiren), ACE inhibitors and angiotensin receptor blockers.<sup>107, 223, 237</sup> Aliskiren has beneficial effects on both the CV and renal systems.<sup>256,128</sup> ACE inhibitors decrease the risk of death, myocardial infarction, and stroke in high risk patients who do not have underlying structural heart disease.<sup>250,257,258</sup> In patients with heart failure, that may also be caused by chemotherapy, ACE inhibitors, including Perindopril, are recommended as Class I medications.<sup>250, 259</sup> Although ACE inhibitors should be administered after LV systolic dysfunction develops,<sup>104, 250, 260-262</sup> there is no consensus recommendation for its prophylactic use to prevent adverse cardiovascular remodelling.<sup>3, 11, 220, 221</sup> Angiotensin receptor blockers, including Valsartan, also decrease morbidity and mortality due to heart failure in a number of landmark clinical trials.<sup>263, 264</sup> RAS

antagonists may also exert anti-fibrotic, antioxidant, anti-inflammatory, and anti-apoptotic properties.<sup>128, 206, 257, 265-270</sup>

A few basic science and clinical trials have investigated the potential role of RAS antagonists in the prevention of cardiac dysfunction due to DOX and/or TRZ.<sup>238, 271, 272</sup> Akolkar and colleagues recently established a chronic murine model in which mice were treated with DOX, TRZ, or DOX+TRZ.<sup>272</sup> These animals were prophylactically given daily placebo, Aliskiren, Perindopril, or Valsartan for a total of 13 weeks.<sup>272</sup> At the end of the study, mice treated with DOX and DOX+TRZ had increased LV cavity dimension with reduced LV systolic function.<sup>272</sup> Administration of RAS antagonists partially attenuated cardiac damage by improving echocardiographic parameters and overall survival of the animals.<sup>272</sup> In a separate study, ACE inhibitors, including Captopril and Enalapril, prevented DOX induced cardiac damage in rats by maintaining the anti-oxidant reserve and respiratory efficiency of mitochondria and decreasing free radical formation.<sup>271,273</sup>

In the clinical setting, treatment with Enalapril was effective in protecting systolic and diastolic heart function in a cancer population receiving anthracycline based chemotherapy.<sup>226</sup> Similarly, the recent PRADA trial evaluated the use of an angiotensin receptor antagonist candesartan or  $\beta$ -blocker metoprolol in breast cancer patients assigned to anthracycline therapy with or without TRZ.<sup>227</sup> Although prophylactic treatment with candesartan prevented an overall decrease in LVEF, metoprolol did not exert any cardioprotective effects.<sup>227</sup> Despite these encouraging findings, no comprehensive studies to date have investigated the prophylactic role of RAS antagonists in the prevention of

BVZ and SNT mediated cardiotoxicity in the settings of CRC and RCC settings, respectively.

## **Chapter 2: Hypothesis, Objectives, and Study Rationale**

### **Hypothesis**

We hypothesize that the cardiotoxic side effects of either BVZ or SNT will be attenuated by the prophylactic use of RAS antagonists, by decreasing OS and expression levels of PARP, Caspase-3, Bax, and Bcl-xL, leading to decreased apoptosis and preservation of overall LV systolic function.

### **Objectives**

1) To evaluate whether early pharmacological inhibition of OS by RAS antagonists will attenuate the cardiotoxic side effects of BVZ or SNT in a chronic *in vivo* murine model;

2) To elucidate potential mechanisms for the cardioprotective effects of RAS antagonism.

### **Study Rationale**

Cancer treatment is multifaceted employing a combination of surgery, radiation, and chemotherapy. An increased understanding of the molecular mechanisms of cancer has led to the development of novel targeted agents, including BVZ and SNT, which are used in CRC and RCC, respectively.<sup>61, 172</sup> Despite the effectiveness of these anti-cancer drugs,<sup>56, 174</sup> an unanticipated side effect of their use is an increased risk of developing cardiotoxicity,<sup>93, 94, 100, 139</sup> highlighting the clinical significance of this serious complication.

Serial assessment of LVEF using echocardiography is an important noninvasive clinical diagnostic tool to monitor patients receiving anticancer therapy.<sup>131-133</sup> A reduction in LVEF signifies that irreversible cardiac injury may have already occurred.<sup>132, 134</sup> Although sensitive echocardiographic techniques including tissue velocity imaging (TVI)

and strain imaging may allow for the early detection of LV systolic dysfunction in cancer patients,<sup>131, 134-137</sup> the more important health concern is whether this injury can be prevented at the onset to improve patient outcomes.

Previous studies have demonstrated that BVZ and SNT mediated cardiotoxicity may be due to an increase in cardiac Ang-II levels with a concomitant upregulation of the RAS, resulting in increased OS, apoptosis, and ultimately heart failure.<sup>97, 104, 113, 119, 201</sup> Although heart failure drugs including RAS inhibitors are commonly used *after* cardiac dysfunction develops in the CRC and RCC settings,<sup>104</sup> their prophylactic role in the prevention of BVZ and SNT mediated cardiotoxicity has yet to be investigated.

## Chapter 3: Materials and Methods

### Animal Model

All animal procedures were conducted in accordance with guidelines of the Canadian Council on Animal Care. The Animal Protocol Review Committee at the University of Manitoba approved all procedures, including drug administration and longitudinal echocardiographic studies (REB: 15-009/1/2 (AC11024)).

A total of 194 wild-type C57Bl/6 male mice (8-12 weeks old; Jackson Laboratories, Bar Harbor, ME, US) were quarantined for 1 week prior to the initiation of the study. All animals were maintained on a 12-hour day/night cycle and received ad libitum access to regular chow and water during their stay in the animal holding facility. Following baseline transthoracic echocardiography (TTE), hemodynamics and weight analyses, all mice were randomly assigned to 3 regimens as indicated in Figure 5:

1. 0.9% Saline (weekly i.p. injections for 4 weeks, n=39);
2. BVZ (10 mg/kg, weekly intravenous (i.v.) tail vein injections for 4 weeks, n=78);<sup>113</sup>
3. SNT (40 mg/kg, daily oral gavage for 4 weeks, n=77).<sup>187</sup>

The doses of targeted therapies BVZ of 10 mg/kg and SNT of 40 mg/kg were sufficient to induce left ventricular systolic dysfunction in this murine model, as previously described by our group and others.<sup>113, 129, 187</sup>

Within each study arm, mice were further randomized to receive daily prophylactic treatment via oral gavage with one of the following agents:

- a) Water (0.1 mL/day);
- b) Hydralazine (0.05 mg/mL);<sup>274</sup>
- c) Aliskiren (50 mg/kg);<sup>275</sup>



- d) Perindopril (4 mg/kg);<sup>276</sup>
- e) Valsartan (2 mg/kg).<sup>206</sup>

Prophylactic treatment with water, Hydralazine, or one of RAS antagonists occurred on the same day, prior to Saline, BVZ, or SNT exposure, for a total of 28 days. The various dosages of Aliskiren, Perindopril, and Valsartan are the widely accepted concentrations to provide adequate inhibition of the RAS in a murine setting.<sup>206, 274-276</sup> These RAS antagonists have been selected due to their water solubility,<sup>206, 274-276</sup> thereby increasing their ease of administration. We hypothesize that the potential cardioprotective effects of Aliskiren, Perindopril, and Valsartan will be independent of their blood pressure lowering effects. Hence, Hydralazine was prophylactically added as potential positive control as it does not affect the RAS pathway.<sup>277</sup>

Body weight of all mice was measured every other day over the study period. Hemodynamic parameters and serial TTE were evaluated on a weekly basis for 4 weeks. All animals were then euthanized by i.p. injection of 150 mg/kg pentobarbital buffered with 2% lidocaine, and hearts were harvested from the thoracic cavity. Each heart was rinsed in 0.9% saline and preserved for further histological, oxolipidomic, and protein analyses.

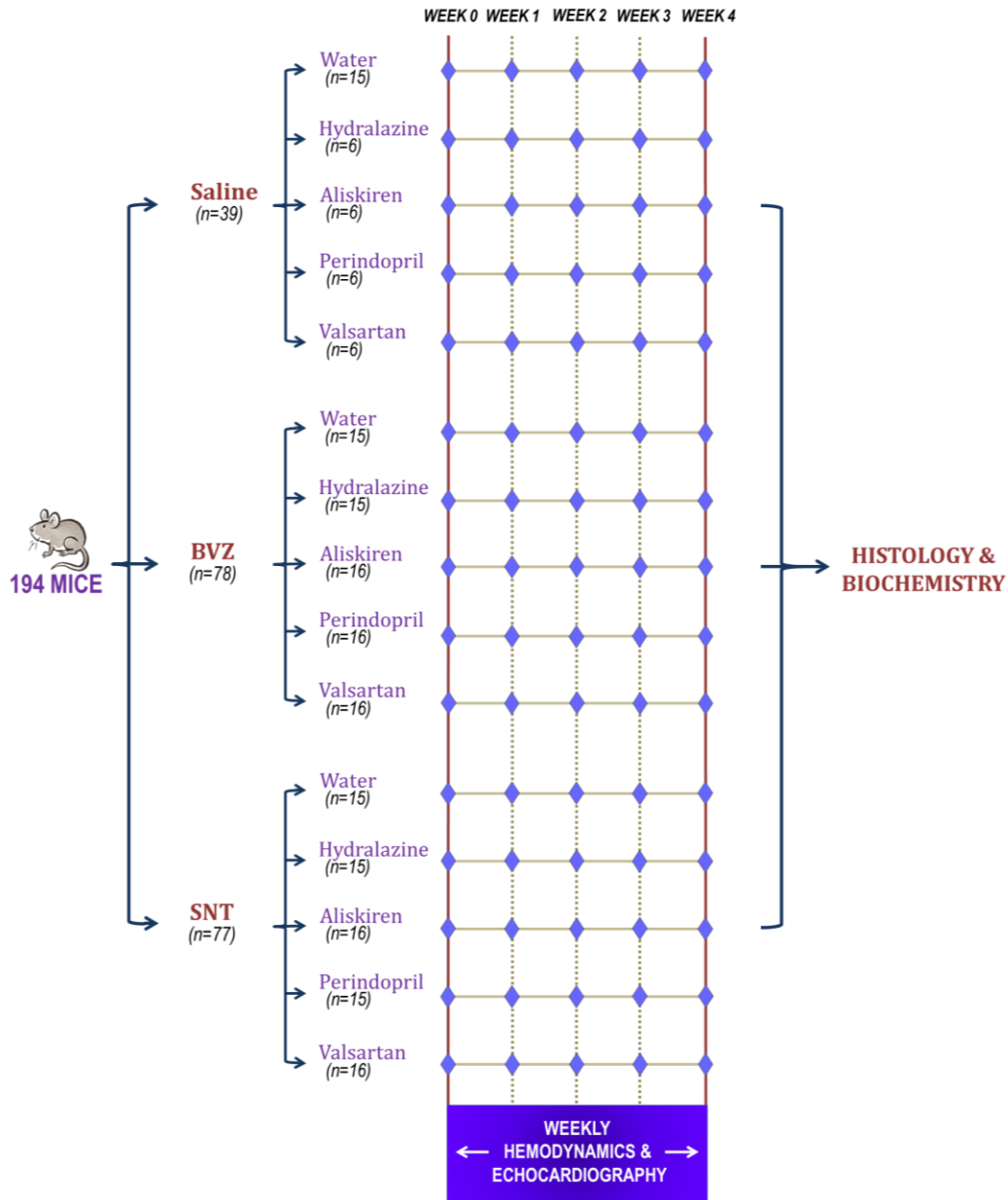


**Figure 5: Experimental Methodology.**

A total of 194 C57Bl/6 male mice were randomly assigned to either: i) 0.9% saline (i.p. weekly; n=39); ii) BVZ (10 mg/kg i.v. weekly for 4 weeks; n=78); or iii) SNT (40 mg/kg/day orally for 4 weeks; n=77). Within each arm, mice were further randomized to receive prophylactic treatment with either water (daily), Hydralazine (0.05 mg/ml/daily),<sup>274</sup> direct renin inhibitor (Aliskiren 50 mg/kg/daily),<sup>275</sup> ACEI (Perindopril 4 mg/kg/daily),<sup>276</sup> or ARB (Valsartan 2 mg/kg/daily)<sup>206</sup> via oral gavage for a total of 28 days. Mice underwent weekly hemodynamic and echocardiographic assessments at 5 time points. At the end of the study, cardiac tissues were collected for histological and biochemical analyses.

## **Hemodynamics**

Non-invasive heart rate and blood pressure measurements were evaluated in non-sedated, restrained mice using a tail-cuff method (CODA system, High Throughput, Kent Scientific, Torrington, CT), as previously reported.<sup>278, 279</sup> Briefly, the holding platform was heated to 30°C, and 9 consecutive blood pressure readings were recorded with 1 minute rest intervals between the readings. Blood pressure was measured at baseline and weekly for a total of 4 weeks, and the average values for mean arterial pressure were computed using 9 individual readings.

## **Murine Echocardiography**

Non-invasive murine TTE was performed in all the animals at baseline and weekly thereafter for the 4-week study. Awake mice underwent echocardiography using a 13-MHz linear array ultrasound probe (Vivid 7, version 11.2, GE Medical Systems, Milwaukee, WI, US). Parasternal long axis (PLAX) and short axis (PSAX) windows were evaluated in all mice as previously described.<sup>134, 239, 279</sup> Upon acquisition of PLAX images, endocardial borders of LV cavity were manually traced in order to determine LV end-diastolic and end-systolic volumes used in the calculation of LVEF (Equation 1). PSAX windows were recorded to derive the M-mode echocardiographic indices, including LV end-diastolic diameter (LVEDD), LV end-systolic diameter (LVESD), posterior wall thickness (PWT), and interventricular septal thickness (IVS). The EchoPAC PC software (Vivid 7, version 11.2, GE Medical Systems, Milwaukee, WI, US) was used for offline post-processing of all images and calculations of LVEF and fractional shortening (FS) (Equations 1 and 2). Echocardiographic data collection and analysis were conducted by observers blinded to the various treatment groups.

**Equation 1: Left Ventricular Ejection Fraction.**

$$LVEF = \frac{(LV \text{ end-diastolic volume} - LV \text{ end-systolic volume})}{LV \text{ end-diastolic volume}} \times 100\%$$

**Equation 2: Fractional Shortening.**

$$FS = \frac{(LVEDD - LVESD)}{LVEDD} \times 100\%$$

To assess the variability of LV cavity dimensions and function, a total of 30 mice were randomly chosen from the various treatment groups. A single observer (DSJ) performed independent measurements of LVEDD and LVEF on two separate days two weeks apart in order to evaluate intra-observer variability. Inter-observer variability was determined separately by two independent observers (VM and DSJ). Intra- and inter-observer variations were defined as the difference between the two observations divided by the means of the observations and expressed as absolute numbers.

**Histological Analysis**

In the preparation for electron microscopy, 3% glutaraldehyde in 0.1M phosphate buffer at pH 7.3 was used to fix the heart tissues for 3 hours at room temperature. They were then rinsed in 0.1M phosphate buffer containing 5% sucrose overnight at 4°C. Post fixation was then performed with 1% osmium tetroxide in 0.1M phosphate buffer for 2 hours at room temperature. Tissues were dehydrated in ascending ethanol concentrations and embedded in Epon 812 as previously described.<sup>280</sup> After the tissue sections were stained with uranyl acetate and lead citrate, they were viewed and photographed with the Philips CM12 electron microscope in order to determine the degree of cellular integrity. To avoid observer bias, grids were coded without prior knowledge of their source.

## Oxolipidomic Analysis

Collected heart tissues were stored in an Eppendorf tube containing a solution of phosphate buffered saline (PBS, pH 7.4) with ethylenediaminetetraacetic acid (EDTA). After gaseous nitrogen was infused into the tubes, they were flash frozen in liquid nitrogen and stored at -80°C. Extraction of phospholipids was performed by the previously described method with modifications.<sup>281</sup> Briefly, thawed heart tissues were placed into a cold mortar with the addition of liquid nitrogen, and ground into a fine powder. The powdered heart tissue was then transferred to a zeroed glass centrifuge tube to obtain tissue weight, followed by the addition of 6 mL ice-cold chloroform:methanol (2:1 CM, vol/vol) containing 0.01% butylated hydroxytoluene (BHT).<sup>282</sup> Once mixed, 100 µL of a global internal standard mixture was added to the tubes followed by 1.5 mL ice-cold PBS. The tubes were then vortexed 3 times and centrifuged (3500rpm) for 5 minutes at 4°C. The lower lipid phase was withdrawn and placed into a new glass tube while the remaining aqueous phase was mixed with 4.5 mL of ice-cold CM-PBS (86:14:1) and centrifuged for 5 minutes at 4°C. The lower lipid phase was transferred to the first organic phase, and evaporation of the combined organic phase solvents was performed using a nitrogen evaporator. Five hundred microliters of CM (2:1) was added to dissolve the lipid extracts. They were then transferred to autosampler vials, flushed with nitrogen and stored at -80°C.

For oxolipidomics analysis, the samples were reconstituted in mobile phase, solvent A (as described below).<sup>282</sup> Thirty microliters of each sample were injected onto an Ascentis Express C18 reversed-phase high performance liquid chromatography (HPLC) column (15 cm x 2.1 mm, 2.7 µm; Supelco Analytical, Bellefonte, Pennsylvania, USA) by means of a Prominence UFLC system (Shimadzu Corporation, Canby, Oregon, USA).<sup>282</sup>

Separation of analytes was performed by using a binary solvent system with solvent A (60:40 acetonitrile:water, vol/vol) and solvent B (90:10 isopropanol:water, vol/vol). Both solvent systems had 10 mM ammonium formate and 0.1% formic acid. The program for mobile phase composition was set at 0.01 min, 32% B; 1.50 min, 32% B; 4.00 min, 45% B; 5.00 min, 52% B; 8.00 min, 58% B; 11.00 min, 66% B; 14.00 min, 70% B; 18.00 min, 75% B; 21.00 min, 97% B; 25.00 min, 97% B; 25.10 min, 32% B; and 30.00 min, 32% B.<sup>282</sup> The elution was stopped at 30.10 min. The flow rate used for chromatographic separation was 260  $\mu$ L/min; moreover, the temperatures of the column and sample trays were maintained at 45 and 4°C, respectively.

The HPLC system was coupled to a 4000 QTRAP triple quadrupole mass spectrometer system with a Turbo V electrospray ion source (AB Sciex, Framingham, Massachusetts, USA). Chromatographic and mass spectral data were collected using Analyst Software 1.6 (AB Sciex). Analyses of the data were performed by MultiQuant Software 2.1 (AB Sciex).<sup>282</sup>

### **Western Blotting**

Frozen heart tissues were ground in the presence of liquid nitrogen into powder. Total protein was extracted from these tissues by homogenization in the radioimmunoprecipitation (RIPA) buffer composed of 50 mM Tris pH 7.4, 150 mM NaCl, 1 mM EDTA, 1 mM EGTA, 0.5% Na-deoxycholate, 1% Triton-X 100, and 0.1% sodium dodecyl sulfate (SDS). The RIPA buffer was supplemented with protease and phosphatase inhibitors (Thermo Scientific) prior to its use. After the samples were incubated on ice and centrifuged for 15 min at 14,000 rpm at 4°C, the supernatants were collected. Total protein concentration was measured by the Bradford assay using the Coomassie Blue Protein

Assay Reagent (ThermoScientific) and bovine serum albumin (BSA) standards (ThermoScientific). 30 µg of protein were separated by sodium dodecyl sulfate polyacrylamide gel electrophoresis (SDS-PAGE) at 55mA for 1.5 hours using the large gel system. Proteins were transferred to 0.2 µm pore size polyvinylidene fluoride (PVDF) membranes at 100V for 1 hour at 10°C. Membranes were blocked in 5% skim milk powder or BSA in 1x Tris Buffered Saline with 0.1% Tween 20 (TBST) for 1 hour at room temperature. Membranes were probed with primary antibodies specific to PARP, Caspase 3, Bax, Bcl-xL, p38, and GAPDH (Cell Signaling) overnight at 4°C. Horseradish peroxidase-conjugated goat anti-rabbit secondary antibody (BioRad) was then used to incubate the membranes. Protein bands were detected using Pierce ECL Western Blotting Substrate (ThermoScientific) on CL-Xposure blue X-ray film (ThermoScientific). Band intensities were quantified by densitometric analysis using QuantityOne software (BioRad) and normalized to GAPDH as the loading control.

### **Statistical Analysis**

All data are expressed as mean  $\pm$  standard deviation (SD). For Western analysis, the data are expressed as mean  $\pm$  standard error mean (SEM). For post hoc analysis, repeated measures of one-way analysis of variance (ANOVA) were used to evaluate for significance between independent factors. P values for main effects and interactions were noted when appropriate. For histological analysis, Mann-Whitney and Kruskal-Wallis tests were applied for non-parametric comparison of scores between each group. The scores ranged from 1 to 4, with 1 representing no tissue injury and 4 representing severe damage. Hemodynamic, echocardiographic, and biochemical analyses were performed by ANOVA with Dunnet's post-hoc analysis. Statistical significance for oxolipidomic analysis was

calculated by one-way ANOVA followed by a Tukey post hoc test. Results with  $p < 0.05$  were considered significant. The statistical software packages SPSS 15.0, SPSS version 24, and Graphpad Prism 5 were utilized to perform the statistical analyses.



## **Chapter 4: Results**

### **Hemodynamics: BVZ Treatment**

Compared to baseline, mean arterial blood pressure (MAP) of mice treated with saline remained unchanged at week 4 ( $119\pm 6$  mmHg vs.  $121\pm 5$  mmHg, respectively). Mice treated with BVZ only demonstrated a significant increase in MAP from  $120\pm 4$  mmHg to  $136\pm 4$  mmHg at week 4 (Figure 6). Addition of Hydralazine completely prevented the increase in MAP in BVZ treated mice, with a value of  $124\pm 3$  mmHg at the end of the study. Similarly, prophylactic treatment with Aliskiren, Perindopril, or Valsartan attenuated the onset of hypertension, with blood pressure values of  $124\pm 4$  mmHg,  $125\pm 5$  mmHg, or  $123\pm 6$  mmHg at week 4, respectively.

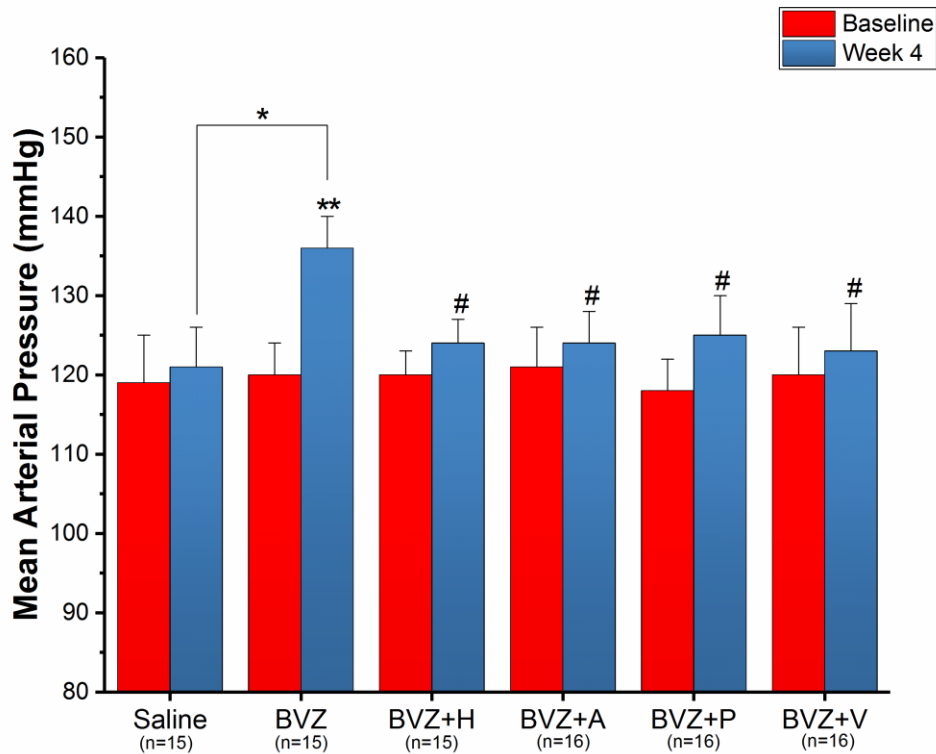


**Figure 6: Mean arterial pressure changes in BVZ treated mice prophylactically receiving anti-hypertensive medications.**

BVZ treatment induced significant increase in MAP at week 4, while prophylactic treatment with anti-hypertensive drugs completely attenuated the development of hypertension in these mice. The results are reported as mean  $\pm$  SD. \* $p < 0.05$  between BVZ at week 4 as compared to Saline. \*\* $p < 0.05$  between BVZ at week 4 as compared to BVZ baseline. # $p < 0.05$  as compared to BVZ at week 4. BVZ, Bevacizumab; MAP, mean arterial pressure; RAS, renin-angiotensin system; H, Hydralazine; A, Aliskiren; P, Perindopril; V, Valsartan.

### **Hemodynamics: SNT Treatment**

Compared to baseline, MAP of mice treated with saline remained unchanged at week 4 ( $121\pm 4$  mmHg vs.  $120\pm 5$  mmHg, respectively). Mice treated with SNT alone demonstrated a significant increase in MAP from  $120\pm 3$  mmHg to  $138\pm 3$  mmHg at week 4 (Figure 7). Conversely, the increase in MAP was attenuated with addition of Hydralazine as a blood pressure value of  $123\pm 3$  mmHg was reported in SNT treated mice at the end of the study. Similarly, prophylactic treatment with RAS antagonists completely prevented the development of hypertension. The MAP of mice receiving SNT and either Aliskiren, Perindopril, or Valsartan was  $124\pm 3$  mmHg,  $125\pm 4$  mmHg, or  $124\pm 5$  mmHg at week 4, respectively.

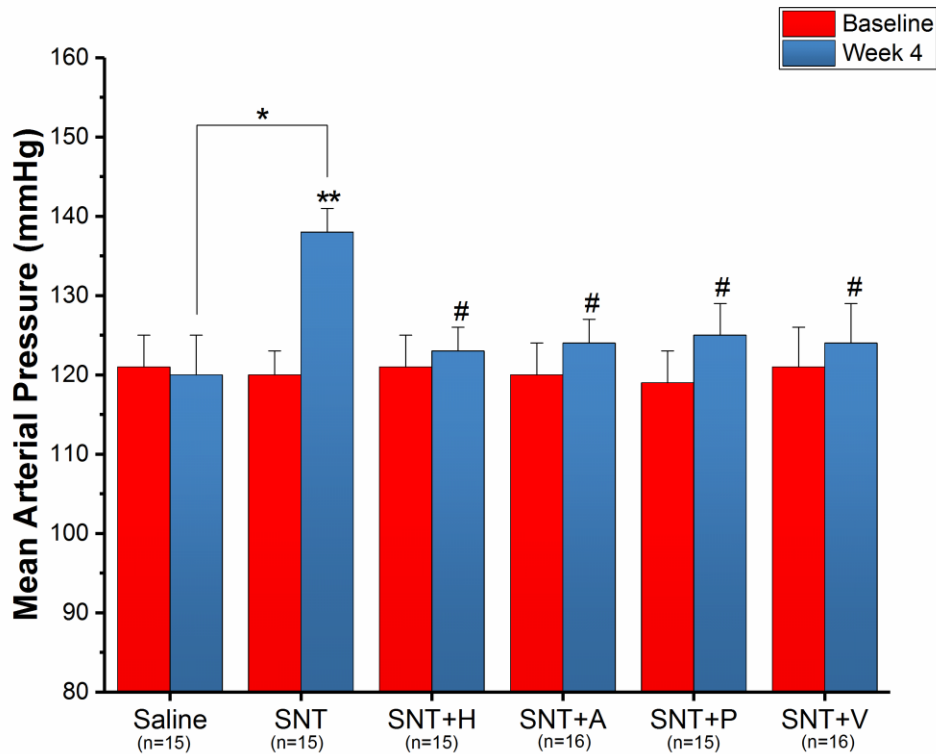


**Figure 7: Mean arterial pressure changes in SNT treated mice prophylactically receiving anti-hypertensive medications.**

SNT treatment induced significant increase in MAP at week 4, while prophylactic treatment with anti-hypertensive drugs completely attenuated the development of hypertension in these mice. The results are reported as mean  $\pm$  SD. \* $p < 0.05$  between SNT at week 4 as compared to Saline. \*\* $p < 0.05$  between SNT at week 4 as compared to SNT baseline. # $p < 0.05$  as compared to SNT at week 4. SNT, Sunitinib; MAP, mean arterial pressure; RAS, renin-angiotensin system; H, Hydralazine; A, Aliskiren; P, Perindopril; V, Valsartan.

### **Murine Echocardiography: BVZ Treatment**

At baseline, echocardiographic parameters including heart rate (HR), IVS, PWT, LVEDD, and LVEF, were similar between all treatment groups (Table 1). HR, IVS, and PWT remained within the normal range for all the treatment groups throughout the duration of the 28 day study.

In the animals treated with BVZ and/or all anti-hypertensive medications, a significant increase in LVEDD is observed beginning at week 2 of the study (Figure 8). At week 4 of the study, LVEDD increased from  $3.2\pm 0.1$  mm at baseline to  $4.4\pm 0.2$  mm in mice treated with BVZ only. A similar trend was observed with prophylactic Hydralazine administration. In particular, addition of Hydralazine did not attenuate LV dilatation, and LVEDD increased from  $3.3\pm 0.1$  mm at baseline to  $4.4\pm 0.1$  mm at week 4 in BVZ treated mice. However, the prophylactic administration of Aliskiren, Perindopril, or Valsartan partially attenuated the increase in LVEDD, with values of  $3.7\pm 0.1$  mm,  $3.8\pm 0.1$  mm, and  $3.8\pm 0.2$  mm, respectively at week 4.

BVZ treatment led to the development of LV systolic dysfunction as LVEF values significantly decreased from  $72\pm 3\%$  at baseline to  $41\pm 2\%$  at week 4 (Figure 9). Similarly, addition of Hydralazine did not preserve cardiac function in BVZ treated mice, causing a significant decline in LVEF to  $43\pm 3\%$ . Prophylactic treatment with Aliskiren, Perindopril, or Valsartan however was partially cardioprotective with LVEF values of  $57\pm 2\%$ ,  $50\pm 2\%$ , or  $51\pm 3\%$  at week 4, respectively ( $p < 0.05$ ).

<b>Echocardiographic variable</b>	<b>Group</b>	<b>Baseline</b>	<b>Week 1</b>	<b>Week 2</b>	<b>Week 3</b>	<b>Week 4</b>	<b>p value</b>
<b>HR (beats/min)</b>	Saline (n=5)	691±8	681±10	675±12	682±9	694±10	0.82
	BVZ (n=11)	694±7	680±7	681±8	680±7	684±8	0.78
	BVZ+H (n=11)	693±1	683±10	678±12	685±8	689±7	0.83
	BVZ+A (n=12)	697±11	688±8	679±11	694±11	690±7	0.85
	BVZ+P (n=12)	693±8	696±11	685±7	679±14	692±4	0.81
	BVZ+V (n=12)	688±11	677±13	691±12	683±11	680±9	0.78
<b>IVS (mm)</b>	Saline (n=5)	0.79±0.01	0.8±0.02	0.78±0.02	0.79±0.02	0.80±0.03	0.82
	BVZ (n=11)	0.79±0.02	0.80±0.01	0.79±0.03	0.80±0.02	0.81±0.03	0.79
	BVZ+H (n=11)	0.78±0.03	0.80±0.02	0.80±0.03	0.80±0.02	0.80±0.02	0.84
	BVZ+A (n=12)	0.80±0.03	0.81±0.02	0.79±0.03	0.81±0.02	0.80±0.03	0.83
	BVZ+P (n=12)	0.78±0.03	0.79±0.02	0.80±0.03	0.80±0.02	0.79±0.03	0.85
	BVZ+V (n=12)	0.79±0.04	0.80±0.02	0.78±0.03	0.81±0.02	0.80±0.03	0.80
<b>PWT (mm)</b>	Saline (n=5)	0.81±0.02	0.81±0.02	0.81±0.02	0.81±0.03	0.79±0.03	0.78
	BVZ (n=11)	0.80±0.02	0.79±0.03	0.80±0.02	0.80±0.02	0.80±0.02	0.81
	BVZ+H (n=11)	0.79±0.02	0.81±0.02	0.78±0.03	0.79±0.03	0.78±0.02	0.78
	BVZ+A (n=12)	0.81±0.02	0.82±0.03	0.82±0.02	0.80±0.02	0.81±0.02	0.85
	BVZ+P (n=12)	0.79±0.03	0.80±0.02	0.80±0.03	0.81±0.03	0.80±0.03	0.87
	BVZ+V (n=12)	0.81±0.03	0.81±0.03	0.81±0.02	0.82±0.02	0.81±0.03	0.83
<b>LVEDD (mm)</b>	Saline (n=5)	3.2±0.2	3.2±0.1	3.3±0.2	3.3±0.2	3.3±0.1	0.82
	BVZ (n=11)	3.2±0.1	3.3±0.1	3.6±0.1*	3.9±0.1*	4.4±0.2*	<0.05
	BVZ+H (n=11)	3.3±0.1	3.3±0.1	3.7±0.1*	3.8±0.2*	4.4±0.1*	<0.05
	BVZ+A (n=12)	3.3±0.1	3.3±0.1	3.4±0.1*	3.6±0.2*	3.7±0.1*#	<0.05
	BVZ+P (n=12)	3.3±0.1	3.3±0.1	3.4±0.1*	3.7±0.2*	3.8±0.1*#	<0.05
	BVZ+V (n=12)	3.3±0.1	3.3±0.1	3.4±0.1*	3.7±0.1*	3.8±0.2*#	<0.05

Echocardiographic variable	Group	Baseline	Week 1	Week 2	Week 3	Week 4	p value
LVEF (%)	Saline (n=5)	72±3	73±3	72±3*	72±3*	72±3	0.91
	BVZ (n=11)	72±3	73±4	57±2*	51±3*	41±2*	<0.05
	BVZ+H (n=11)	73±2	74±4	58±3*	52±4*	43±3*	<0.05
	BVZ+A (n=12)	72±5	73±3	64±3*#	61±1*#	57±2*#	<0.05
	BVZ+P (n=12)	73±3	73±4	63±2*#	58±3*#	50±2*#	<0.05
	BVZ+V (n=12)	73±4	72±4	62±3*#	57±4*#	51±3*#	<0.05

**Table 1: Echocardiographic data from C57Bl/6 mice treated with 0.9% Saline or BVZ with or without prophylactic anti-hypertensive medications from baseline to week 4.**

Assessments of heart rate (HR), interventricular septum (IVS), posterior wall thickness (PWT), left ventricular end diastolic diameter (LVEDD), and left ventricular ejection fraction (LVEF) were performed on a weekly basis during the study period. The values are presented as mean ± SD.

\*p<0.05 as compared to Saline

#p<0.05 as compared to BVZ alone

BVZ, Bevacizumab; RAS, renin-angiotensin system; H, Hydralazine; A, Aliskiren; P, Perindopril; V, Valsartan.

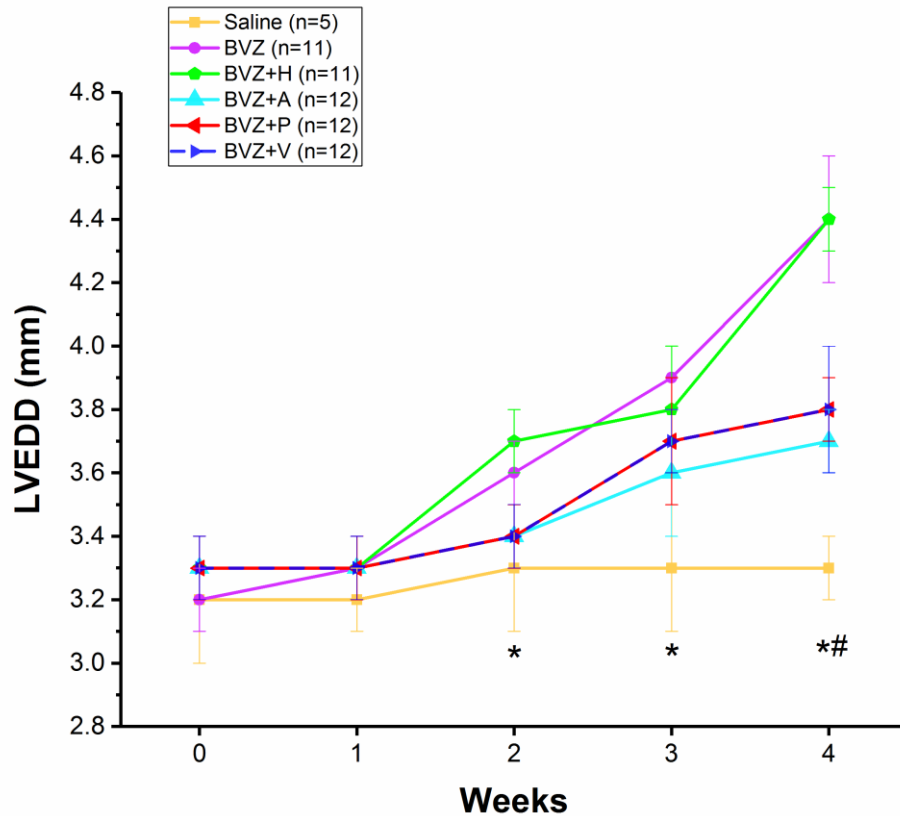


**Figure 8: Changes in LVEDD in BVZ treated mice prophylactically receiving anti-hypertensive medications.**

BVZ treatment resulted in LV cavity dilatation in C57Bl/6 mice at week 4. Prophylactic treatment with Hydralazine did not attenuate the increase in LVEDD at the end of the study. Addition of RAS antagonists partially prevented the increase in LV cavity dimension caused by BVZ administration. The values are presented as mean  $\pm$  SD. \* $p < 0.05$  as compared to Saline. # $p < 0.05$  as compared to SNT alone. LVEDD, left ventricular end diastolic diameter; BVZ, Bevacizumab; RAS, renin-angiotensin system; H, Hydralazine; A, Aliskiren; P, Perindopril; V, Valsartan.



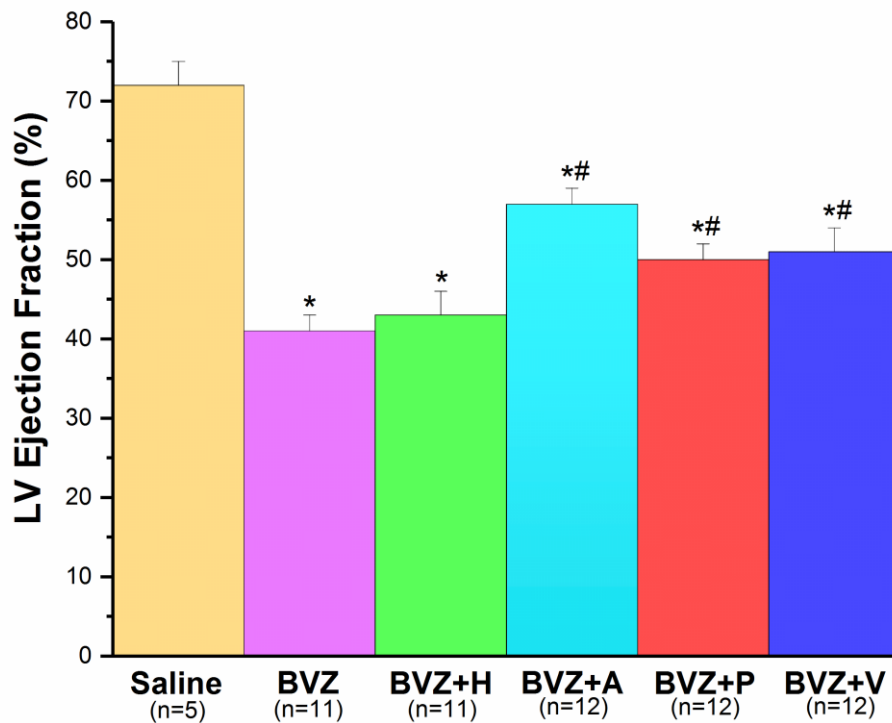


**Figure 9: Changes in LVEF in BVZ treated mice prophylactically receiving anti-hypertensive medications.**

C57Bl/6 mice treated with BVZ developed a significant decrease in LVEF values at week 4. Addition of Hydralazine failed to preserve cardiac function and lowered ejection fraction at the end of the study. LVEF values significantly improved with prophylactic administration of RAS antagonists in animals receiving BVZ. The results are reported as mean  $\pm$  SD. \* $p < 0.05$  as compared to Saline. # $p < 0.05$  as compared to BVZ alone. LV, left ventricular; BVZ, Bevacizumab; RAS, renin-angiotensin system; H, Hydralazine; A, Aliskiren; P, Perindopril; V, Valsartan.

### **Murine Echocardiography: SNT Treatment**

At baseline, the measured echocardiographic parameters, including HR, IVS, PWT, LVEDD, and LVEF, were similar between all treatment groups (Table 2). HR, IVS, and PWT remained within the normal limits for all treatment groups throughout the duration of the 4-week study.

In the animals treated with SNT and/or all anti-hypertensive medications, a significant increase in LV cavity dimension was noted beginning at week 2 of the study (Figure 10). In mice treated with SNT only, LVEDD increased from  $3.3\pm 0.1$  mm at baseline to  $4.6\pm 0.2$  mm at week 4. Left ventricular dilatation was also observed in mice prophylactically treated with Hydralazine as LVEDD increased from  $3.2\pm 0.1$  mm at baseline to  $4.5\pm 0.2$  mm at week 4. The increase in LVEDD was partially attenuated by the prophylactic administration of Aliskiren, Perindopril, or Valsartan, with values of  $3.7\pm 0.1$  mm,  $4.0\pm 0.1$  mm, or  $4.0\pm 0.2$  mm at week 4, respectively.

LVEF decreased from  $73\pm 4\%$  at baseline to  $34\pm 3\%$  in SNT treated mice at week 4, confirming the development of LV systolic dysfunction (Figure 11). Similarly, addition of Hydralazine did not preserve cardiac function as LVEF values significantly decreased to  $33\pm 4\%$ . However, prophylactic administration of Aliskiren, Perindopril, or Valsartan was partially cardioprotective with LVEF values of  $54\pm 2\%$ ,  $45\pm 2\%$ , or  $44\pm 3\%$  at week 4, respectively ( $p < 0.05$ ).

<b>Echocardiographic variable</b>	<b>Group</b>	<b>Baseline</b>	<b>Week 1</b>	<b>Week 2</b>	<b>Week 3</b>	<b>Week 4</b>	<b>p value</b>
<b>HR (beats/min)</b>	Saline (n=5)	688±7	684±8	679±11	680±7	693±9	0.85
	SNT (n=11)	696±8	683±10	685±9	687±11	694±6	0.77
	SNT+H (n=11)	694±5	677±8	684±10	683±9	691±4	0.85
	SNT+A (n=12)	695±11	690±5	684±8	692±11	688±8	0.84
	SNT+P (n=11)	695±10	694±9	691±8	683±12	698±7	0.87
	SNT+V (n=12)	689±9	679±7	692±12	684±11	683±11	0.79
<b>IVS (mm)</b>	Saline (n=5)	0.80±0.02	0.81±0.02	0.79±0.02	0.79±0.03	0.82±0.02	0.83
	SNT (n=11)	0.79±0.03	0.81±0.01	0.80±0.03	0.81±0.02	0.82±0.03	0.84
	SNT+H (n=11)	0.79±0.02	0.80±0.03	0.81±0.03	0.79±0.02	0.81±0.02	0.78
	SNT+A (n=12)	0.81±0.02	0.83±0.02	0.81±0.03	0.80±0.02	0.81±0.03	0.85
	SNT+P (n=11)	0.79±0.02	0.80±0.02	0.81±0.02	0.82±0.02	0.81±0.04	0.82
	SNT+V (n=12)	0.81±0.03	0.80±0.03	0.82±0.03	0.80±0.03	0.82±0.03	0.91
<b>PWT (mm)</b>	Saline (n=5)	0.80±0.03	0.81±0.02	0.82±0.03	0.81±0.02	0.80±0.03	0.81
	SNT (n=11)	0.79±0.03	0.80±0.02	0.80±0.01	0.81±0.02	0.82±0.02	0.80
	SNT+H (n=11)	0.80±0.02	0.80±0.02	0.79±0.02	0.80±0.02	0.81±0.03	0.77
	SNT+A (n=12)	0.80±0.02	0.81±0.03	0.82±0.02	0.80±0.03	0.79±0.03	0.83
	SNT+P (n=11)	0.80±0.01	0.82±0.03	0.81±0.03	0.82±0.03	0.82±0.03	0.82
	SNT+V (n=12)	0.82±0.02	0.80±0.03	0.81±0.02	0.81±0.02	0.82±0.03	0.81
<b>LVEDD (mm)</b>	Saline (n=5)	3.2±0.1	3.2±0.1	3.2±0.2	3.3±0.2	3.2±0.1	0.84
	SNT (n=11)	3.3±0.1	3.3±0.2	3.8±0.1*	4.1±0.1*	4.6±0.2*	<0.05
	SNT+H (n=11)	3.2±0.1	3.2±0.2	3.7±0.2*	4.0±0.2*	4.5±0.2*	<0.05
	SNT+A (n=12)	3.2±0.1	3.3±0.1	3.4±0.1*	3.4±0.2*	3.7±0.1*#	<0.05
	SNT+P (n=11)	3.3±0.1	3.2±0.1	3.6±0.1*	3.9±0.2*	4.0±0.1*#	<0.05
	SNT+V (n=12)	3.2±0.1	3.2±0.1	3.5±0.1*	3.8±0.2*	4.0±0.2*#	<0.05

Echocardiographic variable	Group	Baseline	Week 1	Week 2	Week 3	Week 4	p value
<b>LVEF (%)</b>	Saline (n=5)	73±2	72±4	73±2*	73±3*	73±3	0.91
	SNT (n=11)	73±4	72±3	54±4*	46±3*	34±3*	<0.05
	SNT+H (n=11)	73±2	74±4	55±3*	47±4*	33±4*	<0.05
	SNT+A (n=12)	72±4	71±4	63±2*#	58±3*#	54±2*#	<0.05
	SNT+P (n=11)	74±4	73±2	63±4*#	57±3*#	45±2*#	<0.05
	SNT+V (n=12)	72±4	73±3	64±3*#	56±3*#	44±3*#	<0.05

**Table 2: Echocardiographic data from C57Bl/6 mice treated with 0.9% Saline or SNT with or without prophylactic anti-hypertensive medications from baseline to week 4.**

Assessments of heart rate (HR), interventricular septum (IVS), posterior wall thickness (PWT), left ventricular end diastolic diameter (LVEDD), and left ventricular ejection fraction (LVEF) were performed on a weekly basis during the study period. The values are presented as mean ± SD.

\*p<0.05 as compared to Saline

#p<0.05 as compared to SNT alone

SNT, Sunitinib; RAS, renin-angiotensin system; H, Hydralazine; A, Aliskiren; P, Perindopril; V, Valsartan.

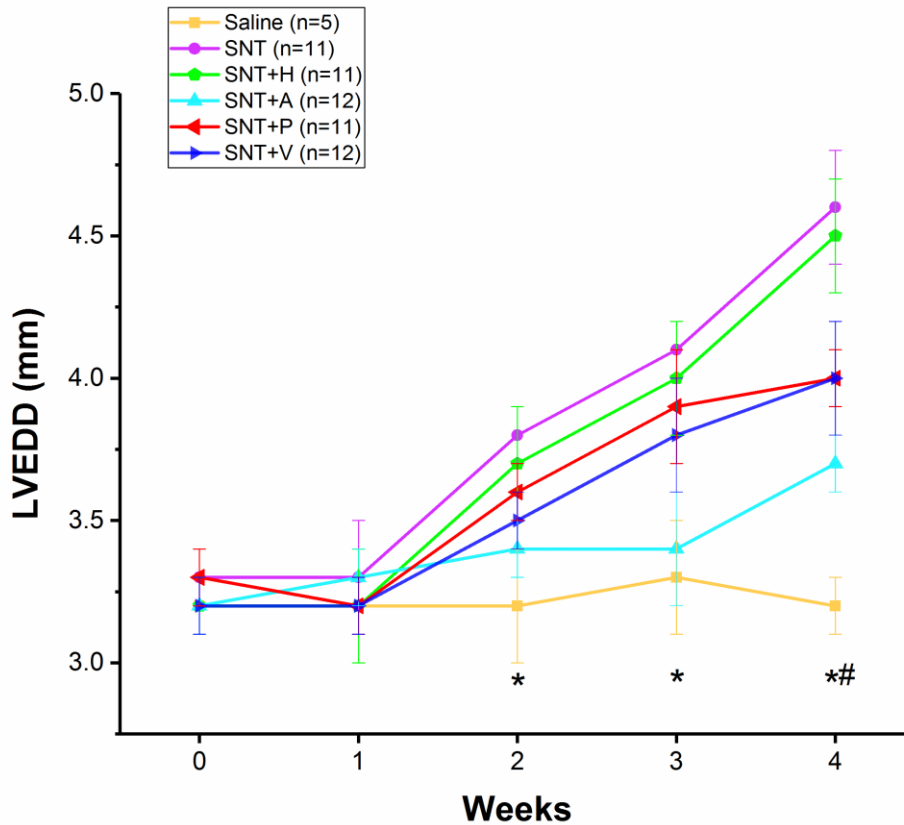


**Figure 10: Changes in LVEDD in SNT treated mice prophylactically receiving anti-hypertensive medications.**

C57Bl/6 mice treated with SNT had increased LV cavity dilatation at week 4. Prophylactic treatment with Hydralazine failed to attenuate the increase in LVEDD at the end of the study. Addition of RAS antagonists partially prevented the increase in LV cavity dimension caused by SNT administration. The values are presented as mean  $\pm$  SD. \* $p < 0.05$  as compared to Saline. # $p < 0.05$  as compared to SNT alone. LVEDD, left ventricular end diastolic diameter; SNT, Sunitinib; RAS, renin-angiotensin system; H, Hydralazine; A, Aliskiren; P, Perindopril; V, Valsartan.

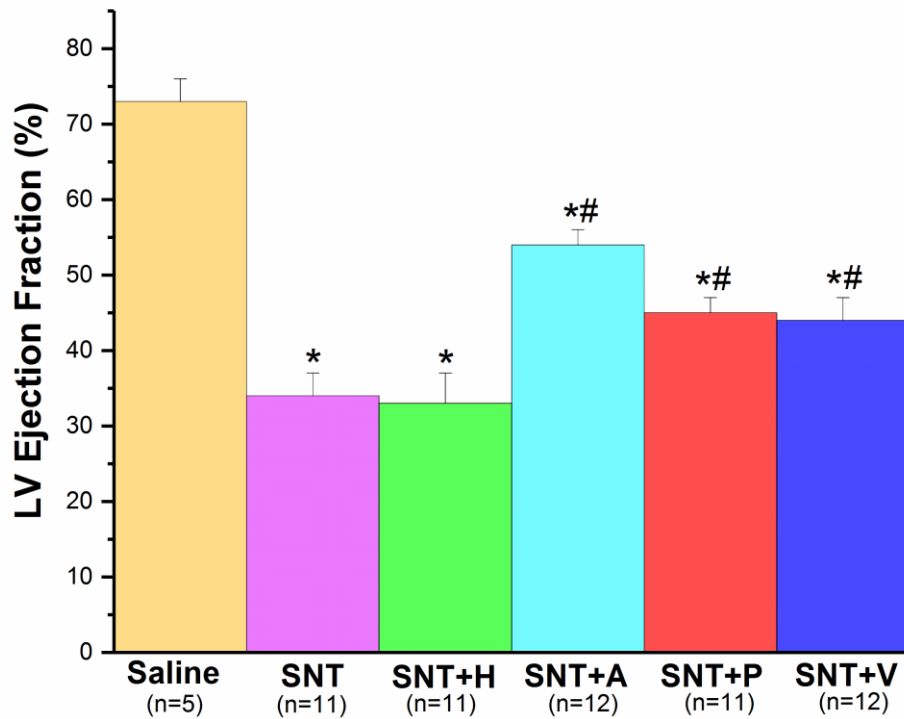


**Figure 11: Changes in LVEF in SNT treated mice prophylactically receiving anti-hypertensive medications.**

A significant reduction in LVEF was observed in C57Bl/6 mice treated with SNT at week 4. Addition of Hydralazine failed to preserve cardiac function and lowered ejection fraction at the end of the study. LVEF values significantly improved with prophylactic administration of RAS antagonists in animals receiving SNT. The results are reported as mean  $\pm$  SD. \* $p < 0.05$  as compared to Saline. # $p < 0.05$  as compared to SNT alone. LV, left ventricular; SNT, Sunitinib; RAS, renin-angiotensin system; H, Hydralazine; A, Aliskiren; P, Perindopril; V, Valsartan.

### **Histological Analysis: BVZ and SNT Treatment**

Approximately 15,000 cells were scanned from 3 random blocks of tissue and assessed for cellular integrity. As compared to saline control, mice in all BVZ and SNT treatment arms demonstrated enlargement of mitochondria and altered cristae at week 4 (Figure 12). The occurrence of swollen mitochondria and disrupted myofilaments was sporadic.

Increased sarcomere disarray and loss of myofibril integrity were observed in mice treated with BVZ alone compared with saline control (Figure 13). Similarly, mice prophylactically treated with Hydralazine failed to preserve cellular integrity, and significant myofibril degeneration was noted at week 4. Addition of Aliskiren and Perindopril partially attenuated cellular damage caused by BVZ ( $p=0.02$  and  $p=0.003$ , respectively). However, prophylactic treatment with Valsartan was not cardioprotective as it did not prevent injury associated with BVZ ( $p=0.08$ ).

Relative to BVZ treatment alone, more pronounced myofibril damage was observed in mice receiving SNT alone as shown in Figure 14 ( $p=0.02$ ). Conversely, prophylactic administration with Hydralazine was associated with significantly less myofibril disruption and sarcomere disarray as compared to SNT treated mice ( $p=0.0006$ ). Similarly results were observed with the addition of RAS antagonists. Aliskiren, Perindopril, and Valsartan were partially effective at preserving myofibril integrity at week 4 ( $p=0.0001$ ;  $p<0.0001$  and  $p<0.0001$ , respectively). Moreover, no evidence of fibrosis was present in any of the treatment arms.

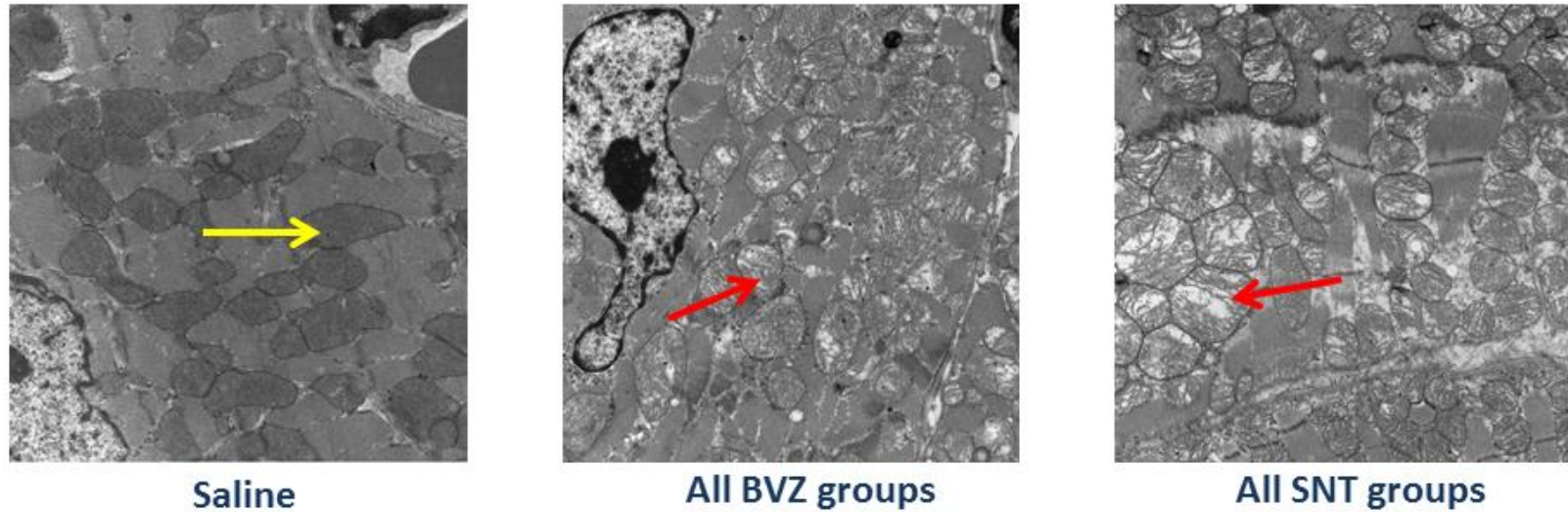


**Figure 12: Structural alterations of mitochondria in all BVZ and SNT treatment arms.**

Representative electron microscopy images of heart samples from C57Bl/6 mice treated with saline, BVZ or SNT. Images were taken at 10,500x magnification. Mitochondria from saline treated mice had normal appearance (yellow arrow). Mitochondrial swellings were observed in mice from all BVZ and SNT treatment arms (red arrows).



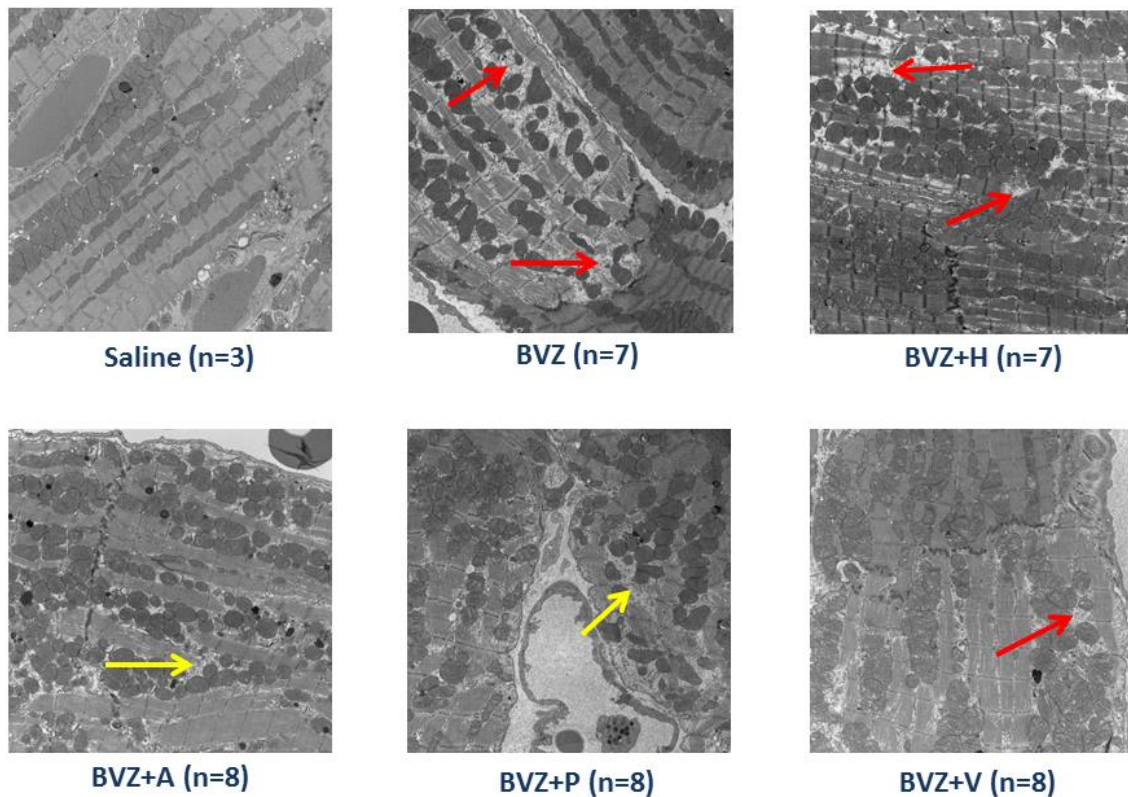


**Figure 13: Cellular alterations in BVZ treated mice prophylactically receiving anti-hypertensive medications.**

Representative electron microscopy images of heart samples from C57Bl/6 mice were taken at 5,800x magnification. Treatment with BVZ alone led to severe damage and loss of myofibrils at week 4 (red arrows). Similar results were observed with Hydralazine administration as this drug did not preserve cellular architecture in BVZ treated mice. Prophylactic treatment with Aliskiren and Perindopril partially prevented the damage associated with BVZ (yellow arrows). Addition of Valsartan however did not offer cardioprotective effects against this monoclonal antibody (red arrow).

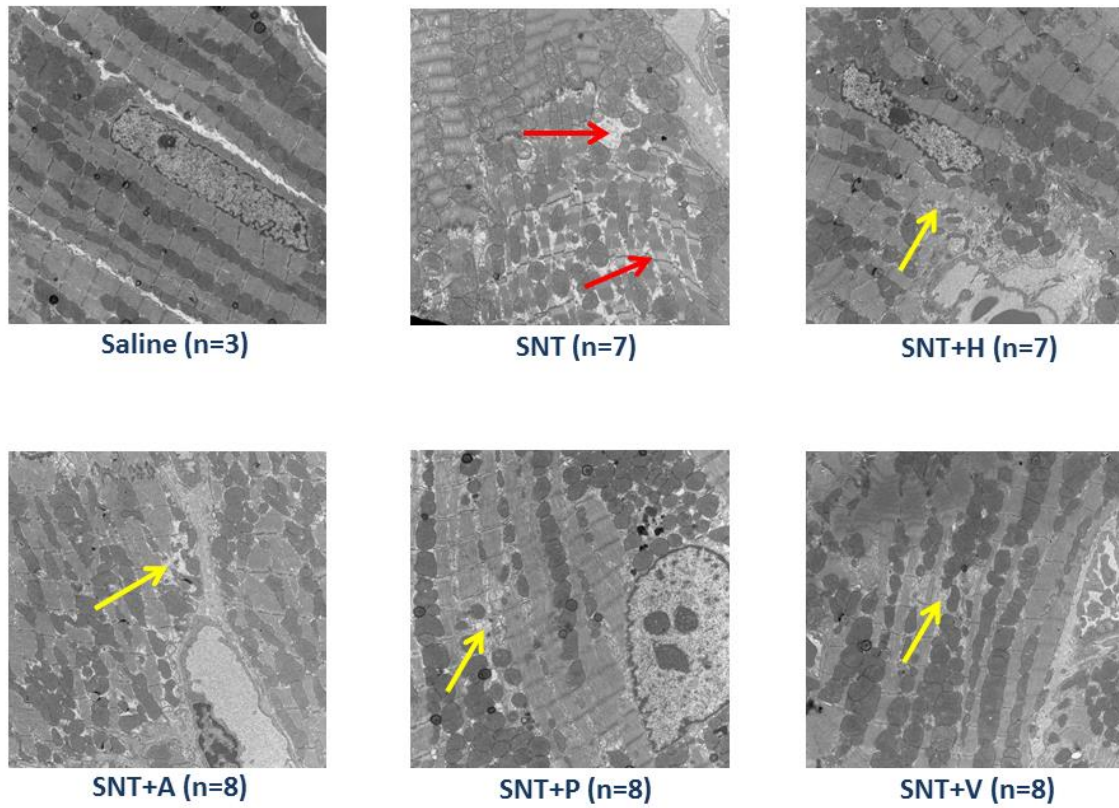


**Figure 14: Cellular alterations in SNT treated mice prophylactically receiving anti-hypertensive medications.**

Representative electron microscopy images of heart samples from C57Bl/6 mice were taken at 5,800x magnification. Red arrows indicate severe damage and loss of myofibrils due to SNT treatment. The prophylactic administration of Hydralazine and RAS antagonists partially attenuated this damage (yellow arrows).

### **Oxolipidomic Analysis**

No significant changes in OxPC levels were observed in mice treated with BVZ or SNT at week 4 (data not shown). Prophylactic administration of Hydralazine, Aliskiren, Perindopril, or Valsartan did not significantly alter OxPC levels as compared to saline and BVZ/SNT treated mice at the end of our study (data not shown).

### **Western Blotting: BVZ Treatment**

At week 4, mice treated with BVZ alone demonstrated a 2.1-fold increase in cleaved PARP protein expression as compared with saline treated mice (Figure 15). Prophylactic treatment with Hydralazine failed to attenuate the expression of cleaved PARP. A similar 2.1-fold increase in this apoptotic marker was observed in mice treated with BVZ. Prophylactic administration of RAS antagonists partially prevented the increase of cleaved PARP expression as compared to BVZ treated animals.

Expressions of apoptotic markers including Caspase-3, Bax, Bcl-xL, and phosphorylated p38 were assessed at day 28. No significant changes were observed between various treatment groups for these markers (data not shown).

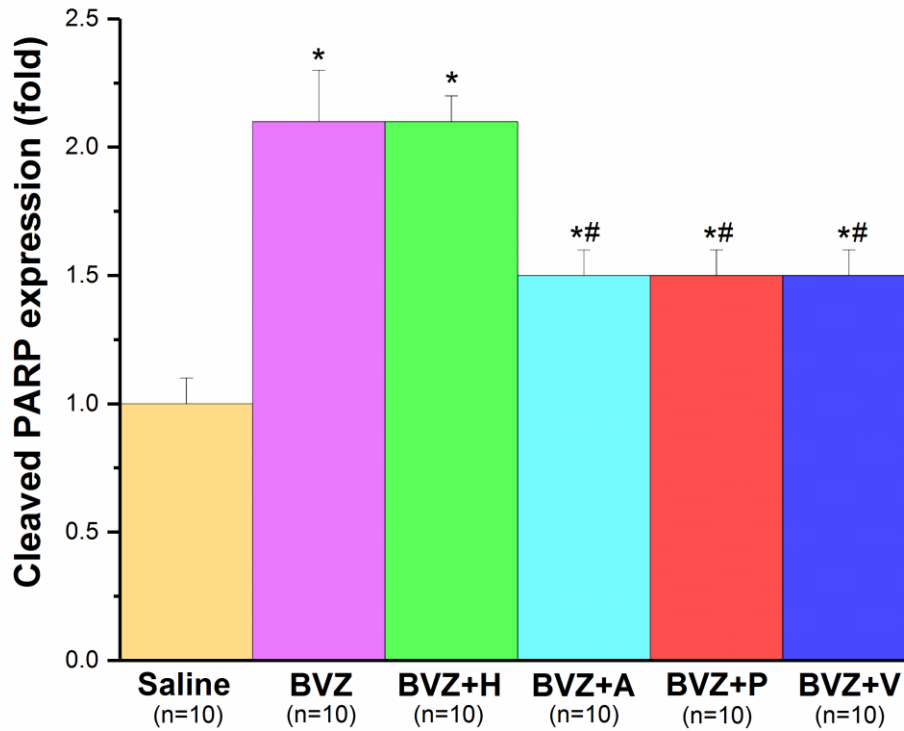


**Figure 15: Changes in cleaved PARP expression in BVZ treated mice prophylactically receiving anti-hypertensive medications.**

Western blot analysis of heart tissue lysates from C57Bl/6 mice treated with saline or BVZ with prophylactic anti-hypertensive medications at week 4. BVZ administration significantly upregulated cleaved PARP expression C57Bl/6 mice. Prophylactic treatment with Hydralazine did not attenuate the degree of cellular apoptosis in BVZ treated mice. Addition of RAS antagonists partially prevented the increase in expression of this marker. The results are normalized to GAPDH loading control and reported as mean  $\pm$  SEM. \* $p$ <0.05 as compared to Saline. # $p$ <0.05 as compared to BVZ alone. PARP – Poly (ADP-ribose) polymerase; BVZ, Bevacizumab; RAS, renin-angiotensin system; H, Hydralazine; A, Aliskiren; P, Perindopril; V, Valsartan.

### **Western Blotting: SNT treatment**

Mice treated with SNT alone demonstrated a 2.3-fold increase in cleaved PARP expression compared with saline treated mice at week 4 (Figure 16). Prophylactic Hydralazine administration failed to prevent activation of cleaved PARP expression as a similar 2.2-fold increase in this apoptotic marker was noted in SNT treated mice. Addition of RAS antagonists, including Aliskiren, Perindopril, or Valsartan, was able to partially attenuate the increase in cleaved PARP as compared to SNT treated animals.

We also observed a 7.7-fold increase in phosphorylated p38 in animals treated with SNT as compared with saline control (Figure 17). Hydralazine administration failed to provide cardioprotective properties as a 6.2-fold increase in this marker was observed in SNT treated mice at week 4. However, treatment with RAS antagonists completely prevented the increase in the expression of phosphorylated p38 at the end of the study.

Expressions of other apoptotic markers including Caspase-3, Bax, and Bcl-xL were assessed at week 4. No significant changes were observed between various treatment groups for these markers (data not shown).

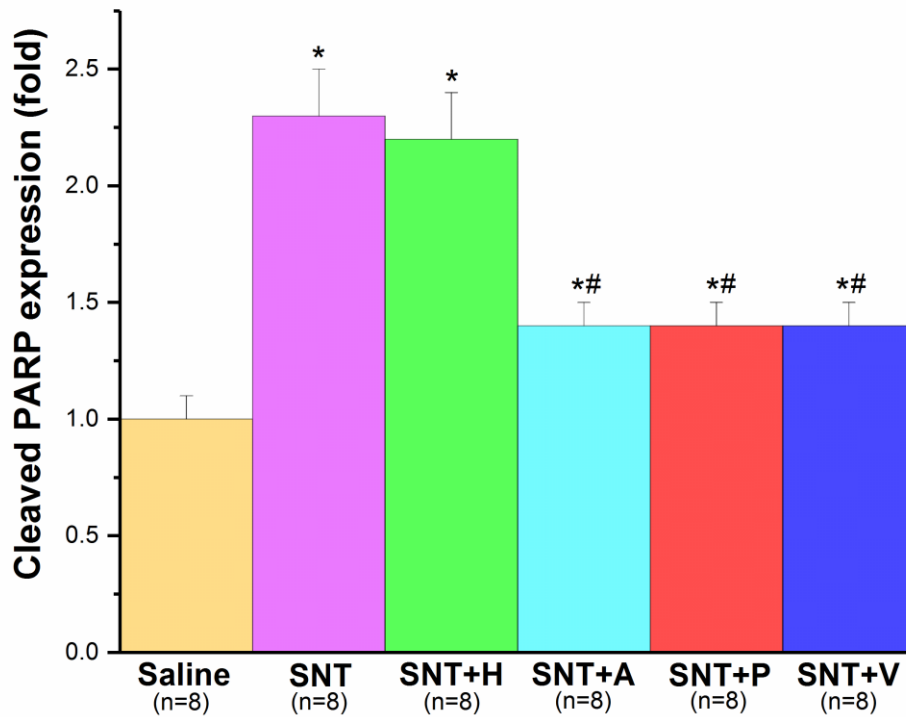


**Figure 16: Changes in cleaved PARP expression in SNT treated mice prophylactically receiving anti-hypertensive medications.**

Western blot analysis of heart tissue lysates from C57Bl/6 mice treated with saline or SNT with prophylactic anti-hypertensive medications at week 4. SNT administration significantly upregulated cleaved PARP expression C57Bl/6 mice. Prophylactic treatment with Hydralazine failed to attenuate the degree of cellular apoptosis in SNT treated mice. Addition of RAS antagonists partially prevented the increase in expression of this marker. The results are normalized to GAPDH loading control and reported as mean  $\pm$  SEM. \* $p$ <0.05 as compared to Saline. # $p$ <0.05 as compared to SNT alone. PARP, Poly (ADP-ribose) polymerase; SNT, Sunitinib; RAS, renin-angiotensin system; H, Hydralazine; A, Aliskiren; P, Perindopril; V, Valsartan.

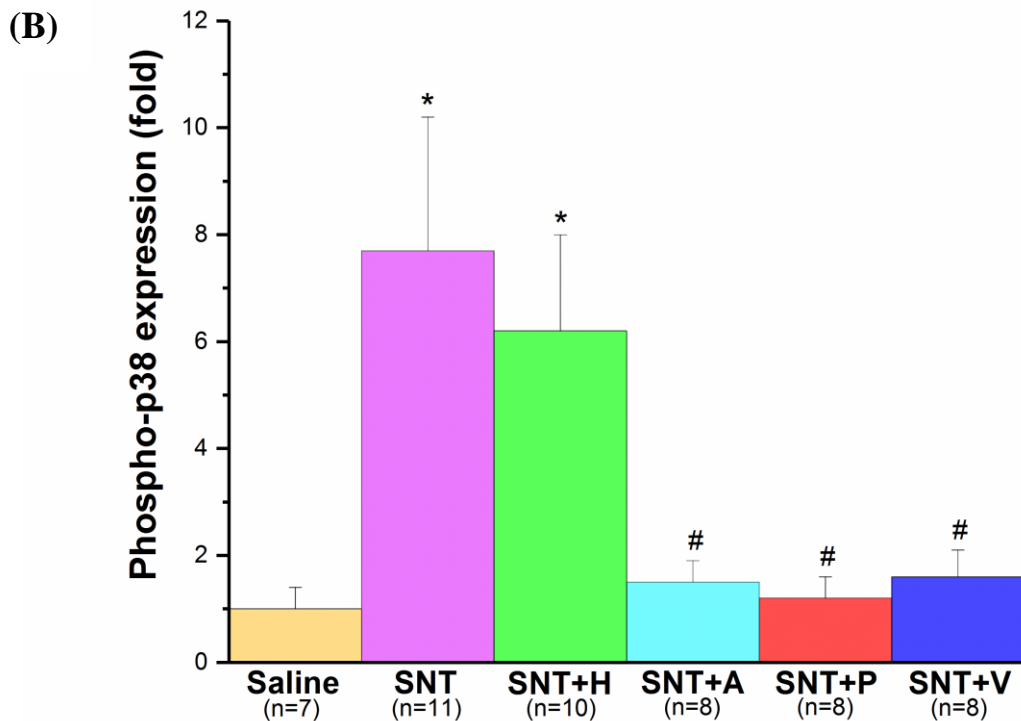
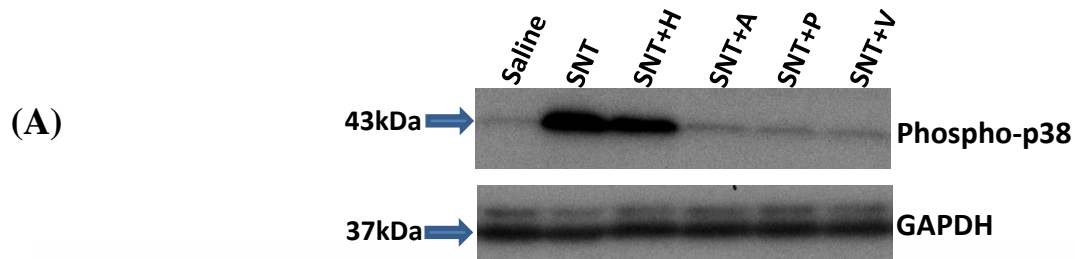


**Figure 17: Changes in phosphorylated p38 expression in SNT treated mice prophylactically receiving anti-hypertensive medications.**

Representative Western blot (A) and data as fold change (B) of phosphorylated p38 protein in C57Bl/6 mice treated with saline or SNT with prophylactic anti-hypertensive medications at week 4. Treatment with SNT resulted in upregulation of phospho-p38 levels. Prophylactic treatment with Hydralazine failed to attenuate phosphorylation of p38 in SNT treated mice. Addition of RAS antagonists, however, normalized the expression of this marker. The results are normalized to GAPDH loading control and reported as mean  $\pm$  SEM \* $p$ <0.05 as compared to Saline. # $p$ <0.05 as compared to SNT alone. SNT, Sunitinib; RAS, renin-angiotensin system; H, Hydralazine; A, Aliskiren; P, Perindopril; V, Valsartan.



## Chapter 4: Discussion

Cardio-oncology is a collaborative discipline that focuses on the detection, management, and prevention of cardiovascular complications caused by cancer therapy.<sup>11</sup> An increased understanding of cancer pathophysiology has led to the development of various targeted agents, including BVZ and SNT, which have been widely used in CRC and RCC patients, respectively.<sup>61, 172</sup> Despite the effectiveness of these anti-cancer drugs,<sup>56, 174</sup> their use is associated with an increased risk of developing cardiotoxicity.<sup>93, 94, 100, 139</sup> Upregulation of RAS pathway is thought to be one of the major contributors of BVZ or SNT mediated cardiac dysfunction.<sup>97, 104, 105, 113, 119, 201</sup> Although pharmacotherapy including RAS antagonists are commonly used after systolic dysfunction develops in the CRC and RCC setting,<sup>104</sup> it would be clinically beneficial to investigate their prophylactic role in the prevention of BVZ or SNT induced cardiotoxicity. The objectives of the current research study were to: 1) determine whether RAS antagonists, including Aliskiren, Perindopril, or Valsartan, would attenuate the cardiotoxic side effects of BVZ or SNT; and 2) to elucidate the potential mechanisms for the cardioprotective effects of RAS antagonism.

In our chronic *in vivo* murine model, prophylactic administration of Hydralazine effectively lowered MAP; however, this medication was not overall cardioprotective. Conversely, we demonstrated that RAS antagonists partially attenuated the cardiotoxic side effects of BVZ or SNT at week 4. In particular, addition of Aliskiren, Perindopril, or Valsartan: i) prevented the rise in MAP; ii) partially prevented adverse cardiovascular remodeling due to BVZ or SNT; iii) partially preserved myofibril structure; and iv) diminished the degree of cardiac apoptosis.

## **BVZ and SNT Mediated Hypertension**

High blood pressure is the most common adverse cardiovascular complication reported in patients treated with BVZ or SNT.<sup>93, 94, 139, 195</sup> These anti-angiogenic agents inhibit the VEGF/VEGFR signaling pathway and facilitate the development of hypertension via the following mechanisms: 1) capillary rarefaction; 2) increased endothelin-1 synthesis; 3) decreased NO production; and 4) RAS stimulation.<sup>96, 97, 100, 102, 139, 201, 202</sup> A myriad of literature demonstrates that the RAS pathway may be the key underlying regulator of blood pressure response.<sup>96, 101, 104, 105, 201</sup> Moreover, the balance between NO and Ang-II is thought to maintain vascular homeostasis due to the antagonistic actions of these molecules.<sup>201,283</sup> NO is known to decrease the expression of ACE and AT<sub>1</sub> receptors whereas Ang-II reduces NO availability by stimulating oxidative stress.<sup>284,285</sup> However, chronic inhibition of NO production enhances the vasoconstrictor actions of Ang-II leading to the development of hypertension, LV hypertrophy, and adverse cardiovascular remodeling.<sup>201, 286</sup>

In their chronic model using C57Bl/6 mice, Belchik *et al.* observed a rapid rise in systolic blood pressure of 17±11% during the first week of treatment with the G6-31 antibody.<sup>105</sup> Increased plasma Ang-II levels were involved in the development of hypertension, leading to increased afterload and LV remodeling.<sup>105</sup> The presence of hypertrophy was congruent with elevated LV mass and end-diastolic wall thickness at week 5 of the study.<sup>105</sup> Conversely, Chu *et al.* observed no changes in blood pressure in an acute model of C57BL/6J mice treated with SNT (40 mg/kg/day) via oral gavage for 12 days.<sup>187</sup> However, this group failed to report on the total number of C57BL/6J mice treated with SNT in their model.<sup>187</sup> Similarly, Chintalgattu and colleagues reported that

C57BL/6 mice receiving SNT (40 mg/kg/d) did not develop an increase in MAP after 21 days of the study.<sup>208</sup> Although SNT was administered via oral gavage, the negligible difference in blood pressure observed in their study may be attributed to their small sample size of only 5-6 mice.<sup>207</sup>

In contrast, we recently demonstrated that C57Bl/6 mice treated with either BVZ (10 mg/kg) or SNT (40 mg/kg/d) developed systemic hypertension on day 7.<sup>113</sup> Specifically, MAP values increased by 50% at day 14 as compared to baseline.<sup>113</sup> In our current study using a chronic model, we confirmed the development of systemic hypertension in mice treated with BVZ or SNT alone. At the end of 4 weeks of administration of these targeted agents, MAP markedly increased by approximately 20 mmHg as compared to baseline. Similar to the clinical setting, the onset of high blood pressure signifies that mice were effectively receiving BVZ or SNT in our chronic study.<sup>95, 195</sup>

In mice that undergo TAC, an increase in systolic blood pressure of 70 mmHg and thickening of posterior wall are observed 2 weeks after surgery.<sup>287</sup> The sudden onset of high blood pressure leads to increase in LV mass by almost 50% within that time period.<sup>288</sup> Chintalgattu *et al.* induced TAC in C57BL/6 mice and administered SNT (40 mg/kg/d) to these animals via oral gavage for 14 days.<sup>208</sup> In this pressure-overload model, mice treated with SNT did not develop cardiac hypertrophy based on the results of normalized organ weight.<sup>208</sup> However, they did not present any data on cardiovascular remodeling using murine echocardiography nor hemodynamic measurements.<sup>208</sup> In our chronic model, we demonstrated that BVZ or SNT administration had no effect on posterior wall dimensions in mice at week 4. This may be due to the fact that a higher

magnitude of change in MAP and longer duration of BVZ or SNT administration may be required for hemodynamic remodeling in mice.<sup>129, 287</sup>

Little is known on the role of anti-hypertensive medications in preventing the development of hypertension in mice receiving either BVZ or SNT. Belcik *et al.* recently evaluated the effect of co-administration of VEGF-A mAb and the ACE inhibitor ramipril (5 mg/kg/d) in C57Bl/6 mice for 5 weeks.<sup>105</sup> The administration of ramipril completely abolished the rise of blood pressure in systole and diastole in mice treated with G6-31.<sup>105</sup> Similarly, our current findings demonstrated that the prophylactic administration of Hydralazine, Aliskiren, Perindopril, or Valsartan completely prevented BVZ or SNT mediated hypertension. In our chronic murine model, all four antihypertensive drugs were equally effective at maintaining the animals in a normotensive state by week 4.

Translating these basic science results into the clinical setting, hypertension was reported in approximately 20% of patients treated with BVZ (5 mg/kg) and 5-FU based chemotherapy.<sup>56</sup> Zhu and colleagues performed a meta-analysis of 1,850 patients who received BVZ for various cancer types, including CRC.<sup>289</sup> The incidence of all grades of hypertension was up to 32% in patients treated with a low dose of BVZ (3, 5, or 7.5 mg/kg) and up to 36% with a high dose concentration of this monoclonal antibody (10 or 15 mg/kg).<sup>289</sup> In a separate clinical study, Mourad *et al.* evaluated metastatic CRC patients treated with chemotherapy and BVZ (5 or 7.5 mg/kg).<sup>290</sup> The mean systolic and diastolic blood pressures were significantly elevated from 129±13/75±7 mmHg at baseline to 145±17/82±7 mmHg after 6 months of therapy, respectively.<sup>290</sup>

Similarly, the development of hypertension has also been reported in clinical trials evaluating the efficacy of the tyrosine kinase inhibitor SNT. Hall *et al.* demonstrated that 53% of metastatic RCC patients receiving SNT developed new or worsening all grade hypertension.<sup>210</sup> Approximately 37% of these patients had grade 3 hypertension, with systolic or diastolic values of  $\geq 160$  mmHg or  $\geq 100$  mmHg, respectively.<sup>210</sup> In support of these findings, Ravaud and colleagues evaluated metastatic RCC patients treated with SNT for 1 year after undergoing nephrectomy.<sup>192</sup> The incidence of all grade hypertension in these patients was found to be approximately 40%.<sup>192</sup> Likewise, Azizi *et al.* demonstrated that metastatic RCC patients who underwent nephrectomy were normotensive prior to 2 cycles of SNT administration.<sup>212</sup> By week 4, blood pressure increased by  $22.2 \pm 6.4$  mmHg in systole and  $17.2 \pm 6.0$  mmHg in diastole.<sup>212</sup> In another clinical study, patients with metastatic RCC or gastrointestinal stromal tumour also developed significant increase in MAP by approximately 15 mmHg at the end of 4 weeks of SNT administration.<sup>291</sup>

No studies to date have evaluated the prophylactic role of antihypertensive drugs, including RAS antagonists, in the prevention of BVZ or SNT mediated cardiotoxicity. In the MANTICORE study,<sup>255</sup> Pitushkin *et al.* recently demonstrated significant reductions in systolic and diastolic blood pressure values when breast cancer patients were co-administered Perindopril (2mg daily) and TRZ adjuvant therapy.<sup>255</sup> Our present basic science research is the first to demonstrate that Hydralazine, Aliskiren, Perindopril, or Valsartan successfully attenuated the increase in MAP with BVZ or SNT treatment, thereby warranting further study in the clinical setting of CRC and RCC.

## **BVZ and SNT Mediated Cardiotoxicity: Echocardiography**

Serial assessment of LVEF is an important clinical diagnostic tool in detecting cardiac dysfunction in the cancer setting.<sup>131-133</sup> A reduction in the LVEF signifies that irreversible cardiac injury may have already occurred.<sup>113, 132, 134</sup> In the evolving field of cardio-oncology, a number of basic science studies have evaluated the role of cardiac imaging in BVZ or SNT induced cardiotoxicity.<sup>105, 113, 129</sup> In a chronic xenograft model of human CRC and breast cancers, treatment of BALB/c mice with 5-FU and BVZ for 6 months resulted in up to 3% incidence of LV systolic dysfunction.<sup>129</sup> Significant decreases in LVEF and cardiac vascular density were reported in the animals treated with this chemotherapeutic regimen.<sup>129</sup> As BVZ inhibits VEGF-A,<sup>59</sup> cardiomyocyte-specific deletion of this gene resulted in reduced LVEF of  $46.8 \pm 1.8\%$  compared to control mice  $62.3 \pm 0.3\%$ .<sup>130</sup> Mice lacking VEGF-A demonstrated dilated cardiac chambers as measured by an increased LVEDD relative to the body weight of mice.<sup>130</sup> In contrast to these findings, this cavity dimension significantly decreased from  $3.4 \pm 0.2$  mm at baseline to  $3.1 \pm 0.3$  mm at week 5 of G6-31 treatment.<sup>105</sup> The reduction in LVEDD and increase in LV mass and wall thickness were congruent with the presence of hypertrophy in mice treated with this VEGF-A antibody.<sup>105</sup>

Bordun *et al.* recently demonstrated that administration of BVZ (10mg/kg) led to an increase in LVEDD from  $3.1 \pm 0.2$  mm at baseline to  $3.9 \pm 0.2$  mm at day 14.<sup>113</sup> Cavity dilatation was also reported in mice treated with SNT (40mg/kg/d).<sup>113</sup> LVEDD values increased from  $3.1 \pm 0.2$  mm at baseline to  $3.9 \pm 0.3$  mm at day 14 in these mice.<sup>113</sup> Moreover, LVEF decreased by approximately 30% as compared to the baseline in mice receiving the anti-cancer agents BVZ or SNT at the end of the 2 week study.<sup>113</sup> The

findings from our chronic model corroborate these results confirming the development of BVZ or SNT induced cardiomyopathy. In mice treated with BVZ, LVEDD increased by 38% and LVEF decreased by 31% as compared to baseline at week 4. We demonstrate greater LV cavity dilatation as compared to the acute model of BVZ mediated cardiotoxicity investigated by Bordun and colleagues.<sup>113</sup> Chronicity of our study and weekly administration of BVZ may have accounted for these detrimental changes on cardiac structure and function. Although a similar decline in LVEF of 30% was observed in both the acute<sup>113</sup> and chronic models of BVZ or SNT mediated cardiotoxicity, we demonstrated a persistent decline in systolic function as compared to baseline. Similarly, in mice treated with SNT, LVEDD increased by 39% and ejection fraction dropped by 39% at week 4. As this targeted agent inhibits more than 50 tyrosine kinase receptors and causes various off-target adverse effects,<sup>199, 200</sup> greater cardiotoxicity is observed in this chronic murine model.

Little is known on the cardioprotective properties of antihypertensive drugs, including RAS antagonists, in the prevention of BVZ or SNT mediated cardiac damage.<sup>11, 220, 221</sup> Five-week treatment with the ACE inhibitor ramipril completely preserved ventricular size and function in mice concomitantly receiving G6-31 monoclonal antibody that targets VEGF-A.<sup>105</sup> In our present study, although prophylactic administration of Hydralazine effectively lowered blood pressure in mice, this drug did not attenuate the cardiotoxic side effects of BVZ or SNT by week 4 as determined by echocardiography. This peripheral vasodilator does not affect the RAS pathway,<sup>277</sup> which is thought to play the key role in the development of cardiac damage caused by anti-cancer drugs.<sup>97, 104, 105, 113, 119</sup> We demonstrated that Hydralazine was not cardioprotective

by echocardiography in the setting of BVZ or SNT induced cardiomyopathy in our chronic *in vivo* murine model, despite a drop in MAP. Conversely, prophylactic administration of RAS antagonists significantly attenuated the degree of cardiac damage in BVZ or SNT treated mice. In our present study, treatment with Aliskiren, Perindopril, or Valsartan partially prevented LV cavity dilatation. In particular, we demonstrated that LVEDD increased by 12-15% in BVZ treated mice and by 16-25% with SNT administration. However, RAS inhibitors partially preserved LV systolic function in our chronic model of cardiotoxicity as a decline in LVEF of 15-22% or 18-28% was observed in BVZ or SNT treated mice, respectively. As both Hydralazine and RAS inhibitors decreased MAP in our chronic murine model, but only the latter prevented adverse cardiovascular remodeling by echocardiography, this would suggest that the cardioprotective effects are independent of the blood pressure lowering effects.

We observed a trend that Aliskiren may be more cardioprotective than Perindopril and Valsartan in our study. This may be due to the fact that the renin inhibitor Aliskiren interferes with the earliest and rate limiting step of the RAS pathway, thereby effectively inhibiting angiotensin I, angiotensin II, and downstream aldosterone production.<sup>104, 256,292</sup> It has also been suggested that Aliskiren may be internalized by cardiomyocytes which are found to increase intracellular Ang-II synthesis in pathological conditions.<sup>293-295</sup> In this situation, local RAS system may not possess all of the components of RAS in myocytes, specifically ACE, and may be dependent on renin and chymase for Ang-II generation.<sup>295</sup> As Ang-II receptor blockers cannot target intracellular Ang-II, direct renin inhibitor Aliskiren may provide better protection on the cardiomyocyte level.<sup>295</sup> In order to confirm that Aliskiren is more effective than Perindopril and Valsartan in our chronic



model of BVZ and SNT mediated cardiotoxicity, similar to the study by Akolkar *et al.*,<sup>272</sup> a larger sample size and longer duration of treatment may be studied in the future.

Although a limited number of clinical studies have revealed potential benefits of RAS antagonists in the setting of anthracycline based chemotherapy,<sup>226, 227, 255</sup> no information is available on their cardioprotective properties in the CRC and RCC setting. Our present basic science study is the first to demonstrate that the cardiotoxic side effects of BVZ or SNT were partially attenuated by the prophylactic administration of Aliskiren, Perindopril, or Valsartan. These inhibitors significantly improved LV structure and function in our chronic murine model. Future clinical studies are necessary to investigate the potential cardioprotective role of these RAS antagonists in the clinical setting of BVZ or SNT mediated cardiotoxicity.

#### **BVZ and SNT Mediated Cardiotoxicity: Histology**

Adverse changes at the cellular level are observed with the anti-cancer therapies BVZ and SNT.<sup>113, 187</sup> Chu and colleagues reported degenerative cardiomyocyte abnormalities, including swelling of mitochondria and disrupted cristae, in C57BL/6J mice treated with SNT (40mg/kg/d) for 12 days.<sup>187</sup> Similarly, in an acute murine model, Bordun *et al.* evaluated hearts from C57Bl/6 mice treated with BVZ or SNT for 14 days using electron microscopy and demonstrated an increased loss of cellular integrity and myofibril disarray at the end of the study.<sup>113</sup>

Our findings corroborate the histological findings in this acute model<sup>113</sup> revealing significant damage in cardiomyocytes due to BVZ or SNT administration at week 4. Both of these targeted agents caused significant structural alterations, including increased myofibril disarray and loss of sarcomere integrity. In addition, we observed enlarged mitochondria with altered cristae in mice treated with either BVZ or SNT. No deposition

of collagen fibers was detected in these mice at week 4, signifying the absence of cardiac fibrosis. Similar to our study, O'Farrell *et al.* demonstrated the absence of cardiac fibrosis in Balb/CJ mice and Sprague-Dawley rats treated with SNT for 4 weeks (40 and 20mg/kg/day, respectively).<sup>203</sup> However, this group reported increased number of lipid droplets in the mouse and rat myocardium, even though myocardial and mitochondrial structure was not adversely affected by SNT.<sup>203</sup> In contrast with these findings, Chen *et al.* reported significantly higher hydroxyproline and collagen levels in BALB/c mice treated with 5-FU and BVZ for a total of 6 months.<sup>129</sup> Prolonged length of anti-cancer drug administration may have resulted in cardiac fibrosis in this study.<sup>129</sup> We speculate that fibrotic markers may be upregulated if we extended the duration of our study to a period of 6 months.<sup>129</sup>

The variation in electron microscopy results may be due to the differences of rodent species used as well as the mode and duration of BVZ and SNT administration.<sup>129, 187, 202, 203, 291</sup> In our chronic model, we demonstrated that addition of Hydralazine did not prevent myofibril damage in the setting of BVZ induced cardiomyopathy, corroborating our echocardiographic findings. Prophylactic treatment with either Aliskiren or Perindopril was cardioprotective as these RAS antagonists partially preserved sarcomere and myofibril integrity in BVZ treated mice. Conversely, addition of Valsartan did not significantly prevent the cellular damage due to BVZ as signified by the p-value of 0.08. However, we anticipate that statistical significance may be reached with a larger sample size in this treatment group in future studies.

More detrimental cellular damage was observed in mice treated with the tyrosine kinase inhibitor SNT. These histological findings were consistent with the significant

changes in cardiac structure and function confirmed by echocardiography. Conversely, prophylactic administration with all antihypertensive medications significantly attenuated myofibril abnormalities in SNT treated mice at week 4. In our chronic model, despite effectively lowering MAP, Hydralazine administration did not prevent LV cavity dilatation and persistent decline in systolic function in mice receiving SNT. As contractile function of cardiomyocytes was impaired, electron microscopy evaluation failed to show these cellular aberrations. This discrepancy may be due to the fact that sarcomere assembly is preserved through an unknown mechanism. Additionally, longer duration of Hydralazine administration may be required for electron microscopy to reveal morphologic changes in SNT treated mice.<sup>187, 202</sup> In our chronic model, mitochondrial dysfunction was not prevented by any of the anti-hypertensive medications in BVZ and SNT treatment arms. However, cardioprotective effects of RAS antagonists were mediated through preservation of cardiac contractile apparatus. Hence, further studies are warranted to elucidate the role of sarcomere and cytoskeleton proteins in BVZ or SNT induced dilated cardiomyopathy.<sup>296-298</sup>

In the clinical setting, histopathological examination is performed by evaluating endomyocardial biopsy samples from cancer patients.<sup>187, 299, 300</sup> Chu *et al.* evaluated tissues from 2 patients who presented with LV systolic dysfunction and heart failure due to SNT administration.<sup>187</sup> Light microscopy revealed hypertrophy of cardiomyocytes, whereas electron microscopy showed structurally normal sarcomeres with swollen anomalous mitochondria.<sup>187</sup> Similarly, Kerkela *et al.* demonstrated aberrant and swollen mitochondria in the tissue from a patient who developed reduced LVEF and CHF due to SNT.<sup>202</sup> Endomyocardial biopsy is necessary to accurately diagnose diseases, including

myocarditis and infiltrative cardiomyopathy.<sup>301</sup> Although this technique is considered to be the gold standard for identifying type I cardiotoxicity, little is known on its use in patients with type II dysfunction.<sup>302</sup> Given this observation, the results from our present study suggest that RAS antagonists may exert cardioprotective effects in CRC and RCC patients, thereby potentially eliminating the need of invasive biopsy<sup>300</sup> in this cancer population. However, our basic science findings require validation of this hypothesis in patients treated with BVZ and SNT.

### **Mechanisms of BVZ or SNT Mediated Cardiotoxicity**

Although the precise mechanisms of BVZ or SNT mediated cardiotoxicity are not completely understood, one of the key signaling processes implicated in this damage is apoptosis.<sup>113</sup> This programmed cell death can be initiated upon activation of certain apoptotic stimuli, including hypoxia, free radicals, toxins, and chemotherapy drugs.<sup>303-305</sup> These stimuli lead to abnormal function of mitochondria and subsequent release of mitochondrial cytochrome *c* into the cytosol, which is regulated by the members of Bcl-2 protein family.<sup>306-308</sup> In particular, pro- and anti-apoptotic proteins, including Bax and Bcl-xL respectively, determine if the cell undergoes cell death or terminates this process.<sup>158, 303, 307</sup> Cytochrome *c* together with pro-caspase-9, and Apaf-1 form the apoptosis complex “apoptosome”.<sup>307</sup> Activated caspase-9 then cleaves effector caspase-3 or caspase-7,<sup>307</sup> which in turn mediates PARP proteolysis, the main feature of apoptosis.<sup>309</sup>

In an *in vivo* model of SNT mediated cardiotoxicity, Chu *et al.* demonstrated increased release of cytochrome *c* from mitochondria, activation of caspase-9, and increased cardiomyocyte apoptosis in neonatal rat ventricular myocytes treated with SNT (1  $\mu$ M).<sup>187</sup> Hasinoff and colleagues reported that up to 10  $\mu$ M of SNT did not change the

levels of pro-apoptotic mediator Bax in ventricular myocytes of Sprague-Dawley rats.<sup>205</sup> However, this group demonstrated that treatment with this targeted agent at the concentration as low as 0.5  $\mu$ M increased activities of caspase-3 and caspase-7 in these myocytes.<sup>205</sup> Corroborating with these findings, Bordun *et al.* revealed that caspase-3 levels were significantly elevated in mice treated with BVZ (10mg/kg) or SNT (40mg/kg/d) for 14 days.<sup>113</sup> Administration of either targeted agent did not change the expression of Bax or PARP proteins by the end of their acute model.<sup>113</sup> In our chronic model, although we observed no change in Bax, Bcl-xL, and Caspase-3, there was a significant increase in the expression of cleaved PARP in mice treated with BVZ or SNT at week 4. Based on these *in vivo* and *in vitro* studies,<sup>113, 205</sup> it is plausible to propose that Bax and Bcl-xL might not be the key regulators of cytochrome *c* release. Therefore, further investigations are warranted on other protein members of the Bcl-2 family that may be involved in this drug mediated cardiotoxicity.

Our findings demonstrate that prophylactic administration of Hydralazine did not attenuate increased cleaved PARP expression induced by BVZ or SNT treatment at week 4. Corroborating the echocardiographic findings, Hydralazine administration was not cardioprotective in our chronic *in vivo* murine model, despite an associated decrease in MAP. Although the addition of this vasodilator resulted in increased cellular damage with BVZ administration, the opposite trend was observed in SNT treated mice, revealing no histological evidence of myofibril loss. The upregulation of cleaved PARP in these animals may have indicated that cardiomyocytes were committed to programmed cell death but they were not actually executing this process at week 4 of our study.

In contrast to these findings, prophylactic administration of RAS antagonists partially attenuated the increase in cleaved PARP expression at week 4 in our chronic model of BVZ or SNT induced cardiomyopathy. As caspase-3 levels did not change in mice with administration of these anti-cancer drugs, it is plausible that cleavage of PARP and, hence, apoptosis may occur via a caspase-3 independent pathway.<sup>307-309</sup> The cleaved PARP protein was detected at about 85-89 kDa in our study.<sup>309</sup> Therefore, expressions of caspase-7, cathepsins, and TGF- $\beta$  proteins should be evaluated in future studies.<sup>309</sup> These proteins are involved in the cleavage of PARP and produce the fragment of similar size we observed in our chronic model.<sup>309</sup>

In response to DNA damage, activated PARP synthesizes poly(ADP-ribose) (PAR) from nicotinamide adenine dinucleotide (NAD<sup>+</sup>) and subsequently transfers PAR to acceptor proteins.<sup>123, 309,310</sup> Poly(ADP-ribosyl)ation leads to chromatin condensation and recruits DNA repair systems.<sup>309-311</sup> In the case of severe DNA damage, PARP activity is greatly elevated resulting in increased NAD<sup>+</sup> consumption and decrease in ATP availability.<sup>309, 311</sup> These processes contribute to PARP cleavage, and inability of this enzyme to respond to DNA breaks leads to programmed cell death.<sup>309, 312</sup> An important protein that senses cellular energy status and regulates its homeostasis is 5' adenosine monophosphate-activated kinase (AMPK).<sup>202,205</sup> It activates energy generating pathways including fatty acid oxidation and glycolysis, thereby increasing ATP levels.<sup>202</sup>

SNT treatment causes AMPK signaling inhibition in both the *in vitro* and *in vivo* settings.<sup>205</sup> This tyrosine kinase inhibitor leads to depletion of ATP levels, reduction of mitochondrial membrane potential, and induction of apoptosis.<sup>202,313,314</sup> As the downstream signal of AMPK is p38, this protein might be involved in apoptosis.<sup>122, 123, 315</sup>

Although AMPK has been shown to regulate p38, there is no compelling evidence that direct phosphorylation is involved in this process.<sup>122, 123, 316</sup> No information is known on the role of p38 in BVZ or SNT mediated cardiotoxicity.<sup>122, 123, 304</sup> Our study is the first to show that phosphorylation of p38 significantly increased in hearts of mice treated with SNT and contributed to apoptotic cell death. Similarly, prophylactic administration with Hydralazine did not prevent activation of phosphorylated p38 due to administration of this tyrosine kinase inhibitor. Therefore, this drug does not exert any apparent cardioprotective effects in the setting of SNT mediated cardiac damage. Treatment with RAS antagonists effectively attenuated the increase in p38 phosphorylation in mice treated with SNT at week 4. Aliskiren, Perindopril, and Valsartan were found to be equally cardioprotective with SNT administration. In contrast with these findings, treatment with the monoclonal antibody BVZ did not elicit any change in the expression of phosphorylated p38 in mice at the end of our chronic study. These findings warrant further investigation on additional apoptotic markers that may be involved in BVZ mediated cardiotoxicity.

Oxidative stress has been found to play an important role in the cardiac damage caused by BVZ and SNT.<sup>113</sup> Amemiya *et al.* demonstrated a decreased ratio of antioxidant glutathione to its oxidized form glutathione disulfide (GSSG) in the hearts of mice treated with SNT.<sup>317</sup> The C57BL/6 mice received this targeted agent (26.7 mg/kg/d) with milk-derived fat (MF) diet for a total of 14 days.<sup>317,318</sup> This group has also performed the thiobarbituric acid reactive substance (TBARS) assay that measures lipid peroxide levels, specifically malondialdehyde.<sup>319</sup> At the end of the study, TBARS levels were significantly elevated in the serum of SNT treated mice.<sup>317</sup> Bordun and colleagues

recently reported a 10-fold increase of OxPC levels in the hearts of mice treated BVZ (10mg/kg) and SNT (40 mg/kg/d) at day 14.<sup>113</sup>

Conversely, in our chronic model, treatment with BVZ (10 mg/kg) or SNT (40 mg/kg/d) for the duration of 4 weeks did not change the levels of OxPC in hearts of these mice. There are several plausible explanations for these findings: 1) As oxidized phospholipids are upregulated in the acute setting,<sup>113</sup> such as myocardial ischemia-reperfusion injury,<sup>320</sup> the levels of OxPCs might have been affected by the longer chronic duration of our study. Most oxidized phospholipids are unstable reactive molecules and have relatively short half-life.<sup>320,321</sup> They can be inactivated by phospholipase cleavage or by antioxidant glutathione peroxidase which reduce these phospholipids.<sup>320</sup> It is plausible that the presence of antioxidant enzymes prevented the increase in OxPC in the mice receiving BVZ or SNT by week 4 of our study; 2) The lack of change in OxPCs levels could have been due to the small sample size of only 4 mice. Therefore, future studies are warranted to evaluate the levels of antioxidant reserve and reactive oxygen species<sup>322</sup> in a larger sample size of mice treated with BVZ or SNT.



## Limitations

There are a number of limitations associated with the current study. First, we only evaluated male C57Bl/6 mice in this chronic *in vivo* model of BVZ or SNT mediated cardiotoxicity. Although males are frequently diagnosed with CRC and RCC in Canada,<sup>1</sup> cardiac damage due to these anti-cancer drugs can affect both males and females.<sup>56, 323</sup> It will be useful to evaluate potential cardioprotective role of Aliskiren, Perindopril, and Valsartan in the chronic model of female mice treated with either BVZ or SNT. Second, we did not evaluate the effect of RAS inhibitors on the tumor suppressing actions of BVZ or SNT. Some ACE inhibitors and angiotensin receptor blockers (ARBs) are known to reduce proliferation of neoplasms in animal models.<sup>324, 325</sup> In the clinical setting, BVZ or SNT treated patients receiving ACE antagonists and ARBs had better overall survival and progression free survival as compared to patients given targeted agents alone.<sup>326-331</sup> Whether RAS antagonists affect the cytotoxic abilities of BVZ or SNT in the cancer setting should be evaluated in future studies. Third, although Aliskiren, Perindopril, and Valsartan improved the cardiac structure and function in mice treated with BVZ or SNT, we did not test other agents that could potentially exert cardioprotective properties. As Ang-II stimulates the secretion of aldosterone,<sup>107</sup> the role of mineralocorticoid antagonists<sup>332</sup> may be investigated in this chronic murine model in future studies.

## **Future directions**

The following *in vivo* research directions should be undertaken in order to fully investigate BVZ or SNT mediated cardiotoxicity and its primary prophylaxis with pharmacotherapy:

1. Future studies are warranted in evaluating whether RAS antagonists can prevent cardiotoxicity in the chronic model of female mice treated with BVZ or SNT.
2. Using the xenograft model of metastatic CRC or RCC,<sup>129, 324</sup> it is necessary to determine whether the RAS antagonists will affect the cytotoxic abilities of BVZ or SNT in an *in vivo* setting.
3. The levels of antioxidant enzymes and OxPCs should be investigated on a weekly basis, as they could vary with the duration of anti-cancer drug administration.<sup>113</sup> This may provide potential insights into the mechanistic actions of BVZ or SNT in the chronic murine model.
4. Comprehensive investigation is required on the role other cell death pathways, including necrosis and autophagy,<sup>307, 333</sup> play in the development of BVZ or SNT mediated cardiotoxicity.
5. As Ang-II stimulates TGF- $\beta$ 1 expression and downstream activation of the SMAD pathway,<sup>111, 334</sup> mediating the synthesis of collagen and development of cardiac fibrosis,<sup>111, 334</sup> this overall cascade should be characterized in the setting of BVZ or SNT administration.

## **Clinical Implications**

Despite the beneficial effects of BVZ and SNT on tumour suppression in CRC and RCC patients,<sup>56, 174</sup> respectively, the use of these targeted agents is associated with an elevated risk of cardiotoxicity.<sup>93, 94, 139</sup> Our study is the first to highlight the potential cardioprotective role of RAS antagonists in the prevention of cardiovascular complications due to BVZ or SNT. The results of this basic science study provide encouraging evidence for us to translate our findings to the clinical setting by investigating the prophylactic role of RAS antagonists in the prevention of cardiotoxicity in CRC and RCC patients. This clinical study may allow clinicians to adjust treatment and/or administer these cardioprotective drugs before irreversible cardiac injury develops, thereby improving overall morbidity and mortality in cancer patients treated with either BVZ or SNT. Moreover, the role of other heart failure medications, including anti-oxidants,  $\beta$ -blockers and/or statins<sup>5, 21, 229, 335</sup> should be evaluated in the murine and clinical settings. These studies would help develop appropriate strategies and guidelines to prevent adverse cardiac events in CRC and RCC population.

## Chapter 6: Conclusion

Our study demonstrated that Hydralazine was effective in lowering blood pressure but was not cardioprotective in BVZ or SNT treated mice. However, prophylactic administration of RAS antagonists partially attenuated BVZ or SNT mediated cardiomyopathy. In our chronic *in vivo* murine model, RAS antagonists: i) prevented the rise in mean arterial pressure; ii) partially improved LV function and cavity dimensions; iii) partially preserved myofibril structure; and iv) diminished the degree of cardiac apoptosis. Future clinical studies are warranted to investigate the role of RAS inhibition in preventing the cardiotoxic side effects of BVZ and SNT in CRC and RCC, respectively.

## Chapter 7: References

1. Canadian Cancer Society's Advisory Committee on Cancer Statistics. *Canadian Cancer Statistics 2017*. Canadian Cancer Society. 2017. Toronto, ON. <http://www.cancer.ca/~media/cancer.ca/CW/cancer%20information/cancer%20101/Canadian%20cancer%20statistics/Canadian-Cancer-Statistics-2017-EN.pdf?la=en>. Accessed August 20, 2017.
2. Parent S, Pituskin E, Paterson DI. The Cardio-oncology Program: A Multidisciplinary Approach to the Care of Cancer Patients With Cardiovascular Disease. *Can J Cardiol*. 2016;32:847-851.
3. O'Hare M, Murphy K, Mookadam F, Sharma A, Lee H. Cardio-oncology Part II: the monitoring, prevention, detection and treatment of chemotherapeutic cardiac toxicity. *Expert Rev Cardiovasc Ther*. 2015;13:519-527.
4. Coleman MP, Quaresma M, Berrino F, Lutz JM, De Angelis R, Capocaccia R, Baili P, Rachet B, Gatta G, Hakulinen T, Micheli A, Sant M, Weir HK, Elwood JM, Tsukuma H, Koifman S, GA ES, Francisci S, Santaquilani M, Verdecchia A, Storm HH, Young JL. Cancer survival in five continents: a worldwide population-based study (CONCORD). *Lancet Oncol*. 2008;9:730-756.
5. Marwick TH. Cancer Therapy-Related Cardiac Dysfunction: Unresolved Issues. *Can J Cardiol*. 2016;32:842-846.
6. Bellinger AM, Arteaga CL, Force T, Humphreys BD, Demetri GD, Druker BJ, Moslehi JJ. Cardio-Oncology: How New Targeted Cancer Therapies and Precision Medicine Can Inform Cardiovascular Discovery. *Circulation*. 2015;132:2248-2258.
7. Larsen CM, Mulvagh SL. Cardio-oncology: what you need to know now for clinical practice and echocardiography. *Echo Res Pract*. 2017;4:R33-r41.
8. Moslehi J. The cardiovascular perils of cancer survivorship. *N Engl J Med*. 2013;368:1055-1056.
9. Swain SM, Whaley FS, Ewer MS. Congestive heart failure in patients treated with doxorubicin: a retrospective analysis of three trials. *Cancer*. 2003;97:2869-2879.
10. Bair SM, Choueiri TK, Moslehi J. Cardiovascular complications associated with novel angiogenesis inhibitors: emerging evidence and evolving perspectives. *Trends Cardiovasc Med*. 2013;23:104-113.
11. Virani SA, Dent S, Brezden-Masley C, Clarke B, Davis MK, Jassal DS, Johnson C, Lemieux J, Paterson I, Sebag IA, Simmons C, Sulpher J, Thain K, Thavendiranathan P, Wentzell JR, Wurtele N, Cote MA, Fine NM, Haddad H, Hayley BD, Hopkins S, Joy AA, Rayson D, Stadnick E, Straatman L. Canadian Cardiovascular Society Guidelines for Evaluation and Management of Cardiovascular Complications of Cancer Therapy. *Can J Cardiol*. 2016;32:831-841.
12. Chen-Scarabelli C, McRee C, Leeser MA, Hage FG, Scarabelli TM. Comprehensive review on cardio-oncology: Role of multimodality imaging. *J Nucl Cardiol*. 2016
13. NCI Dictionary of Cancer Terms. National Cancer Institute. <https://www.cancer.gov/publications/dictionaries/cancer-terms?cdrid=44004>. Accessed April 30, 2017.

14. Moudgil R, Yeh ET. Mechanisms of Cardiotoxicity of Cancer Chemotherapeutic Agents: Cardiomyopathy and Beyond. *Can J Cardiol.* 2016;32:863-870.e865.
15. Seidman A, Hudis C, Pierri MK, Shak S, Paton V, Ashby M, Murphy M, Stewart SJ, Keefe D. Cardiac dysfunction in the trastuzumab clinical trials experience. *J Clin Oncol.* 2002;20:1215-1221.
16. Plana JC, Galderisi M, Barac A, Ewer MS, Ky B, Scherrer-Crosbie M, Ganame J, Sebag IA, Agler DA, Badano LP, Banchs J, Cardinale D, Carver J, Cerqueira M, DeCara JM, Edvardsen T, Flamm SD, Force T, Griffin BP, Jerusalem G, Liu JE, Magalhaes A, Marwick T, Sanchez LY, Sicari R, Villarraga HR, Lancellotti P. Expert consensus for multimodality imaging evaluation of adult patients during and after cancer therapy: a report from the American Society of Echocardiography and the European Association of Cardiovascular Imaging. *Eur Heart J Cardiovasc Imaging.* 2014;15:1063-1093.
17. Nathan PC, Amir E, Abdel-Qadir H. Cardiac Outcomes in Survivors of Pediatric and Adult Cancers. *Can J Cardiol.* 2016;32:871-880.
18. Zhang S, Liu X, Bawa-Khalfe T, Lu LS, Lyu YL, Liu LF, Yeh ET. Identification of the molecular basis of doxorubicin-induced cardiotoxicity. *Nat Med.* 2012;18:1639-1642.
19. Friedman MA, Bozdech MJ, Billingham ME, Rider AK. Doxorubicin cardiotoxicity. Serial endomyocardial biopsies and systolic time intervals. *Jama.* 1978;240:1603-1606.
20. Moslehi JJ. Cardiovascular Toxic Effects of Targeted Cancer Therapies. *N Engl J Med.* 2016;375:1457-1467.
21. Curigliano G, Cardinale D, Dent S, Criscitiello C, Aseyev O, Lenihan D, Cipolla CM. Cardiotoxicity of anticancer treatments: Epidemiology, detection, and management. *CA Cancer J Clin.* 2016;66:309-325.
22. Barrett-Lee PJ, Dixon JM, Farrell C, Jones A, Leonard R, Murray N, Palmieri C, Plummer CJ, Stanley A, Verrill MW. Expert opinion on the use of anthracyclines in patients with advanced breast cancer at cardiac risk. *Ann Oncol.* 2009;20:816-827.
23. Von Hoff DD, Layard MW, Basa P, Davis HL, Jr., Von Hoff AL, Rozenzweig M, Muggia FM. Risk factors for doxorubicin-induced congestive heart failure. *Ann Intern Med.* 1979;91:710-717.
24. Tromp J, Steggink LC, Van Veldhuisen DJ, Gietema JA, van der Meer P. Cardio-Oncology: Progress in Diagnosis and Treatment of Cardiac Dysfunction. *Clin Pharmacol Ther.* 2017;101:481-490.
25. Herrmann J, Lerman A, Sandhu NP, Villarraga HR, Mulvagh SL, Kohli M. Evaluation and management of patients with heart disease and cancer: cardio-oncology. *Mayo Clin Proc.* 2014;89:1287-1306.
26. Ewer MS, Lippman SM. Type II chemotherapy-related cardiac dysfunction: time to recognize a new entity. *J Clin Oncol.* 2005;23:2900-2902.
27. Lenneman CG, Sawyer DB. Cardio-Oncology: An Update on Cardiotoxicity of Cancer-Related Treatment. *Circ Res.* 2016;118:1008-1020.
28. Walker JR, Singal PK, Jassal DS. The art of healing broken hearts in breast cancer patients: Trastuzumab and heart failure. *Exp Clin Cardiol.* 2009;14:e62-67.

29. Raschi E, De Ponti F. Cardiovascular toxicity of anticancer-targeted therapy: emerging issues in the era of cardio-oncology. *Intern Emerg Med.* 2012;7:113-131.
30. Cautela J, Lalevee N, Ammar C, Ederhy S, Peyrol M, Debourdeau P, Serin D, Le Dolley Y, Michel N, Orabona M, Barraud J, Laine M, Bonello L, Paganelli F, Barlesi F, Thuny F. Management and research in cancer treatment-related cardiovascular toxicity: Challenges and perspectives. *Int J Cardiol.* 2016;224:366-375.
31. Yeh ET, Tong AT, Lenihan DJ, Yusuf SW, Swafford J, Champion C, Durand JB, Gibbs H, Zafarmand AA, Ewer MS. Cardiovascular complications of cancer therapy: diagnosis, pathogenesis, and management. *Circulation.* 2004;109:3122-3131.
32. Johnson CB, Davis MK, Law A, Sulpher J. Shared Risk Factors for Cardiovascular Disease and Cancer: Implications for Preventive Health and Clinical Care in Oncology Patients. *Can J Cardiol.* 2016;32:900-907.
33. Brenner H, Kloor M, Pox CP. Colorectal cancer. *Lancet.* 2014;383:1490-1502.
34. Weitz J, Koch M, Debus J, Hohler T, Galle PR, Buchler MW. Colorectal cancer. *Lancet.* 2005;365:153-165.
35. Ferlay J, Shin HR, Bray F, Forman D, Mathers C, Parkin DM. Estimates of worldwide burden of cancer in 2008: GLOBOCAN 2008. *Int J Cancer.* 2010;127:2893-2917.
36. Brody H. Colorectal cancer. *Nature.* 2015;521:S1.
37. Labianca R, Beretta GD, Kildani B, Milesi L, Merlin F, Mosconi S, Pessi MA, Prochilo T, Quadri A, Gatta G, de Braud F, Wils J. Colon cancer. *Crit Rev Oncol Hematol.* 2010;74:106-133.
38. Arvelo F, Sojo F, Cotte C. Biology of colorectal cancer. *Ecancermedicalscience.* 2015;9:520.
39. Cunningham D, Atkin W, Lenz HJ, Lynch HT, Minsky B, Nordlinger B, Starling N. Colorectal cancer. *Lancet.* 2010;375:1030-1047.
40. Yoruker EE, Holdenrieder S, Gezer U. Blood-based biomarkers for diagnosis, prognosis and treatment of colorectal cancer. *Clin Chim Acta.* 2016;455:26-32.
41. Lynch HT, de la Chapelle A. Hereditary colorectal cancer. *N Engl J Med.* 2003;348:919-932.
42. Jasperson K, Burt RW. The Genetics of Colorectal Cancer. *Surg Oncol Clin N Am.* 2015;24:683-703.
43. Yiu AJ, Yiu CY. Biomarkers in Colorectal Cancer. *Anticancer Res.* 2016;36:1093-1102.
44. Grady WM, Carethers JM. Genomic and epigenetic instability in colorectal cancer pathogenesis. *Gastroenterology.* 2008;135:1079-1099.
45. Majumdar SR, Fletcher RH, Evans AT. How does colorectal cancer present? Symptoms, duration, and clues to location. *Am J Gastroenterol.* 1999;94:3039-3045.
46. Jorgensen B, Knudtson J. Stop cancer colon. Colorectal cancer screening--updated guidelines. *S D Med.* 2015;Spec No:82-87.
47. Bacchus CM, Dunfield L, Gorber SC, Holmes NM, Birtwhistle R, Dickinson JA, Lewin G, Singh H, Klarenbach S, Mai V, Tonelli M. Recommendations on screening for colorectal cancer in primary care. *Cmaj.* 2016;188:340-348.

48. Willyard C. Screening: Early alert. *Nature*. 2015;521:S4-5.
49. El Zoghbi M, Cummings LC. New era of colorectal cancer screening. *World J Gastrointest Endosc*. 2016;8:252-258.
50. Ransohoff DF, Sox HC. Clinical Practice Guidelines for Colorectal Cancer Screening: New Recommendations and New Challenges. *Jama*. 2016;315:2529-2531.
51. Leddin D, Hunt R, Champion M, Cockeram A, Flook N, Gould M, Kim YI, Love J, Morgan D, Natsheh S, Sadowski D. Canadian Association of Gastroenterology and the Canadian Digestive Health Foundation: Guidelines on colon cancer screening. *Can J Gastroenterol*. 2004;18:93-99.
52. Ribeiro Gomes J, Belotto M, D'Alpino Peixoto R. The role of surgery for unusual sites of metastases from colorectal cancer: A review of the literature. *Eur J Surg Oncol*. 2017;43:15-19.
53. Riihimaki M, Hemminki A, Sundquist J, Hemminki K. Patterns of metastasis in colon and rectal cancer. *Sci Rep*. 2016;6:29765.
54. Goldstein DA, Zeichner SB, Bartnik CM, Neustadter E, Flowers CR. Metastatic Colorectal Cancer: A Systematic Review of the Value of Current Therapies. *Clin Colorectal Cancer*. 2016;15:1-6.
55. McRee AJ, Goldberg RM. Optimal management of metastatic colorectal cancer: current status. *Drugs*. 2011;71:869-884.
56. Hurwitz H, Fehrenbacher L, Novotny W, Cartwright T, Hainsworth J, Heim W, Berlin J, Baron A, Griffing S, Holmgren E, Ferrara N, Fyfe G, Rogers B, Ross R, Kabbinavar F. Bevacizumab plus irinotecan, fluorouracil, and leucovorin for metastatic colorectal cancer. *N Engl J Med*. 2004;350:2335-2342.
57. Mulder K, Scarfe A, Chua N, Spratlin J. The role of bevacizumab in colorectal cancer: understanding its benefits and limitations. *Expert Opin Biol Ther*. 2011;11:405-413.
58. McCormack PL, Keam SJ. Bevacizumab: a review of its use in metastatic colorectal cancer. *Drugs*. 2008;68:487-506.
59. Keating GM. Bevacizumab: a review of its use in advanced cancer. *Drugs*. 2014;74:1891-1925.
60. Presta LG, Chen H, O'Connor SJ, Chisholm V, Meng YG, Krummen L, Winkler M, Ferrara N. Humanization of an anti-vascular endothelial growth factor monoclonal antibody for the therapy of solid tumors and other disorders. *Cancer Res*. 1997;57:4593-4599.
61. Ferrara N, Hillan KJ, Gerber HP, Novotny W. Discovery and development of bevacizumab, an anti-VEGF antibody for treating cancer. *Nat Rev Drug Discov*. 2004;3:391-400.
62. Ohhara Y, Fukuda N, Takeuchi S, Honma R, Shimizu Y, Kinoshita I, Dosaka-Akita H. Role of targeted therapy in metastatic colorectal cancer. *World J Gastrointest Oncol*. 2016;8:642-655.
63. Zondor SD, Medina PJ. Bevacizumab: an angiogenesis inhibitor with efficacy in colorectal and other malignancies. *Ann Pharmacother*. 2004;38:1258-1264.
64. Degirmenci M, Karaca B, Gorumlu G, Durusoy R, Demir Piskin G, Bozkurt MT, Cirak Y, Tunali D, Karabulut B, Sanli UA, Uslu R. Efficacy and safety of



- bevacizumab plus capecitabine and irinotecan regimen for metastatic colorectal cancer. *Med Oncol*. 2010;27:585-591.
65. Eskander RN, Tewari KS. Development of bevacizumab in advanced cervical cancer: pharmacodynamic modeling, survival impact and toxicology. *Future Oncol*. 2015;11:909-922.
  66. Falk AT, Barriere J, Francois E, Follana P. Bevacizumab: A dose review. *Crit Rev Oncol Hematol*. 2015;94:311-322.
  67. Rosen LS. Clinical experience with angiogenesis signaling inhibitors: focus on vascular endothelial growth factor (VEGF) blockers. *Cancer Control*. 2002;9:36-44.
  68. Kramer I, Lipp HP. Bevacizumab, a humanized anti-angiogenic monoclonal antibody for the treatment of colorectal cancer. *J Clin Pharm Ther*. 2007;32:1-14.
  69. Arjaans M, Schroder CP, Oosting SF, Dafni U, Kleibeuker JE, de Vries EG. VEGF pathway targeting agents, vessel normalization and tumor drug uptake: from bench to bedside. *Oncotarget*. 2016;7:21247-21258.
  70. Matsumoto K, Ema M. Roles of VEGF-A signalling in development, regeneration, and tumours. *J Biochem*. 2014;156:1-10.
  71. Ranieri G, Patruno R, Ruggieri E, Montemurro S, Valerio P, Ribatti D. Vascular endothelial growth factor (VEGF) as a target of bevacizumab in cancer: from the biology to the clinic. *Curr Med Chem*. 2006;13:1845-1857.
  72. Kerbel RS. Tumor angiogenesis. *N Engl J Med*. 2008;358:2039-2049.
  73. Alon T, Hemo I, Itin A, Pe'er J, Stone J, Keshet E. Vascular endothelial growth factor acts as a survival factor for newly formed retinal vessels and has implications for retinopathy of prematurity. *Nat Med*. 1995;1:1024-1028.
  74. Taimah Z, Loughran J, Birks EJ, Bolli R. Vascular endothelial growth factor in heart failure. *Nat Rev Cardiol*. 2013;10:519-530.
  75. Di Lisi D, Madonna R, Zito C, Bronte E, Badalamenti G, Parrella P, Monte I, Tocchetti CG, Russo A, Novo G. Anticancer therapy-induced vascular toxicity: VEGF inhibition and beyond. *Int J Cardiol*. 2017;227:11-17.
  76. Koch S, Tugues S, Li X, Gualandi L, Claesson-Welsh L. Signal transduction by vascular endothelial growth factor receptors. *Biochem J*. 2011;437:169-183.
  77. Holmes K, Roberts OL, Thomas AM, Cross MJ. Vascular endothelial growth factor receptor-2: structure, function, intracellular signalling and therapeutic inhibition. *Cell Signal*. 2007;19:2003-2012.
  78. Cross MJ, Dixelius J, Matsumoto T, Claesson-Welsh L. VEGF-receptor signal transduction. *Trends Biochem Sci*. 2003;28:488-494.
  79. Mousa L, Salem ME, Mikhail S. Biomarkers of Angiogenesis in Colorectal Cancer. *Biomark Cancer*. 2015;7:13-19.
  80. van Geel RM, Beijnen JH, Bernards R, Schellens JH. Treatment Individualization in Colorectal Cancer. *Curr Colorectal Cancer Rep*. 2015;11:335-344.
  81. Schubbert S, Shannon K, Bollag G. Hyperactive Ras in developmental disorders and cancer. *Nat Rev Cancer*. 2007;7:295-308.
  82. Downward J. Targeting RAS and PI3K in lung cancer. *Nat Med*. 2008;14:1315-1316.
  83. Snyder SH, Jaffrey SR. Vessels vivified by Akt acting on NO synthase. *Nat Cell Biol*. 1999;1:E95-96.

84. Pavlidis ET, Pavlidis TE. Role of bevacizumab in colorectal cancer growth and its adverse effects: a review. *World J Gastroenterol.* 2013;19:5051-5060.
85. Hall RD, Le TM, Haggstrom DE, Gentzler RD. Angiogenesis inhibition as a therapeutic strategy in non-small cell lung cancer (NSCLC). *Transl Lung Cancer Res.* 2015;4:515-523.
86. Jain RK, Duda DG, Clark JW, Loeffler JS. Lessons from phase III clinical trials on anti-VEGF therapy for cancer. *Nat Clin Pract Oncol.* 2006;3:24-40.
87. Willett CG, Boucher Y, di Tomaso E, Duda DG, Munn LL, Tong RT, Chung DC, Sahani DV, Kalva SP, Kozin SV, Mino M, Cohen KS, Scadden DT, Hartford AC, Fischman AJ, Clark JW, Ryan DP, Zhu AX, Blaszkowsky LS, Chen HX, Shellito PC, Lauwers GY, Jain RK. Direct evidence that the VEGF-specific antibody bevacizumab has antivasculature effects in human rectal cancer. *Nat Med.* 2004;10:145-147.
88. Giantonio BJ, Catalano PJ, Meropol NJ, O'Dwyer PJ, Mitchell EP, Alberts SR, Schwartz MA, Benson AB, 3rd. Bevacizumab in combination with oxaliplatin, fluorouracil, and leucovorin (FOLFOX4) for previously treated metastatic colorectal cancer: results from the Eastern Cooperative Oncology Group Study E3200. *J Clin Oncol.* 2007;25:1539-1544.
89. Kabbinavar FF, Hambleton J, Mass RD, Hurwitz HI, Bergsland E, Sarkar S. Combined analysis of efficacy: the addition of bevacizumab to fluorouracil/leucovorin improves survival for patients with metastatic colorectal cancer. *J Clin Oncol.* 2005;23:3706-3712.
90. Kabbinavar F, Hurwitz HI, Fehrenbacher L, Meropol NJ, Novotny WF, Lieberman G, Griffing S, Bergsland E. Phase II, randomized trial comparing bevacizumab plus fluorouracil (FU)/leucovorin (LV) with FU/LV alone in patients with metastatic colorectal cancer. *J Clin Oncol.* 2003;21:60-65.
91. Tocchetti CG, Gallucci G, Coppola C, Piscopo G, Cipresso C, Maurea C, Giudice A, Iaffaioli RV, Arra C, Maurea N. The emerging issue of cardiac dysfunction induced by antineoplastic angiogenesis inhibitors. *Eur J Heart Fail.* 2013;15:482-489.
92. Abdel-Qadir H, Ethier JL, Lee DS, Thavendiranathan P, Amir E. Cardiovascular toxicity of angiogenesis inhibitors in treatment of malignancy: A systematic review and meta-analysis. *Cancer Treat Rev.* 2017;53:120-127.
93. Yeh ET, Bickford CL. Cardiovascular complications of cancer therapy: incidence, pathogenesis, diagnosis, and management. *J Am Coll Cardiol.* 2009;53:2231-2247.
94. Economopoulou P, Kotsakis A, Kapiris I, Kentepozidis N. Cancer therapy and cardiovascular risk: focus on bevacizumab. *Cancer Manag Res.* 2015;7:133-143.
95. Scartozzi M, Galizia E, Chiellini S, Giampieri R, Berardi R, Pierantoni C, Cascinu S. Arterial hypertension correlates with clinical outcome in colorectal cancer patients treated with first-line bevacizumab. *Ann Oncol.* 2009;20:227-230.
96. Syrigos KN, Karapanagiotou E, Boura P, Manegold C, Harrington K. Bevacizumab-induced hypertension: pathogenesis and management. *BioDrugs.* 2011;25:159-169.
97. Wasserstrum Y, Kornowski R, Raanani P, Leader A, Pasvolsky O, Iakobishvili Z. Hypertension in cancer patients treated with anti-angiogenic based regimens. *Cardio-Oncology.* 2015;1:6.

98. Souza VB, Silva EN, Ribeiro ML, Martins Wde A. Hypertension in patients with cancer. *Arq Bras Cardiol.* 2015;104:246-252.
99. Moreno-Munoz D, de la Haba-Rodriguez JR, Conde F, Lopez-Sanchez LM, Valverde A, Hernandez V, Martinez A, Villar C, Gomez-Espana A, Porras I, Rodriguez-Ariza A, Aranda E. Genetic variants in the renin-angiotensin system predict response to bevacizumab in cancer patients. *Eur J Clin Invest.* 2015;45:1325-1332.
100. Brinda BJ, Viganego F, Vo T, Dolan D, Fradley MG. Anti-VEGF-Induced Hypertension: a Review of Pathophysiology and Treatment Options. *Curr Treat Options Cardiovasc Med.* 2016;18:33.
101. Shord SS, Bressler LR, Tierney LA, Cuellar S, George A. Understanding and managing the possible adverse effects associated with bevacizumab. *Am J Health Syst Pharm.* 2009;66:999-1013.
102. Robinson ES, Khankin EV, Karumanchi SA, Humphreys BD. Hypertension induced by vascular endothelial growth factor signaling pathway inhibition: mechanisms and potential use as a biomarker. *Semin Nephrol.* 2010;30:591-601.
103. Hayman SR, Leung N, Grande JP, Garovic VD. VEGF inhibition, hypertension, and renal toxicity. *Curr Oncol Rep.* 2012;14:285-294.
104. Vaklavas C, Lenihan D, Kurzrock R, Tsimberidou AM. Anti-vascular endothelial growth factor therapies and cardiovascular toxicity: what are the important clinical markers to target? *Oncologist.* 2010;15:130-141.
105. Belcik JT, Qi Y, Kaufmann BA, Xie A, Bullens S, Morgan TK, Bagby SP, Kolumam G, Kowalski J, Oyer JA, Bunting S, Lindner JR. Cardiovascular and systemic microvascular effects of anti-vascular endothelial growth factor therapy for cancer. *J Am Coll Cardiol.* 2012;60:618-625.
106. Dostal DE, Baker KM. The cardiac renin-angiotensin system: conceptual, or a regulator of cardiac function? *Circ Res.* 1999;85:643-650.
107. Wal P, Wal A, Rai AK, Dixit A. Aliskiren: An orally active renin inhibitor. *J Pharm Bioallied Sci.* 2011;3:189-193.
108. Sparks MA, Crowley SD, Gurley SB, Mirotsoy M, Coffman TM. Classical Renin-Angiotensin system in kidney physiology. *Compr Physiol.* 2014;4:1201-1228.
109. Harada K, Komuro I, Hayashi D, Sugaya T, Murakami K, Yazaki Y. Angiotensin II type 1a receptor is involved in the occurrence of reperfusion arrhythmias. *Circulation.* 1998;97:315-317.
110. Bridgman P, Aronovitz MA, Kakkar R, Oliverio MI, Coffman TM, Rand WM, Konstam MA, Mendelsohn ME, Patten RD. Gender-specific patterns of left ventricular and myocyte remodeling following myocardial infarction in mice deficient in the angiotensin II type 1a receptor. *Am J Physiol Heart Circ Physiol.* 2005;289:H586-592.
111. Hao J, Wang B, Jones SC, Jassal DS, Dixon IM. Interaction between angiotensin II and Smad proteins in fibroblasts in failing heart and in vitro. *Am J Physiol Heart Circ Physiol.* 2000;279:H3020-3030.
112. Lankhorst S, Kappers MH, van Esch JH, Danser AH, van den Meiracker AH. Hypertension during vascular endothelial growth factor inhibition: focus on nitric oxide, endothelin-1, and oxidative stress. *Antioxid Redox Signal.* 2014;20:135-145.

113. Bordun KA, Premecz S, daSilva M, Mandal S, Goyal V, Glavinovic T, Cheung M, Cheung D, White CW, Chaudhary R, Freed DH, Villarraga HR, Herrmann J, Kohli M, Ravandi A, Thliveris J, Pitz M, Singal PK, Mulvagh S, Jassal DS. The utility of cardiac biomarkers and echocardiography for the early detection of bevacizumab- and sunitinib-mediated cardiotoxicity. *Am J Physiol Heart Circ Physiol*. 2015;309:H692-701.
114. Zhao W, Ahokas RA, Weber KT, Sun Y. ANG II-induced cardiac molecular and cellular events: role of aldosterone. *Am J Physiol Heart Circ Physiol*. 2006;291:H336-343.
115. Myers CE, McGuire WP, Liss RH, Ifrim I, Grotzinger K, Young RC. Adriamycin: the role of lipid peroxidation in cardiac toxicity and tumor response. *Science*. 1977;197:165-167.
116. Singal PK, Khaper N, Palace V, Kumar D. The role of oxidative stress in the genesis of heart disease. *Cardiovasc Res*. 1998;40:426-432.
117. Ushio-Fukai M, Nakamura Y. Reactive oxygen species and angiogenesis: NADPH oxidase as target for cancer therapy. *Cancer Lett*. 2008;266:37-52.
118. Kumar D, Kirshenbaum L, Li T, Danelisen I, Singal P. Apoptosis in isolated adult cardiomyocytes exposed to adriamycin. *Ann N Y Acad Sci*. 1999;874:156-168.
119. Touyz RM. Reactive oxygen species and angiotensin II signaling in vascular cells - implications in cardiovascular disease. *Braz J Med Biol Res*. 2004;37:1263-1273.
120. Mehta PK, Griendling KK. Angiotensin II cell signaling: physiological and pathological effects in the cardiovascular system. *Am J Physiol Cell Physiol*. 2007;292:C82-97.
121. Lou H, Danelisen I, Singal PK. Involvement of mitogen-activated protein kinases in adriamycin-induced cardiomyopathy. *Am J Physiol Heart Circ Physiol*. 2005;288:H1925-1930.
122. Cuenda A, Rousseau S. p38 MAP-kinases pathway regulation, function and role in human diseases. *Biochim Biophys Acta*. 2007;1773:1358-1375.
123. Habiro A, Tanno S, Koizumi K, Izawa T, Nakano Y, Osanai M, Mizukami Y, Okumura T, Kohgo Y. Involvement of p38 mitogen-activated protein kinase in gemcitabine-induced apoptosis in human pancreatic cancer cells. *Biochem Biophys Res Commun*. 2004;316:71-77.
124. Ichijo H, Nishida E, Irie K, ten Dijke P, Saitoh M, Moriguchi T, Takagi M, Matsumoto K, Miyazono K, Gotoh Y. Induction of apoptosis by ASK1, a mammalian MAPKKK that activates SAPK/JNK and p38 signaling pathways. *Science*. 1997;275:90-94.
125. Matsuzawa A, Nishitoh H, Tobiume K, Takeda K, Ichijo H. Physiological roles of ASK1-mediated signal transduction in oxidative stress- and endoplasmic reticulum stress-induced apoptosis: advanced findings from ASK1 knockout mice. *Antioxid Redox Signal*. 2002;4:415-425.
126. Dhingra S, Sharma AK, Arora RC, Slezak J, Singal PK. IL-10 attenuates TNF-alpha-induced NF kappaB pathway activation and cardiomyocyte apoptosis. *Cardiovasc Res*. 2009;82:59-66.
127. Lemarie CA, Paradis P, Schiffrin EL. New insights on signaling cascades induced by cross-talk between angiotensin II and aldosterone. *J Mol Med (Berl)*. 2008;86:673-678.

128. Westermann D, Riad A, Lettau O, Roks A, Savvatis K, Becher PM, Escher F, Jan Danser AH, Schultheiss HP, Tschöpe C. Renin inhibition improves cardiac function and remodeling after myocardial infarction independent of blood pressure. *Hypertension*. 2008;52:1068-1075.
129. Chen CT, Yamaguchi H, Lee HJ, Du Y, Lee HH, Xia W, Yu WH, Hsu JL, Yen CJ, Sun HL, Wang Y, Yeh ET, Hortobagyi GN, Hung MC. Dual targeting of tumor angiogenesis and chemotherapy by endostatin-cytosine deaminase-uracil phosphoribosyltransferase. *Mol Cancer Ther*. 2011;10:1327-1336.
130. Giordano FJ, Gerber HP, Williams SP, VanBruggen N, Bunting S, Ruiz-Lozano P, Gu Y, Nath AK, Huang Y, Hickey R, Dalton N, Peterson KL, Ross J, Jr., Chien KR, Ferrara N. A cardiac myocyte vascular endothelial growth factor paracrine pathway is required to maintain cardiac function. *Proc Natl Acad Sci U S A*. 2001;98:5780-5785.
131. Fallah-Rad N, Walker JR, Wassef A, Lytwyn M, Bohonis S, Fang T, Tian G, Kirkpatrick ID, Singal PK, Krahn M, Grenier D, Jassal DS. The utility of cardiac biomarkers, tissue velocity and strain imaging, and cardiac magnetic resonance imaging in predicting early left ventricular dysfunction in patients with human epidermal growth factor receptor II-positive breast cancer treated with adjuvant trastuzumab therapy. *J Am Coll Cardiol*. 2011;57:2263-2270.
132. Neilan TG, Jassal DS, Perez-Sanz TM, Raheer MJ, Pradhan AD, Buys ES, Ichinose F, Bayne DB, Halpern EF, Weyman AE, Derumeaux G, Bloch KD, Picard MH, Scherrer-Crosbie M. Tissue Doppler imaging predicts left ventricular dysfunction and mortality in a murine model of cardiac injury. *Eur Heart J*. 2006;27:1868-1875.
133. Ducas R, Tsang W, Chong AA, Jassal DS, Lang RM, Leong-Poi H, Chan KL. Echocardiography and vascular ultrasound: new developments and future directions. *Can J Cardiol*. 2013;29:304-316.
134. Jassal DS, Han SY, Hans C, Sharma A, Fang T, Ahmadie R, Lytwyn M, Walker JR, Bhalla RS, Czarnecki A, Moussa T, Singal PK. Utility of tissue Doppler and strain rate imaging in the early detection of trastuzumab and anthracycline mediated cardiomyopathy. *J Am Soc Echocardiogr*. 2009;22:418-424.
135. Di Lisi D, Bonura F, Macaione F, Peritore A, Meschisi M, Cuttitta F, Novo G, D'Alessandro N, Novo S. Chemotherapy-induced cardiotoxicity: role of the tissue Doppler in the early diagnosis of left ventricular dysfunction. *Anticancer Drugs*. 2011;22:468-472.
136. Sebag IA, Handschumacher MD, Ichinose F, Morgan JG, Hataishi R, Rodrigues AC, Guerrero JL, Steudel W, Raheer MJ, Halpern EF, Derumeaux G, Bloch KD, Picard MH, Scherrer-Crosbie M. Quantitative assessment of regional myocardial function in mice by tissue Doppler imaging: comparison with hemodynamics and sonomicrometry. *Circulation*. 2005;111:2611-2616.
137. Sawaya H, Sebag IA, Plana JC, Januzzi JL, Ky B, Cohen V, Gosavi S, Carver JR, Wieggers SE, Martin RP, Picard MH, Gerszten RE, Halpern EF, Passeri J, Kuter I, Scherrer-Crosbie M. Early detection and prediction of cardiotoxicity in chemotherapy-treated patients. *Am J Cardiol*. 2011;107:1375-1380.
138. Thavendiranathan P, Poulin F, Lim KD, Plana JC, Woo A, Marwick TH. Use of myocardial strain imaging by echocardiography for the early detection of

- cardiotoxicity in patients during and after cancer chemotherapy: a systematic review. *J Am Coll Cardiol*. 2014;63:2751-2768.
139. Gupta R, Maitland ML. Sunitinib, hypertension, and heart failure: a model for kinase inhibitor-mediated cardiotoxicity. *Curr Hypertens Rep*. 2011;13:430-435.
  140. Senkus E, Jassem J. Cardiovascular effects of systemic cancer treatment. *Cancer Treat Rev*. 2011;37:300-311.
  141. Qi WX, Fu S, Zhang Q, Guo XM. Bevacizumab increases the risk of severe congestive heart failure in cancer patients: an up-to-date meta-analysis with a focus on different subgroups. *Clin Drug Investig*. 2014;34:681-690.
  142. Chen ZI, Ai DI. Cardiotoxicity associated with targeted cancer therapies. *Mol Clin Oncol*. 2016;4:675-681.
  143. Zeglinski M JD. Prevalence of Bevacizumab mediated cardiomyopathy in the real world setting. *Canadian Journal of Cardiology*. 2012 (Abstract).
  144. Ranpura V, Hapani S, Chuang J, Wu S. Risk of cardiac ischemia and arterial thromboembolic events with the angiogenesis inhibitor bevacizumab in cancer patients: a meta-analysis of randomized controlled trials. *Acta Oncol*. 2010;49:287-297.
  145. Scappaticci FA, Skillings JR, Holden SN, Gerber HP, Miller K, Kabbinavar F, Bergsland E, Ngai J, Holmgren E, Wang J, Hurwitz H. Arterial thromboembolic events in patients with metastatic carcinoma treated with chemotherapy and bevacizumab. *J Natl Cancer Inst*. 2007;99:1232-1239.
  146. Ridge CA, Pua BB, Madoff DC. Epidemiology and staging of renal cell carcinoma. *Semin Intervent Radiol*. 2014;31:3-8.
  147. Graves A, Hessamodini H, Wong G, Lim WH. Metastatic renal cell carcinoma: update on epidemiology, genetics, and therapeutic modalities. *Immunotargets Ther*. 2013;2:73-90.
  148. Hancock SB, Georgiades CS. Kidney Cancer. *Cancer J*. 2016;22:387-392.
  149. Hsieh JJ, Purdue MP, Signoretti S, Swanton C, Albiges L, Schmidinger M, Heng DY, Larkin J, Ficarra V. Renal cell carcinoma. *Nat Rev Dis Primers*. 2017;3:17009.
  150. Haddad AQ, Margulis V. Tumour and patient factors in renal cell carcinoma-towards personalized therapy. *Nat Rev Urol*. 2015;12:253-262.
  151. Reaume MN, Graham GE, Tomiak E, Kamel-Reid S, Jewett MA, Bjarnason GA, Blais N, Care M, Drachenberg D, Gedye C, Grant R, Heng DY, Kapoor A, Kollmannsberger C, Lattouf JB, Maher ER, Pause A, Ruether D, Soulieres D, Tanguay S, Turcotte S, Violette PD, Wood L, Basiuk J, Pautler SE. Canadian guideline on genetic screening for hereditary renal cell cancers. *Can Urol Assoc J*. 2013;7:319-323.
  152. Turajlic S, Larkin J, Swanton C. SnapShot: Renal Cell Carcinoma. *Cell*. 2015;163:1556-1556.e1551.
  153. Jonasch E, Gao J, Rathmell WK. Renal cell carcinoma. *Bmj*. 2014;349:g4797.
  154. Twardowski PW, Mack PC, Lara PN, Jr. Papillary renal cell carcinoma: current progress and future directions. *Clin Genitourin Cancer*. 2014;12:74-79.
  155. Pignot G, Elie C, Conquy S, Vieillefond A, Flam T, Zerbib M, Debre B, Amsellem-Ouazana D. Survival analysis of 130 patients with papillary renal cell

- carcinoma: prognostic utility of type 1 and type 2 subclassification. *Urology*. 2007;69:230-235.
156. Yang XJ, Tan MH, Kim HL, Ditlev JA, Betten MW, Png CE, Kort EJ, Futami K, Furge KA, Takahashi M, Kanayama HO, Tan PH, Teh BS, Luan C, Wang K, Pins M, Tretiakova M, Anema J, Kahnoski R, Nicol T, Stadler W, Vogelzang NG, Amato R, Seligson D, Figlin R, Beldegrun A, Rogers CG, Teh BT. A molecular classification of papillary renal cell carcinoma. *Cancer Res*. 2005;65:5628-5637.
  157. Klatter T, Pantuck AJ, Said JW, Seligson DB, Rao NP, LaRochelle JC, Shuch B, Zisman A, Kabbinavar FF, Beldegrun AS. Cytogenetic and molecular tumor profiling for type 1 and type 2 papillary renal cell carcinoma. *Clin Cancer Res*. 2009;15:1162-1169.
  158. Seeger-Nukpezah T, Geynisman DM, Nikonova AS, Benzing T, Golemis EA. The hallmarks of cancer: relevance to the pathogenesis of polycystic kidney disease. *Nat Rev Nephrol*. 2015;11:515-534.
  159. Kabaria R, Klaassen Z, Terris MK. Renal cell carcinoma: links and risks. *Int J Nephrol Renovasc Dis*. 2016;9:45-52.
  160. Gupta S. Obesity: The fat advantage. *Nature*. 2016;537:S100-102.
  161. Albiges L, Hakimi AA, Xie W, McKay RR, Simantov R, Lin X, Lee JL, Rini BI, Srinivas S, Bjarnason GA, Ernst S, Wood LA, Vaishamayan UN, Rha SY, Agarwal N, Yuasa T, Pal SK, Bamias A, Zabor EC, Skanderup AJ, Furberg H, Fay AP, de Velasco G, Preston MA, Wilson KM, Cho E, McDermott DF, Signoretti S, Heng DY, Choueiri TK. Body Mass Index and Metastatic Renal Cell Carcinoma: Clinical and Biological Correlations. *J Clin Oncol*. 2016
  162. Brown C. Targeted therapy: An elusive cancer target. *Nature*. 2016;537:S106-108.
  163. Ljungberg B, Hanbury DC, Kuczyk MA, Merseburger AS, Mulders PF, Patard JJ, Sinescu IC. Renal cell carcinoma guideline. *Eur Urol*. 2007;51:1502-1510.
  164. Motzer RJ, Hutson TE, Tomczak P, Michaelson MD, Bukowski RM, Rixe O, Oudard S, Negrier S, Szczylik C, Kim ST, Chen I, Bycott PW, Baum CM, Figlin RA. Sunitinib versus interferon alfa in metastatic renal-cell carcinoma. *N Engl J Med*. 2007;356:115-124.
  165. Rendon RA, Kapoor A, Breau R, Leveridge M, Feifer A, Black PC, So A. Surgical management of renal cell carcinoma: Canadian Kidney Cancer Forum Consensus. *Can Urol Assoc J*. 2014;8:E398-412.
  166. Lee-Ying R, Lester R, Heng D. Current management and future perspectives of metastatic renal cell carcinoma. *Int J Urol*. 2014;21:847-855.
  167. Leslie S, Goh AC, Gill IS. Partial nephrectomy--contemporary indications, techniques and outcomes. *Nat Rev Urol*. 2013;10:275-283.
  168. Sivarajan G, Huang WC. Current practice patterns in the surgical management of renal cancer in the United States. *Urol Clin North Am*. 2012;39:149-160, v.
  169. Adibi M, Thomas AZ, Borregales LD, Matin SF, Wood CG, Karam JA. Surgical considerations for patients with metastatic renal cell carcinoma. *Urol Oncol*. 2015;33:528-537.
  170. Krabbe LM, Haddad AQ, Westerman ME, Margulis V. Surgical management of metastatic renal cell carcinoma in the era of targeted therapies. *World J Urol*. 2014;32:615-622.

171. North SA, Basappa N, Basiuk J, Bjarnason G, Breau R, Canil C, Heng D, Jewett MA, Kapoor A, Kollmannsberger C, Potvin K, Neil Reaume M, Dean Ruether J, Venner P, Wood L. Management of advanced kidney cancer: Canadian Kidney Cancer Forum consensus update. *Can Urol Assoc J*. 2015;9:164-170.
172. Chow LQ, Eckhardt SG. Sunitinib: from rational design to clinical efficacy. *J Clin Oncol*. 2007;25:884-896.
173. Suarez C, Rini BI. Determining the optimal dose and schedule of sunitinib: some answers, more questions. *Cancer*. 2012;118:1178-1180.
174. Motzer RJ, Hutson TE, Tomczak P, Michaelson MD, Bukowski RM, Oudard S, Negrier S, Szczylik C, Pili R, Bjarnason GA, Garcia-del-Muro X, Sosman JA, Solska E, Wilding G, Thompson JA, Kim ST, Chen I, Huang X, Figlin RA. Overall survival and updated results for sunitinib compared with interferon alfa in patients with metastatic renal cell carcinoma. *J Clin Oncol*. 2009;27:3584-3590.
175. Hao Z, Sadek I. Sunitinib: the antiangiogenic effects and beyond. *Onco Targets Ther*. 2016;9:5495-5505.
176. Khakoo AY, Kassiotis CM, Tannir N, Plana JC, Halushka M, Bickford C, Trent J, 2nd, Champion JC, Durand JB, Lenihan DJ. Heart failure associated with sunitinib malate: a multitargeted receptor tyrosine kinase inhibitor. *Cancer*. 2008;112:2500-2508.
177. Deeks ED, Keating GM. Sunitinib. *Drugs*. 2006;66:2255-2266; discussion 2267-2258.
178. Kalra S, Rini BI, Jonasch E. Alternate sunitinib schedules in patients with metastatic renal cell carcinoma. *Ann Oncol*. 2015;26:1300-1304.
179. Faivre S, Demetri G, Sargent W, Raymond E. Molecular basis for sunitinib efficacy and future clinical development. *Nat Rev Drug Discov*. 2007;6:734-745.
180. Gotink KJ, Verheul HM. Anti-angiogenic tyrosine kinase inhibitors: what is their mechanism of action? *Angiogenesis*. 2010;13:1-14.
181. Ferrara N, Gerber HP, LeCouter J. The biology of VEGF and its receptors. *Nat Med*. 2003;9:669-676.
182. Shaw G. The silent disease. *Nature*. 2016;537:S98-99.
183. Schmidt C. Immunotherapy: Controlled attack. *Nature*. 2016;537:S109-110.
184. Schmid TA, Gore ME. Sunitinib in the treatment of metastatic renal cell carcinoma. *Ther Adv Urol*. 2016;8:348-371.
185. Segaliny AI, Tellez-Gabriel M, Heymann MF, Heymann D. Receptor tyrosine kinases: Characterisation, mechanism of action and therapeutic interests for bone cancers. *J Bone Oncol*. 2015;4:1-12.
186. Force T, Kolaja KL. Cardiotoxicity of kinase inhibitors: the prediction and translation of preclinical models to clinical outcomes. *Nat Rev Drug Discov*. 2011;10:111-126.
187. Chu TF, Rupnick MA, Kerkela R, Dallabrida SM, Zurakowski D, Nguyen L, Woulfe K, Pravda E, Cassiola F, Desai J, George S, Morgan JA, Harris DM, Ismail NS, Chen JH, Schoen FJ, Van den Abbeele AD, Demetri GD, Force T, Chen MH. Cardiotoxicity associated with tyrosine kinase inhibitor sunitinib. *Lancet*. 2007;370:2011-2019.
188. Greineder CF, Kohnstamm S, Ky B. Heart failure associated with sunitinib: lessons learned from animal models. *Curr Hypertens Rep*. 2011;13:436-441.



189. Atkins M, Jones CA, Kirkpatrick P. Sunitinib maleate. *Nat Rev Drug Discov.* 2006;5:279-280.
190. Demoulin JB, Essagher A. PDGF receptor signaling networks in normal and cancer cells. *Cytokine Growth Factor Rev.* 2014;25:273-283.
191. Heldin CH. Targeting the PDGF signaling pathway in tumor treatment. *Cell Commun Signal.* 2013;11:97.
192. Ravaud A, Motzer RJ, Pandha HS, George DJ, Pantuck AJ, Patel A, Chang YH, Escudier B, Donskov F, Magheli A, Carteni G, Laguerre B, Tomczak P, Breza J, Gerletti P, Lechuga M, Lin X, Martini JF, Ramaswamy K, Casey M, Staehler M, Patard JJ. Adjuvant Sunitinib in High-Risk Renal-Cell Carcinoma after Nephrectomy. *N Engl J Med.* 2016;375:2246-2254.
193. Joensuu H. Cardiac toxicity of sunitinib. *Lancet.* 2007;370:1978-1980.
194. Jain D, Russell RR, Schwartz RG, Panjra GS, Aronow W. Cardiac Complications of Cancer Therapy: Pathophysiology, Identification, Prevention, Treatment, and Future Directions. *Curr Cardiol Rep.* 2017;19:36.
195. Kollmannsberger C. Sunitinib side effects as surrogate biomarkers of efficacy. *Can Urol Assoc J.* 2016;10:S245-s247.
196. Steingart RM, Bakris GL, Chen HX, Chen MH, Force T, Ivy SP, Leier CV, Liu G, Lenihan D, Lindenfeld J, Maitland ML, Remick SC, Tang WH. Management of cardiac toxicity in patients receiving vascular endothelial growth factor signaling pathway inhibitors. *Am Heart J.* 2012;163:156-163.
197. Numico G, Sicuro M, Silvestris N, Mozzicafreddo A, Trogu A, Malossi A, Cristofano A, Thiebat B. Takotsubo syndrome in a patient treated with sunitinib for renal cancer. *J Clin Oncol.* 2012;30:e218-220.
198. Uraizee I, Cheng S, Moslehi J. Reversible cardiomyopathy associated with sunitinib and sorafenib. *N Engl J Med.* 2011;365:1649-1650.
199. Witteles RM, Telli M. Underestimating cardiac toxicity in cancer trials: lessons learned? *J Clin Oncol.* 2012;30:1916-1918.
200. Cheng H, Force T. Why do kinase inhibitors cause cardiotoxicity and what can be done about it? *Prog Cardiovasc Dis.* 2010;53:114-120.
201. Aparicio-Gallego G, Afonso-Afonso FJ, Leon-Mateos L, Firvida-Perez JL, Vazquez-Estevez S, Lazaro-Quintela M, Ramos-Vazquez M, Fernandez-Calvo O, Campos-Balea B, Anton-Aparicio LM. Molecular basis of hypertension side effects induced by sunitinib. *Anticancer Drugs.* 2011;22:1-8.
202. Kerkela R, Woulfe KC, Durand JB, Vagnozzi R, Kramer D, Chu TF, Beahm C, Chen MH, Force T. Sunitinib-induced cardiotoxicity is mediated by off-target inhibition of AMP-activated protein kinase. *Clin Transl Sci.* 2009;2:15-25.
203. O'Farrell AC, Evans R, Silvola JM, Miller IS, Conroy E, Hector S, Cary M, Murray DW, Jarzabek MA, Maratha A, Alamanou M, Udipi GM, Shiels L, Pallaud C, Saraste A, Liljenback H, Jauhiainen M, Oikonen V, Ducret A, Cutler P, McAuliffe FM, Rousseau JA, Lecomte R, Gascon S, Arany Z, Ky B, Force T, Knuuti J, Gallagher WM, Roivainen A, Byrne AT. A Novel Positron Emission Tomography (PET) Approach to Monitor Cardiac Metabolic Pathway Remodeling in Response to Sunitinib Malate. *PLoS One.* 2017;12:e0169964.
204. Yang Y, Bu P. Progress on the cardiotoxicity of sunitinib: Prognostic significance, mechanism and protective therapies. *Chem Biol Interact.* 2016;257:125-131.

205. Hasinoff BB, Patel D, O'Hara KA. Mechanisms of myocyte cytotoxicity induced by the multiple receptor tyrosine kinase inhibitor sunitinib. *Mol Pharmacol.* 2008;74:1722-1728.
206. Yong QC, Thomas CM, Seqqat R, Chandel N, Baker KM, Kumar R. Angiotensin type 1a receptor-deficient mice develop diabetes-induced cardiac dysfunction, which is prevented by renin-angiotensin system inhibitors. *Cardiovasc Diabetol.* 2013;12:169.
207. Chintalgattu V, Ai D, Langley RR, Zhang J, Bankson JA, Shih TL, Reddy AK, Coombes KR, Daher IN, Pati S, Patel SS, Pocius JS, Taffet GE, Buja LM, Entman ML, Khakoo AY. Cardiomyocyte PDGFR-beta signaling is an essential component of the mouse cardiac response to load-induced stress. *J Clin Invest.* 2010;120:472-484.
208. Chintalgattu V, Rees ML, Culver JC, Goel A, Jiffar T, Zhang J, Dunner K, Jr., Pati S, Bankson JA, Pasqualini R, Arap W, Bryan NS, Taegtmeier H, Langley RR, Yao H, Kupferman ME, Entman ML, Dickinson ME, Khakoo AY. Coronary microvascular pericytes are the cellular target of sunitinib malate-induced cardiotoxicity. *Sci Transl Med.* 2013;5:187ra169.
209. Hahn VS, Lenihan DJ, Ky B. Cancer therapy-induced cardiotoxicity: basic mechanisms and potential cardioprotective therapies. *J Am Heart Assoc.* 2014;3:e000665.
210. Hall PS, Harshman LC, Srinivas S, Witteles RM. The frequency and severity of cardiovascular toxicity from targeted therapy in advanced renal cell carcinoma patients. *JACC Heart Fail.* 2013;1:72-78.
211. Bono P, Rautiola J, Utriainen T, Joensuu H. Hypertension as predictor of sunitinib treatment outcome in metastatic renal cell carcinoma. *Acta Oncol.* 2011;50:569-573.
212. Azizi M, Chedid A, Oudard S. Home blood-pressure monitoring in patients receiving sunitinib. *N Engl J Med.* 2008;358:95-97.
213. Richards CJ, Je Y, Schutz FA, Heng DY, Dallabrida SM, Moslehi JJ, Choueiri TK. Incidence and risk of congestive heart failure in patients with renal and nonrenal cell carcinoma treated with sunitinib. *J Clin Oncol.* 2011;29:3450-3456.
214. Telli ML, Witteles RM, Fisher GA, Srinivas S. Cardiotoxicity associated with the cancer therapeutic agent sunitinib malate. *Ann Oncol.* 2008;19:1613-1618.
215. Gore ME, Szczylik C, Porta C, Bracarda S, Bjarnason GA, Oudard S, Lee SH, Haanen J, Castellano D, Vrdoljak E, Schoffski P, Mainwaring P, Hawkins RE, Crino L, Kim TM, Carteni G, Eberhardt WE, Zhang K, Fly K, Matczak E, Lechuga MJ, Hariharan S, Bukowski R. Final results from the large sunitinib global expanded-access trial in metastatic renal cell carcinoma. *Br J Cancer.* 2015;113:12-19.
216. Goldstein D, Rosenberg JE, Figlin RA, Townsend RR, McCann L, Carpenter C, Pandite L. Is change in blood pressure a biomarker of pazopanib and sunitinib efficacy in advanced/metastatic renal cell carcinoma? *Eur J Cancer.* 2016;53:96-104.
217. Bax JJ, Delgado V, Sogaard P, Singh JP, Abraham WT, Borer JS, Dickstein K, Gras D, Brugada J, Robertson M, Ford I, Krum H, Holzmeister J, Ruschitzka F, Gorcsan J. Prognostic implications of left ventricular global longitudinal strain in

- heart failure patients with narrow QRS complex treated with cardiac resynchronization therapy: a subanalysis of the randomized EchoCRT trial. *Eur Heart J*. 2017;38:720-726.
218. Bottinor WJ, Migliore CK, Lenneman CA, Stoddard MF. Echocardiographic Assessment of Cardiotoxic Effects of Cancer Therapy. *Curr Cardiol Rep*. 2016;18:99.
  219. Tops LF, Delgado V, Marsan NA, Bax JJ. Myocardial strain to detect subtle left ventricular systolic dysfunction. *Eur J Heart Fail*. 2017;19:307-313.
  220. Davis MK, Virani SA. Routine Prophylactic Cardioprotective Therapy Should Not Be Given to All Recipients of Potentially Cardiotoxic Cancer Chemotherapy. *Can J Cardiol*. 2016;32:926-930.
  221. Abdel-Qadir H, Amir E, Thavendiranathan P. Prevention, Detection, and Management of Chemotherapy-Related Cardiac Dysfunction. *Can J Cardiol*. 2016;32:891-899.
  222. Yancy CW, Jessup M, Bozkurt B, Butler J, Casey DE, Jr., Colvin MM, Drazner MH, Filippatos GS, Fonarow GC, Givertz MM, Hollenberg SM, Lindenfeld J, Masoudi FA, McBride PE, Peterson PN, Stevenson LW, Westlake C. 2017 ACC/AHA/HFSA Focused Update of the 2013 ACCF/AHA Guideline for the Management of Heart Failure: A Report of the American College of Cardiology/American Heart Association Task Force on Clinical Practice Guidelines and the Heart Failure Society of America. *Circulation*. 2017
  223. Kalam K, Marwick TH. Role of cardioprotective therapy for prevention of cardiotoxicity with chemotherapy: a systematic review and meta-analysis. *Eur J Cancer*. 2013;49:2900-2909.
  224. Seicean S, Seicean A, Plana JC, Budd GT, Marwick TH. Effect of statin therapy on the risk for incident heart failure in patients with breast cancer receiving anthracycline chemotherapy: an observational clinical cohort study. *J Am Coll Cardiol*. 2012;60:2384-2390.
  225. Cardinale D, Colombo A, Sandri MT, Lamantia G, Colombo N, Civelli M, Martinelli G, Veglia F, Fiorentini C, Cipolla CM. Prevention of high-dose chemotherapy-induced cardiotoxicity in high-risk patients by angiotensin-converting enzyme inhibition. *Circulation*. 2006;114:2474-2481.
  226. Janbabai G, Nabati M, Faghihinia M, Azizi S, Borhani S, Yazdani J. Effect of Enalapril on Preventing Anthracycline-Induced Cardiomyopathy. *Cardiovasc Toxicol*. 2017;17:130-139.
  227. Gulati G, Heck SL, Ree AH, Hoffmann P, Schulz-Menger J, Fagerland MW, Gravdehaug B, von Knobelsdorff-Brenkenhoff F, Bratland A, Storås TH, Håge TA, Rosjo H, Steine K, Geisler J, Omland T. Prevention of cardiac dysfunction during adjuvant breast cancer therapy (PRADA): a 2 x 2 factorial, randomized, placebo-controlled, double-blind clinical trial of candesartan and metoprolol. *Eur Heart J*. 2016;37:1671-1680.
  228. Riad A, Bien S, Westermann D, Becher PM, Loya K, Landmesser U, Kroemer HK, Schultheiss HP, Tschope C. Pretreatment with statin attenuates the cardiotoxicity of Doxorubicin in mice. *Cancer Res*. 2009;69:695-699.

229. Zhang J, Cui X, Yan Y, Li M, Yang Y, Wang J, Zhang J. Research progress of cardioprotective agents for prevention of anthracycline cardiotoxicity. *Am J Transl Res.* 2016;8:2862-2875.
230. Okwuosa TM, Anzevino S, Rao R. Cardiovascular disease in cancer survivors. *Postgrad Med J.* 2017;93:82-90.
231. Ramanjaneyulu SV, Trivedi PP, Kushwaha S, Vikram A, Jena GB. Protective role of atorvastatin against doxorubicin-induced cardiotoxicity and testicular toxicity in mice. *J Physiol Biochem.* 2013;69:513-525.
232. Ishida J, Konishi M, Ebner N, Springer J. Repurposing of approved cardiovascular drugs. *J Transl Med.* 2016;14:269.
233. Oliveira PJ, Bjork JA, Santos MS, Leino RL, Froberg MK, Moreno AJ, Wallace KB. Carvedilol-mediated antioxidant protection against doxorubicin-induced cardiac mitochondrial toxicity. *Toxicol Appl Pharmacol.* 2004;200:159-168.
234. Jasinska M, Owczarek J, Orszulak-Michalak D. Statins: a new insight into their mechanisms of action and consequent pleiotropic effects. *Pharmacol Rep.* 2007;59:483-499.
235. Chotenimitkhun R, D'Agostino R, Jr., Lawrence JA, Hamilton CA, Jordan JH, Vasu S, Lash TL, Yeboah J, Herrington DM, Hundley WG. Chronic statin administration may attenuate early anthracycline-associated declines in left ventricular ejection function. *Can J Cardiol.* 2015;31:302-307.
236. Acar Z, Kale A, Turgut M, Demircan S, Durna K, Demir S, Meric M, Agac MT. Efficiency of atorvastatin in the protection of anthracycline-induced cardiomyopathy. *J Am Coll Cardiol.* 2011;58:988-989.
237. Fanous I, Dillon P. Cancer treatment-related cardiac toxicity: prevention, assessment and management. *Med Oncol.* 2016;33:84.
238. Goyal V, Bews H, Cheung D, Premecz S, Mandal S, Shaikh B, Best R, Bhindi R, Chaudhary R, Ravandi A, Thliveris J, Singal PK, Niraula S, Jassal DS. The Cardioprotective Role of N-Acetyl Cysteine Amide in the Prevention of Doxorubicin and Trastuzumab-Mediated Cardiac Dysfunction. *Can J Cardiol.* 2016;32:1513-1519.
239. Walker JR, Sharma A, Lytwyn M, Bohonis S, Thliveris J, Singal PK, Jassal DS. The cardioprotective role of probucol against anthracycline and trastuzumab-mediated cardiotoxicity. *J Am Soc Echocardiogr.* 2011;24:699-705.
240. Ludke AR, Al-Shudiefat AA, Dhingra S, Jassal DS, Singal PK. A concise description of cardioprotective strategies in doxorubicin-induced cardiotoxicity. *Can J Physiol Pharmacol.* 2009;87:756-763.
241. Yamashita S, Masuda D, Matsuzawa Y. Did we abandon probucol too soon? *Curr Opin Lipidol.* 2015;26:304-316.
242. Zucoloto AZ, Manchope MF, Staurengo-Ferrari L, Pinho-Ribeiro FA, Zarpelon AC, Saraiva ALL, Cecilio NT, Alves-Filho JC, Cunha TM, Menezes GB, Cunha FQ, Casagrande R, Verri WA, Jr. Probucol attenuates lipopolysaccharide-induced leukocyte recruitment and inflammatory hyperalgesia: effect on NF-small ka, CyrillicB activation and cytokine production. *Eur J Pharmacol.* 2017;809:52-63.
243. Siveski-Iliskovic N, Kaul N, Singal PK. Probucol promotes endogenous antioxidants and provides protection against adriamycin-induced cardiomyopathy in rats. *Circulation.* 1994;89:2829-2835.

244. Kumar D, Kirshenbaum LA, Li T, Danelisen I, Singal PK. Apoptosis in adriamycin cardiomyopathy and its modulation by probucol. *Antioxid Redox Signal*. 2001;3:135-145.
245. Li T, Singal PK. Adriamycin-induced early changes in myocardial antioxidant enzymes and their modulation by probucol. *Circulation*. 2000;102:2105-2110.
246. Grinberg L, Fibach E, Amer J, Atlas D. N-acetylcysteine amide, a novel cell-permeating thiol, restores cellular glutathione and protects human red blood cells from oxidative stress. *Free Radic Biol Med*. 2005;38:136-145.
247. Sunitha K, Hemshekhar M, Thushara RM, Santhosh MS, Yariswamy M, Kemparaju K, Girish KS. N-Acetylcysteine amide: a derivative to fulfill the promises of N-Acetylcysteine. *Free Radic Res*. 2013;47:357-367.
248. Ates B, Abraham L, Ercal N. Antioxidant and free radical scavenging properties of N-acetylcysteine amide (NACA) and comparison with N-acetylcysteine (NAC). *Free Radic Res*. 2008;42:372-377.
249. Shi R, Huang CC, Aronstam RS, Ercal N, Martin A, Huang YW. N-acetylcysteine amide decreases oxidative stress but not cell death induced by doxorubicin in H9c2 cardiomyocytes. *BMC Pharmacol*. 2009;9:7.
250. Hunt SA, Baker DW, Chin MH, Cinquegrani MP, Feldman AM, Francis GS, Ganiats TG, Goldstein S, Gregoratos G, Jessup ML, Noble RJ, Packer M, Silver MA, Stevenson LW, Gibbons RJ, Antman EM, Alpert JS, Faxon DP, Fuster V, Gregoratos G, Jacobs AK, Hiratzka LF, Russell RO, Smith SC, Jr. ACC/AHA Guidelines for the Evaluation and Management of Chronic Heart Failure in the Adult: Executive Summary A Report of the American College of Cardiology/American Heart Association Task Force on Practice Guidelines (Committee to Revise the 1995 Guidelines for the Evaluation and Management of Heart Failure): Developed in Collaboration With the International Society for Heart and Lung Transplantation; Endorsed by the Heart Failure Society of America. *Circulation*. 2001;104:2996-3007.
251. Coelho M, Soares-Silva C, Brandao D, Marino F, Cosentino M, Ribeiro L. beta-Adrenergic modulation of cancer cell proliferation: available evidence and clinical perspectives. *J Cancer Res Clin Oncol*. 2017;143:275-291.
252. Kalay N, Basar E, Ozdogru I, Er O, Cetinkaya Y, Dogan A, Inanc T, Oguzhan A, Eryol NK, Topsakal R, Ergin A. Protective effects of carvedilol against anthracycline-induced cardiomyopathy. *J Am Coll Cardiol*. 2006;48:2258-2262.
253. Yun S, Vincelette ND, Abraham I. Cardioprotective role of beta-blockers and angiotensin antagonists in early-onset anthracyclines-induced cardiotoxicity in adult patients: a systematic review and meta-analysis. *Postgrad Med J*. 2015;91:627-633.
254. Bosch X, Rovira M, Sitges M, Domenech A, Ortiz-Perez JT, de Caralt TM, Morales-Ruiz M, Perea RJ, Monzo M, Esteve J. Enalapril and carvedilol for preventing chemotherapy-induced left ventricular systolic dysfunction in patients with malignant hemopathies: the OVERCOME trial (prevention of left Ventricular dysfunction with Enalapril and carvedilol in patients submitted to intensive Chemotherapy for the treatment of Malignant hemopathies). *J Am Coll Cardiol*. 2013;61:2355-2362.

255. Pituskin E, Mackey JR, Koshman S, Jassal D, Pitz M, Haykowsky MJ, Pagano JJ, Chow K, Thompson RB, Vos LJ, Ghosh S, Oudit GY, Ezekowitz JA, Paterson DI. Multidisciplinary Approach to Novel Therapies in Cardio-Oncology Research (MANTICORE 101-Breast): A Randomized Trial for the Prevention of Trastuzumab-Associated Cardiotoxicity. *J Clin Oncol*. 2017;35:870-877.
256. Volpe M. Cardiovascular risk in hypertension - can we ask for more? : focus on aliskiren. *High Blood Press Cardiovasc Prev*. 2008;15:255-268.
257. Wzgarda A, Kleszcz R, Prokop M, Regulska K, Regulski M, Paluszczak J, Stanisz BJ. Unknown face of known drugs - what else can we expect from angiotensin converting enzyme inhibitors? *Eur J Pharmacol*. 2017;797:9-19.
258. Yusuf S, Sleight P, Pogue J, Bosch J, Davies R, Dagenais G. Effects of an angiotensin-converting-enzyme inhibitor, ramipril, on cardiovascular events in high-risk patients. *N Engl J Med*. 2000;342:145-153.
259. Sonnenblick EH. Perindopril treatment for congestive heart failure. *Am J Cardiol*. 2001;88:19i-27i.
260. Howlett JG, Chan M, Ezekowitz JA, Harkness K, Heckman GA, Kouz S, Leblanc MH, Moe GW, O'Meara E, Abrams H, Ducharme A, Grzeslo A, Hamilton PG, Koshman SL, Lepage S, McDonald M, McKelvie R, Rajda M, Swiggum E, Virani S, Zieroth S. The Canadian Cardiovascular Society Heart Failure Companion: Bridging Guidelines to Your Practice. *Can J Cardiol*. 2016;32:296-310.
261. Yusuf S, Pepine CJ, Garces C, Pouleur H, Salem D, Kostis J, Benedict C, Rousseau M, Bourassa M, Pitt B. Effect of enalapril on myocardial infarction and unstable angina in patients with low ejection fractions. *Lancet*. 1992;340:1173-1178.
262. Rutherford JD, Pfeffer MA, Moye LA, Davis BR, Flaker GC, Kowey PR, Lamas GA, Miller HS, Packer M, Rouleau JL, et al. Effects of captopril on ischemic events after myocardial infarction. Results of the Survival and Ventricular Enlargement trial. SAVE Investigators. *Circulation*. 1994;90:1731-1738.
263. Cohn JN, Tognoni G. A randomized trial of the angiotensin-receptor blocker valsartan in chronic heart failure. *N Engl J Med*. 2001;345:1667-1675.
264. White HD. Candesartan and heart failure: the allure of CHARM. *Lancet*. 2003;362:754-755.
265. Miao J, Wang L, Zhang X, Zhu C, Cui L, Ji H, Liu Y, Wang X. Protective Effect of Aliskiren in Experimental Ischemic Stroke: Up-Regulated p-PI3K, p-AKT, Bcl-2 Expression, Attenuated Bax Expression. *Neurochem Res*. 2016;41:2300-2310.
266. Abuelezz SA, Hendawy N, Osman WM. Aliskiren attenuates bleomycin-induced pulmonary fibrosis in rats: focus on oxidative stress, advanced glycation end products, and matrix metalloproteinase-9. *Naunyn Schmiedebergs Arch Pharmacol*. 2016;389:897-909.
267. Simao S, Santos DF, Silva GA. Aliskiren decreases oxidative stress and angiogenic markers in retinal pigment epithelium cells. *Angiogenesis*. 2017;20:175-181.
268. Ju H, Zhao S, Jassal DS, Dixon IM. Effect of AT1 receptor blockade on cardiac collagen remodeling after myocardial infarction. *Cardiovasc Res*. 1997;35:223-232.
269. Khaper N, Singal PK. Modulation of oxidative stress by a selective inhibition of angiotensin II type 1 receptors in MI rats. *J Am Coll Cardiol*. 2001;37:1461-1466.

270. Asker SA, Mazroa SA, Boshra V, Hassan AM. Biochemical and histological impact of direct renin inhibition by aliskiren on myofibroblasts activation and differentiation in bleomycin induced pulmonary fibrosis in adult mice. *Tissue Cell*. 2015;47:373-381.
271. Hiona A, Lee AS, Nagendran J, Xie X, Connolly AJ, Robbins RC, Wu JC. Pretreatment with angiotensin-converting enzyme inhibitor improves doxorubicin-induced cardiomyopathy via preservation of mitochondrial function. *J Thorac Cardiovasc Surg*. 2011;142:396-403.e393.
272. Akolkar G, Bhullar N, Bews H, Shaikh B, Premecz S, Bordun KA, Cheung DY, Goyal V, Sharma AK, Garber P, Singal PK, Jassal DS. The role of renin angiotensin system antagonists in the prevention of doxorubicin and trastuzumab induced cardiotoxicity. *Cardiovasc Ultrasound*. 2015;13:18.
273. Abd El-Aziz MA, Othman AI, Amer M, El-Missiry MA. Potential protective role of angiotensin-converting enzyme inhibitors captopril and enalapril against adriamycin-induced acute cardiac and hepatic toxicity in rats. *J Appl Toxicol*. 2001;21:469-473.
274. Suda O, Tsutsui M, Morishita T, Tanimoto A, Horiuchi M, Tasaki H, Huang PL, Sasaguri Y, Yanagihara N, Nakashima Y. Long-term treatment with N(omega)-nitro-L-arginine methyl ester causes arteriosclerotic coronary lesions in endothelial nitric oxide synthase-deficient mice. *Circulation*. 2002;106:1729-1735.
275. Zhi H, Luptak I, Alreja G, Shi J, Guan J, Metes-Kosik N, Joseph J. Effects of direct Renin inhibition on myocardial fibrosis and cardiac fibroblast function. *PLoS One*. 2013;8:e81612.
276. Lo CS, Liu F, Shi Y, Maachi H, Chenier I, Godin N, Filep JG, Ingelfinger JR, Zhang SL, Chan JS. Dual RAS blockade normalizes angiotensin-converting enzyme-2 expression and prevents hypertension and tubular apoptosis in Akita angiotensinogen-transgenic mice. *Am J Physiol Renal Physiol*. 2012;302:F840-852.
277. Cohn JN, McInnes GT, Shepherd AM. Direct-acting vasodilators. *J Clin Hypertens (Greenwich)*. 2011;13:690-692.
278. Feng M, Whitesall S, Zhang Y, Beibel M, D'Alecy L, DiPetrillo K. Validation of volume-pressure recording tail-cuff blood pressure measurements. *Am J Hypertens*. 2008;21:1288-1291.
279. Ahmadi R, Santiago JJ, Walker J, Fang T, Le K, Zhao Z, Azordegan N, Bage S, Lytwyn M, Rattan S, Dixon IM, Kardami E, Moghadasian MH, Jassal DS. A high-lipid diet potentiates left ventricular dysfunction in nitric oxide synthase 3-deficient mice after chronic pressure overload. *J Nutr*. 2010;140:1438-1444.
280. Luft JH. Improvements in epoxy resin embedding methods. *J Biophys Biochem Cytol*. 1961;9:409-414.
281. Folch J, Lees M, Sloane Stanley GH. A simple method for the isolation and purification of total lipides from animal tissues. *J Biol Chem*. 1957;226:497-509.
282. Hasanally D, Edel A, Chaudhary R, Ravandi A. Identification of Oxidized Phosphatidylinositols Present in OxLDL and Human Atherosclerotic Plaque. *Lipids*. 2017;52:11-26.
283. Millatt LJ, Abdel-Rahman EM, Siragy HM. Angiotensin II and nitric oxide: a question of balance. *Regul Pept*. 1999;81:1-10.

284. Zhou MS, Schulman IH, Raij L. Role of angiotensin II and oxidative stress in vascular insulin resistance linked to hypertension. *Am J Physiol Heart Circ Physiol*. 2009;296:H833-839.
285. Yan C, Kim D, Aizawa T, Berk BC. Functional interplay between angiotensin II and nitric oxide: cyclic GMP as a key mediator. *Arterioscler Thromb Vasc Biol*. 2003;23:26-36.
286. Bataineh A, Raij L. Angiotensin II, nitric oxide, and end-organ damage in hypertension. *Kidney Int Suppl*. 1998;68:S14-19.
287. Li L, Zhou N, Gong H, Wu J, Lin L, Komuro I, Ge J, Zou Y. Comparison of angiotensin II type 1-receptor blockers to regress pressure overload-induced cardiac hypertrophy in mice. *Hypertens Res*. 2010;33:1289-1297.
288. Patten RD, Hall-Porter MR. Small animal models of heart failure: development of novel therapies, past and present. *Circ Heart Fail*. 2009;2:138-144.
289. Zhu X, Wu S, Dahut WL, Parikh CR. Risks of proteinuria and hypertension with bevacizumab, an antibody against vascular endothelial growth factor: systematic review and meta-analysis. *Am J Kidney Dis*. 2007;49:186-193.
290. Mourad JJ, des Guetz G, Debbabi H, Levy BI. Blood pressure rise following angiogenesis inhibition by bevacizumab. A crucial role for microcirculation. *Ann Oncol*. 2008;19:927-934.
291. Kappers MH, van Esch JH, Sluiter W, Sleijfer S, Danser AH, van den Meiracker AH. Hypertension induced by the tyrosine kinase inhibitor sunitinib is associated with increased circulating endothelin-1 levels. *Hypertension*. 2010;56:675-681.
292. Siragy HM, Kar S, Kirkpatrick P. Aliskiren. *Nat Rev Drug Discov*. 2007;6:779-780.
293. Thomas CM, Yong QC, Seqqat R, Chandel N, Feldman DL, Baker KM, Kumar R. Direct renin inhibition prevents cardiac dysfunction in a diabetic mouse model: comparison with an angiotensin receptor antagonist and angiotensin-converting enzyme inhibitor. *Clin Sci (Lond)*. 2013;124:529-541.
294. Feldman DL. New insights into the renoprotective actions of the renin inhibitor aliskiren in experimental renal disease. *Hypertens Res*. 2010;33:279-287.
295. Singh VP, Baker KM, Kumar R. Activation of the intracellular renin-angiotensin system in cardiac fibroblasts by high glucose: role in extracellular matrix production. *Am J Physiol Heart Circ Physiol*. 2008;294:H1675-1684.
296. Saito T, Asai K, Sato S, Takano H, Mizuno K, Shimizu W. Ultrastructural features of cardiomyocytes in dilated cardiomyopathy with initially decompensated heart failure as a predictor of prognosis. *Eur Heart J*. 2015;36:724-732.
297. Carmeliet P, Ng YS, Nuyens D, Theilmeier G, Brusselmans K, Cornelissen I, Ehler E, Kakkar VV, Stalmans I, Mattot V, Perriard JC, Dewerchin M, Flameng W, Nagy A, Lupu F, Moons L, Collen D, D'Amore PA, Shima DT. Impaired myocardial angiogenesis and ischemic cardiomyopathy in mice lacking the vascular endothelial growth factor isoforms VEGF164 and VEGF188. *Nat Med*. 1999;5:495-502.
298. Harvey PA, Leinwand LA. The cell biology of disease: cellular mechanisms of cardiomyopathy. *J Cell Biol*. 2011;194:355-365.
299. Torti FM, Bristow MM, Lum BL, Carter SK, Howes AE, Aston DA, Brown BW, Jr., Hannigan JF, Jr., Meyers FJ, Mitchell EP, et al. Cardiotoxicity of epirubicin



- and doxorubicin: assessment by endomyocardial biopsy. *Cancer Res.* 1986;46:3722-3727.
300. Cooper LT, Baughman KL, Feldman AM, Frustaci A, Jessup M, Kuhl U, Levine GN, Narula J, Starling RC, Towbin J, Virmani R. The role of endomyocardial biopsy in the management of cardiovascular disease: a scientific statement from the American Heart Association, the American College of Cardiology, and the European Society of Cardiology. Endorsed by the Heart Failure Society of America and the Heart Failure Association of the European Society of Cardiology. *J Am Coll Cardiol.* 2007;50:1914-1931.
  301. From AM, Maleszewski JJ, Rihal CS. Current status of endomyocardial biopsy. *Mayo Clin Proc.* 2011;86:1095-1102.
  302. Saidi A, Alharethi R. Management of chemotherapy induced cardiomyopathy. *Curr Cardiol Rev.* 2011;7:245-249.
  303. Elmore S. Apoptosis: a review of programmed cell death. *Toxicol Pathol.* 2007;35:495-516.
  304. Assefa Z, Vantieghem A, Garmyn M, Declercq W, Vandenaabeele P, Vandenneede JR, Bouillon R, Merlevede W, Agostinis P. p38 mitogen-activated protein kinase regulates a novel, caspase-independent pathway for the mitochondrial cytochrome c release in ultraviolet B radiation-induced apoptosis. *J Biol Chem.* 2000;275:21416-21421.
  305. Prickett TD, Brautigan DL. Cytokine activation of p38 mitogen-activated protein kinase and apoptosis is opposed by alpha-4 targeting of protein phosphatase 2A for site-specific dephosphorylation of MEK3. *Mol Cell Biol.* 2007;27:4217-4227.
  306. Brown DA, Perry JB, Allen ME, Sabbah HN, Stauffer BL, Shaikh SR, Cleland JG, Colucci WS, Butler J, Voors AA, Anker SD, Pitt B, Pieske B, Filippatos G, Greene SJ, Gheorghide M. Expert consensus document: Mitochondrial function as a therapeutic target in heart failure. *Nat Rev Cardiol.* 2017;14:238-250.
  307. Chiong M, Wang ZV, Pedrozo Z, Cao DJ, Troncoso R, Ibacache M, Criollo A, Nemchenko A, Hill JA, Lavandero S. Cardiomyocyte death: mechanisms and translational implications. *Cell Death Dis.* 2011;2:e244.
  308. Cande C, Cecconi F, Dessen P, Kroemer G. Apoptosis-inducing factor (AIF): key to the conserved caspase-independent pathways of cell death? *J Cell Sci.* 2002;115:4727-4734.
  309. Chaitanya GV, Steven AJ, Babu PP. PARP-1 cleavage fragments: signatures of cell-death proteases in neurodegeneration. *Cell Commun Signal.* 2010;8:31.
  310. Yelamos J, Farres J, Llacuna L, Ampurdanes C, Martin-Caballero J. PARP-1 and PARP-2: New players in tumour development. *Am J Cancer Res.* 2011;1:328-346.
  311. Luo X, Kraus WL. On PAR with PARP: cellular stress signaling through poly(ADP-ribose) and PARP-1. *Genes Dev.* 2012;26:417-432.
  312. Boulares AH, Yakovlev AG, Ivanova V, Stoica BA, Wang G, Iyer S, Smulson M. Role of poly(ADP-ribose) polymerase (PARP) cleavage in apoptosis. Caspase 3-resistant PARP mutant increases rates of apoptosis in transfected cells. *J Biol Chem.* 1999;274:22932-22940.
  313. Will Y, Dykens JA, Nadanaciva S, Hirakawa B, Jamieson J, Marroquin LD, Hynes J, Patyna S, Jessen BA. Effect of the multitargeted tyrosine kinase inhibitors

- imatinib, dasatinib, sunitinib, and sorafenib on mitochondrial function in isolated rat heart mitochondria and H9c2 cells. *Toxicol Sci.* 2008;106:153-161.
314. French KJ, Coatney RW, Renninger JP, Hu CX, Gales TL, Zhao S, Storck LM, Davis CB, McSurdy-Freed J, Chen E, Frazier KS. Differences in effects on myocardium and mitochondria by angiogenic inhibitors suggest separate mechanisms of cardiotoxicity. *Toxicol Pathol.* 2010;38:691-702.
  315. Lee YK, Hwang JT, Kwon DY, Surh YJ, Park OJ. Induction of apoptosis by quercetin is mediated through AMPK $\alpha$ 1/ASK1/p38 pathway. *Cancer Lett.* 2010;292:228-236.
  316. Cardaci S, Filomeni G, Ciriolo MR. Redox implications of AMPK-mediated signal transduction beyond energetic clues. *J Cell Sci.* 2012;125:2115-2125.
  317. Amemiya T, Honma M, Kariya Y, Ghosh S, Kitano H, Kurachi Y, Fujita K-i, Sasaki Y, Homma Y, Abernethy DR, Kume H, Suzuki H. Elucidation of the molecular mechanisms underlying adverse reactions associated with a kinase inhibitor using systems toxicology. *npj Systems Biology and Applications.* 2015;1:15005.
  318. Devkota S, Wang Y, Musch MW, Leone V, Fehlner-Peach H, Nadimpalli A, Antonopoulos DA, Jabri B, Chang EB. Dietary-fat-induced taurocholic acid promotes pathobiont expansion and colitis in Il10 $^{-/-}$  mice. *Nature.* 2012;487:104-108.
  319. Ayala A, Munoz MF, Arguelles S. Lipid peroxidation: production, metabolism, and signaling mechanisms of malondialdehyde and 4-hydroxy-2-nonenal. *Oxid Med Cell Longev.* 2014;2014:360438.
  320. Bochkov VN, Oskolkova OV, Birukov KG, Levonen AL, Binder CJ, Stockl J. Generation and biological activities of oxidized phospholipids. *Antioxid Redox Signal.* 2010;12:1009-1059.
  321. Samhan-Arias AK, Ji J, Demidova OM, Sparvero LJ, Feng W, Tyurin V, Tyurina YY, Epperly MW, Shvedova AA, Greenberger JS, Bayir H, Kagan VE, Amoscato AA. Oxidized phospholipids as biomarkers of tissue and cell damage with a focus on cardiolipin. *Biochim Biophys Acta.* 2012;1818:2413-2423.
  322. Lu L, Quinn MT, Sun Y. Oxidative stress in the infarcted heart: role of de novo angiotensin II production. *Biochem Biophys Res Commun.* 2004;325:943-951.
  323. Schmidinger M, Zielinski CC, Vogl UM, Bojic A, Bojic M, Schukro C, Ruhsam M, Hejna M, Schmidinger H. Cardiac toxicity of sunitinib and sorafenib in patients with metastatic renal cell carcinoma. *J Clin Oncol.* 2008;26:5204-5212.
  324. Verhoest G, Dolley-Hitze T, Jouan F, Belaud-Rotureau MA, Oger E, Lavenue A, Bensalah K, Arlot-Bonnemains Y, Collet N, Rioux-Leclercq N, Vigneau C. Sunitinib combined with angiotensin-2 type-1 receptor antagonists induces more necrosis: a murine xenograft model of renal cell carcinoma. *Biomed Res Int.* 2014;2014:901371.
  325. Neo JH, Malcontenti-Wilson C, Muralidharan V, Christophi C. Effect of ACE inhibitors and angiotensin II receptor antagonists in a mouse model of colorectal cancer liver metastases. *J Gastroenterol Hepatol.* 2007;22:577-584.
  326. McKay RR, Rodriguez GE, Lin X, Kaymakcalan MD, Hamnvik OP, Sabbisetti VS, Bhatt RS, Simantov R, Choueiri TK. Angiotensin system inhibitors and

- survival outcomes in patients with metastatic renal cell carcinoma. *Clin Cancer Res.* 2015;21:2471-2479.
327. Osumi H, Matsusaka S, Wakatsuki T, Suenaga M, Shinozaki E, Mizunuma N. Angiotensin II type-1 receptor blockers enhance the effects of bevacizumab-based chemotherapy in metastatic colorectal cancer patients. *Mol Clin Oncol.* 2015;3:1295-1300.
  328. Childers WK. Interactions of the renin-angiotensin system in colorectal cancer and metastasis. *Int J Colorectal Dis.* 2015;30:749-752.
  329. Izzedine H, Derosa L, Le Teuff G, Albiges L, Escudier B. Hypertension and angiotensin system inhibitors: impact on outcome in sunitinib-treated patients for metastatic renal cell carcinoma. *Ann Oncol.* 2015;26:1128-1133.
  330. Derosa L, Izzedine H, Albiges L, Escudier B. Hypertension and Angiotensin System Inhibitors in Patients with Metastatic Renal Cell Carcinoma. *Oncol Rev.* 2016;10:298.
  331. Keizman D, Huang P, Eisenberger MA, Pili R, Kim JJ, Antonarakis ES, Hammers H, Carducci MA. Angiotensin system inhibitors and outcome of sunitinib treatment in patients with metastatic renal cell carcinoma: a retrospective examination. *Eur J Cancer.* 2011;47:1955-1961.
  332. Delyani JA. Mineralocorticoid receptor antagonists: the evolution of utility and pharmacology. *Kidney Int.* 2000;57:1408-1411.
  333. Edinger AL, Thompson CB. Death by design: apoptosis, necrosis and autophagy. *Curr Opin Cell Biol.* 2004;16:663-669.
  334. Zhao W, Zhao T, Chen Y, Ahokas RA, Sun Y. Oxidative stress mediates cardiac fibrosis by enhancing transforming growth factor-beta1 in hypertensive rats. *Mol Cell Biochem.* 2008;317:43-50.
  335. Albin A, Pennesi G, Donatelli F, Cammarota R, De Flora S, Noonan DM. Cardiotoxicity of anticancer drugs: the need for cardio-oncology and cardio-oncological prevention. *J Natl Cancer Inst.* 2010;102:14-25.